

REGULATED CELL DEATH: APOPTOSIS AND NECROPTOSIS IN U937 CELL LINE

Ph.D thesis

Zsuzsanna A. Dunai

Pathological Sciences Doctoral School
Semmelweis University



Supervisor: Dr. Rudolf Mihalik Ph.D.

Official reviewers:

Dr. Gabor Koncz, Ph.D.

Dr. Tibor Vantus, Ph.D.

Head of the Final Examination Committee:

Dr. Gabor Banhegyi, M.D., D.Sc.

Members of the Final Examination Committee:

Dr. Andras Kiss, M.D., Ph.D.

Dr. Gabor Rez, Ph.D.

Budapest, 2012

Table of Contents

Table of Contents.....	2
The list of Abbreviations	5
1. Introduction	10
1. 1. Types of cell death subroutines and actual questions of nomenclature	10
1. 2. Apoptosis, secondary necrosis, necrosis and necroptosis	11
1. 2. 1. Apoptosis	13
1. 2. 1. 1. Molecular background of apoptosis.....	13
1. 2. 1. 2. Caspases are the central initiators and executioners of the apoptotic process	13
1. 2. 2. Secondary necrosis	16
1. 2. 3. Necrosis	17
1. 2. 4. Necroptosis	18
1. 3. Extrinsic cell death pathway and/or survival induction – through TNFR1	19
1. 3. 1. NF- κ B activation – induction of the survival pathway.....	19
1. 3. 2. Apoptosis induction – a route to cell death	21
1. 3. 3. Necroptosis induction	23
1. 4. Extrinsic cell death and survival induction – through Fas/CD95 and TRAIL receptors.....	26
1. 4. 1. Apoptosis and necroptosis induction.....	26
1. 5. Intrinsic apoptotic pathway.....	29
1. 6. Further type of programmed necrosis.....	32
1. 6. 1. PARP-AIF-mediated programmed necrotic pathway.....	32
1. 7. Physiological and pathological aspects of programmed necrotic cell death.....	33
1. 7. 1. Physiological aspects	33
1. 7. 2. Pathological aspects.....	36
2. Objectives	41
3. Methods	42
3. 1. Materials	42
3. 2. Cell culture.....	42
3. 3. Detection of the cell death-associated functional changes by flow cytometry ...	43

3. 3. 1. Assay of PI uptake of native cells representing the damage of plasma membrane	43
3. 3. 2. Characterization of PS distribution in the plasma membrane by flow cytometric analysis of Annexin V-FITC and PI double-labeled cells	44
3. 3. 3. Changes of mitochondrial transmembrane potential were characterized by the DiOC ₆ (3) uptake method	45
3. 3. 4. Functioning lysosomal compartments are characterized by the red fluorescence of acridine orange emitted in the acidic environment of lysosomes .	45
3. 3. 5. Determination of oligonucleosomal DNA fragmentation by the measurement of sub-G1 population of cells	46
3. 3. 6. Representation of side scatter change and DNA fragmentation	46
3. 4. Agarose gel electrophoresis	47
3. 5. Light microscopic studies	47
3. 6. Fluorescent microscopic studies	48
3. 7. Western blot representation of PARP-1 and RIPK1 cleavage.....	48
3. 8. DEVD-ase activity assay	49
3. 9. Statistics	49
4. Results	50
4. 1. TRAIL induces necroptosis in U937 cell line in the presence of a caspase inhibitor.....	50
4. 2. STS induces primary necrosis in the presence of a caspase inhibitor.....	52
4. 3. STS and TRAIL induce RIPK1 and MLKL-dependent necroptosis	59
4. 4. 3-MA inhibits STS-induced necroptosis.....	63
4. 5. CA inhibits both the TRAIL and STS-induced necroptosis in the presence of a caspase inhibitor	64
4. 6. PJ-34 does not arrest either the TRAIL or STS-induced necroptosis in the presence of a caspase inhibitor	70
5. Discussion.....	73
6. Conclusions	78
7. Summary.....	80
8. Összefoglaló	82
9. Bibliography	84

10. Publications	104
10. 1. Publications related to the thesis.....	104
10. 2. Publications not directly related to the thesis	104
11. Acknowledgements.....	105

The list of Abbreviations

A20	dual E3 ligase and hydrolase cleaves off K63-linked polyubiquitin chains
aa	amino acid
AA	arachidonic acid
ACAT	acyl-CoA:cholesterol acyltransferase
ADP	adenosine diphosphate
AIF	apoptosis-inducing factor
ALL	acute lymphoblastic leukemia
AMC	7-amino-4-methylcoumarin
AML	acute myeloid leukemia
ANT	adenine nucleotide translocase, ADP/ATP translocase
AO	acridine orange
Apaf1	apoptotic protease activating factor-1
<i>atg1</i>	autophagy related 1 homolog gene
ATP	adenosine triphosphate
BAD	BCL-2 antagonist of cell death
BAK	BCL-2 homologous antagonist/killer
BAX	BCL-2-like protein 4
BCL-2	B-cell lymphoma 2
BCL-X _L	BCL-2-like protein 1
BHA	butylated hydroxyanisole
BID	BH3 interacting domain death agonist
<i>C. elegans</i>	<i>Caenorhabditis elegans</i>
CA	cathepsin-B inhibitor, CA-074-OMe
CARD	caspase recruitment domain
CCI	controlled cortical impact
cFLIP	cellular FLICE-like inhibitory protein, CASP8 and FADD-like apoptosis regulator
CHAPS	3-[(3-cholamidopropyl)dimethylammonio]-1-propanesulfonate
CHOP	C/EBP homologous protein

CICD	caspase-independent cell death
CYLD	ubiquitin carboxyl-terminal hydrolase
CYPD	cyclophilin D
<i>D. melanogaster</i>	<i>Drosophila melanogaster</i>
DAMP	danger-associated molecular pattern molecule
DED	death effector domain
DIF-1	differentiation-inducing factor
DiOC ₆ (3)	3,3'-Dihexyloxacarbocyanine iodide
DISC	death-inducing signaling complex
DNA	deoxyribonucleic acid
DR	death receptor
DR4	TRAILR1, tumor necrosis factor-related apoptosis-inducing ligand receptor 1, tumor necrosis factor receptor superfamily member 10A
DR5	TRAILR2, tumor necrosis factor-related apoptosis-inducing ligand receptor 2, tumor necrosis factor receptor superfamily member 10B
DRP1	mitochondrial fission factor
DTT	DL-Dithiothreitol
EDTA	ethylenediamine-tetraacetic acid
EtBr	ethidium bromide
FACS	fluorescence-activated cell sorting, flow cytometer
FADD	Fas-associated death domain protein
Fas receptor	also known CD95 receptor, tumor necrosis factor receptor superfamily member 6
FasL	also known CD95L, tumor necrosis factor ligand superfamily member 6
FSC	forward scatter
GA	geldanamycin
GLUD1	glutamate dehydrogenase 1
GLUL	glutamate–ammonia ligase, glutamine synthetase
GM-CSF	granulocyte-macrophage colony stimulating factor
GSH	glutathione
HEPES	4-(2-Hydroxyethyl)piperazine-1-ethanesulfonic acid sodium salt

HMGB	high mobility group box protein
hr-	human recombinant
HSP70	heat-shock protein 70
HSP90	heat-shock protein 90
IAP-1	inhibitor of apoptosis protein 1, baculoviral IAP repeat-containing protein 3
IAP-2	inhibitor of apoptosis protein 2, baculoviral IAP repeat-containing protein 2
IKK	I κ B kinase
IKK α and β	alpha and beta kinases of IKK complex
I κ B	inhibitor of κ B
JNK	c-Jun N-terminal kinase 1, mitogen-activated protein kinase 8
LDH	lactate dehydrogenase
LOX	lypoxigenase
MA	3-methyladenine
MDR-ABC	multi-drug resistant ATP binding cassette
MEF	mouse embryonic fibroblast
MLKL	mixed lineage kinase domain-like protein
MNNG	N-methyl-N'-nitro-N-nitrosoguanidine, DNA alkylating agent
MnSOD	superoxide dismutase [Mn]
NAD	nicotinamide adenine dinucleotide
NCCD	Nomenclature Committee on Cell Death
Nec	necrostatin-1
NEMO	NF-kappa-B essential modulator
NF- κ B	nuclear factor kappa-B
NK cell	natural killer cell
NMDA	N-Methyl-D-aspartate
NO	nitric oxide
NOX1	plasma membrane NADPH oxidase-1
NSA	necrosulfonamide, inhibitor of MLKL
Omi/HtrA2	high temperature requirement protein A2, serine protease, IAP antagonist

PAR	poly(ADP-ribose)
PARP-1	poly(ADP-ribose) polymerase-1
PBS	phosphate buffered saline
PCD	programmed cell death
PGAM5	serine/threonine-protein phosphatase
PI	propidium iodide
PJ-34	N-(6-Oxo-5,6-dihydrophenanthridin-2-yl)-(N,N-dimethylamino)acetamide hydrochloride, PARP inhibitor
PRR	pathogen recognition receptor
PS	phosphatidylserine
PTPC	mitochondrial permeability transition pore complex
PYGL	glycogen phosphorylase
RHIM	RIP homotypic interaction motif
RIPK1	also known RIP1, receptor-interacting protein kinase 1, receptor-interacting serine/threonine-protein kinase 1
RIPK3	also known RIP3, receptor-interacting protein kinase 3, receptor-interacting serine/threonine-protein kinase 3
RNA	ribonucleic acid
RNase A	ribonuclease A
ROS	reactive oxygen species
SDS	sodium dodecyl sulfate
Smac mimetics	cIAP inhibitors, facilitate the proteasomal degradation of cIAPs and sensitize various type of tumor cell to death
Smac/Diablo	IAP-binding mitochondrial protein
SSC	side scatter
STS	staurosporine
TBI	traumatic brain injury
tBID	truncated BID
TNFR1	tumor necrosis factor receptor 1, tumor necrosis factor receptor superfamily member 1A
TNF α	tumor necrosis factor-alpha, tumor necrosis factor

TRADD	TNF α receptor-associated death domain protein, tumor necrosis factor receptor type 1-associated death domain protein
TRAF2	TNF α receptor-associated factor 2, TNF receptor-associated factor 2, E3 ligase enzyme
TRAIL	also known Apo-2L, tumor necrosis factor-related apoptosis-inducing ligand, tumor necrosis factor ligand superfamily member 10
TRAILR1	tumor necrosis factor-related apoptosis-inducing ligand receptor 1, tumor necrosis factor receptor superfamily member 10A, DR4
TRIS-HCl	tris(hydroxymethyl)aminomethane hydrochloride
VDAC	voltage-dependent anion channel
XIAP	X-linked inhibitor of apoptosis protein
z-DEVD.amc	Benzyloxycarbonyl-Asp(OMe)-Glu(OMe)-Val-DL-Asp(OMe)-7 aminomethylcoumarin
zVAD.fmk	<i>N</i> -Benzyloxycarbonyl-Val-Ala-Asp(OMe)-fluoromethyl ketone
zVD.fmk	z-Val-DL-Asp-fluoromethylketone

1. Introduction

In 1972 Kerr, Wyllie and Currie proposed a controlled cell elimination process, which acts complementary but opposite to cell division, to keep tissue homeostasis. That was suggested to be an active and programmed process which can be initiated or inhibited by various physiological or pathological stimuli [1]. Since then, apoptosis as they termed, became a widely investigated cell physiological process. Later Horvitz *et al.* described the molecular genetic pathway responsible for apoptosis that leads to genetically determined cell elimination during the development of the model organism *Caenorhabditis elegans* [2]. Apoptosis has become a widely used term and is often considered to be synonymous with programmed cell death (PCD), while necrosis remained a cell death type lacking the morphological signs of apoptosis. In the last decades accumulating evidences imply that necrotic cell death can also be a genetically regulated event and can be classified as programmed cell death in line with apoptosis. However, contrary to the fairly well characterized pathways of apoptosis the molecular constituents of necrotic pathway(s) are hardly known.

1. 1. Types of cell death subroutines and actual questions of nomenclature

As the experimental scope widened various sub-types of basic cell death forms were defined based not only on morphological criteria but also considering other biochemical, functional or immunological aspects too. Besides the morphology based classification of Clarke: type I. cell death - apoptosis, type II. cell death mediated through autophagy, type III. - necrosis [3], new expressions such as caspase-independent cell death (CICD) [4], non-apoptotic PCD [5], tyrosine kinase inhibitor-triggered Clarke III cell death [6], oncosis [7], necrapoptosis [8], necrotic-like cell death [9], paraptosis [10] or programmed necrosis [11] were established to better define the variegated appearance of cell death types. Some of these terms refer to a cell death type characterized by necrotic morphology but reported as a regulated event.

At the same time, this expansion of cell death related terminologies, without precisely defined terms of cell death subtypes caused confusions in interpretation of results. The term of PCD is often used as a synonym of apoptosis although it has been proved that necrosis can also be a programmed process, as a result of the involvement of a regulated signaling cascade [12-14]. Moreover necrosis can be genetically regulated programmed cell death type too [15-18]. In comparison, during CICD the dying cells can display the morphological signs of apoptosis, necrosis or autophagy [19,20]. Additionally in some cases apoptosis may provoke immune response too [21].

Due to the need for a more precise classification of cell death types, the Nomenclature Committee on Cell Death (NCCD) has been set up by the Editors of Cell Death and Differentiation with the following goals: *“The Nomenclature Committee on Cell Death (NCCD) proposes unified criteria for the definition of cell death and of different cell death morphologies, while formulating several caveats against the misuse of words and concepts that slow down progress in the area of cell death research. Nomenclature must be open to improvements and amendments to entail new discoveries, and the NCCD will help to update and clarify these points.”* [19]. *„The NCCD provides a forum in which names describing distinct modalities of cell death are critically evaluated and recommendations on their definition and use are formulated, hoping that a non-rigid, yet uniform, nomenclature will facilitate the communication among scientists and ultimately accelerate the pace of discovery.”* [22]

The NCCD published its recommendations in 2005, 2009 and 2012 [19,22,23]. These reviews define dying cell, point of no return and the point of cell death, contain guidelines for functional classification of cell death types, suggest methods for detection of the different cell death types, and present the main biochemical features and examples of inhibitory interventions [19,22,23]. In the last review the NCCD discussed 13 different types of regulated cell death subroutines including necroptosis.

1. 2. Apoptosis, secondary necrosis, necrosis and necroptosis

Conventional knowledge considers apoptosis as a caspase-dependent, programmed, non-immunogenic process, characterized by cellular shrinkage, membrane blebbing, chromatin condensation and DNA degradation. During apoptosis dying cell loses its

contacts to the neighbouring cells and finally is fragmented into compact membrane-enclosed structures, called apoptotic bodies. Under normal physiological circumstances apoptotic bodies are engulfed by macrophages and are removed from the tissue without activating immune response.

It is accepted that the main, but not obligate, hallmarks of apoptosis are the activation of caspases resulting in cleavage of a selective pool of proteins, the loss of phospholipid asymmetry of the plasma membrane, cell shrinkage and the early oligonucleosomal DNA fragmentation (Table 1).

In absence of corpse clearing mechanism the apoptotic process is terminated in an autolytic necrotic outcome, with loss of plasma membrane integrity (Table 1). This phenomena was called as secondary necrosis by Wyllie *et al.* [24] with the intention to better distinguish this mode of cell elimination from “cellular necrosis occurring *ab initio*”, which should be called “primary necrosis” [25].

Table 1. Morphological features of apoptosis, secondary necrosis and (primary) necrosis

Apoptosis	Secondary necrosis¹	(Primary) necrosis
Cell shrinkage	Karyolysis (dissolution of the chromatin matter)	Cell volume increase
Intense chromatin condensation (pyknosis)	Pyknosis	Dilatation of ER, mitochondria
Nuclear fragmentation (karyorrhexis)	Karyorrhexis	Chromatin clamping
Oligonucleosomal DNA fragmentation	<i>Cytoplasmic swelling</i>	Karyolysis
Intact cytoplasmic membrane	<i>Rupture of lysosomal membrane</i>	Rupture of cytoplasmic and lysosomal membrane
Phosphatidylserine externalization	<i>Rupture of cytoplasmic membrane</i>	

¹Apoptotic and necrotic features are in bold and in italic, respectively.

Originally the word necrosis was used as a pathological term which describes the morphology of dead cells observed in many human diseases such as neurodegenerative diseases with necrotic outcome [26] as pancreas adiponecrosis [27], trauma [28], ischemia-reperfusion in myocardial infarction [29] or in cerebral infarction [30],

bacterial infection [31,32] tumor malignancies [33,34] and not as description characterising the way how cells die. Morphologically, necrosis is marked by oncosis accompanied by early loss of the integrity of plasma membrane and intracellular compartments. (Table 1.) Due to the bias, that this is a passive type of cell death without underlying regulatory mechanisms involved, the general research interest was turned away from this field of cell death.

Nevertheless, accumulating evidences have confirmed that necrotic cell death can also be a regulated event and therefore be classified as programmed cell death in line with apoptosis [9,14,35-38] (see at 1.2.2).

1. 2. 1. Apoptosis

1. 2. 1. 1. Molecular background of apoptosis

The definitive evidences for the genetic control of the apoptotic machinery were gained in the studies using the nematode *C. elegans* as experimental object [2]. Horvitz and his colleagues identified the crucial genes involved in the process of apoptosis [39]. The cysteine protease CED-3 is the executioner molecule of apoptosis in *C. elegans* and is proteolytically activated from its pro-form with the help of CED-4 protein [39]. Activation of the CED-3/4 complex is regulated by the product of the apoptosis inhibitor gene, *ced-9* and also by the apoptosis inducer *egl-1* gene product, during the developmental cell loss of *C. elegans* [39]. *ced-3* shows similarity to the mammalian caspases, *ced-4* corresponds to apoptotic protease activating factor-1 (Apaf1), while *egl-1* and *ced-9* are members of the *bcl-2* family of pro- and antiapoptotic genes respectively [40]. Subsequent studies in *Drosophila melanogaster* and mammalian cells demonstrated that the core components of the apoptotic cell death machinery are highly conserved through evolution [41].

1. 2. 1. 2. Caspases are the central initiators and executioners of the apoptotic process

Mammalian cysteine proteases show homology to the *C. elegans* CED-3 protein, play crucial role in the signaling network of apoptosis. The acronym word caspase derives from the cystein-dependent aspartate-specific protease expression. The catalytic activity of these enzymes depends on the –SH group of the cysteine residue located at the active

site of the enzyme in the middle of a characteristic QACXG sequence (where X is R, Q or G) [42,43]. Upon binding, caspases specifically cleave their substrates at carboxyl groups of aspartates present in the recognition sequence within the substrate protein [42]. Caspases are synthesized as inactive zymogens. Procaspsases carry a prodomain at their N-terminus site, followed by a polypeptide from where the large and small subunits of the enzyme will be carved out [44-46] (Fig. 1A). The active caspase is a heterotetramer, a homodimer of two heterodimers [46]. The prodomain is also frequently but not necessarily removed from the procaspase upon activation (Fig. 1A).

In the procaspase family 14 member have been identified, that are play essential roles in apoptosis and inflammation (Fig. 1B). Eleven members of this family have been identified in the human genome: caspase-1 to caspase-10, and caspase-14. Based on their homology in amino acid sequences and their function, caspases are divided into three groups (Fig. 1B): Group I - Inflammatory mediators (procaspase-1, -4, -5, -11, -12, -13, -14). Group II - The initiator, apical or apoptosis activator caspases derives from procaspase-2, -8, -9, -10 and Group III - The effector or executioner caspases (procaspase-3, -6, -7) [47]. While the effector caspases have short prodomains, the initiator caspases possess long prodomains. The death effector domain (DED) is present in the prodomains of procaspase-8 and -10, while the caspase recruitment domain (CARD) can be found in the prodomains of procaspase-1, -2, -4, -5, -9, -11, -12, -13. Via their prodomains initiator procaspases can be recruited and activated by the close proximity model at death inducing signaling complexes through homotypic interactions [48,49].

Much less is known about how caspases are involved in apoptosis-related events like phosphatidylserine (PS) externalization, cellular shrinkage, chromatin condensation apoptotic body formation, etc. The inflammatory caspases appear to be much more specific proteases than those involved in apoptosis [50].

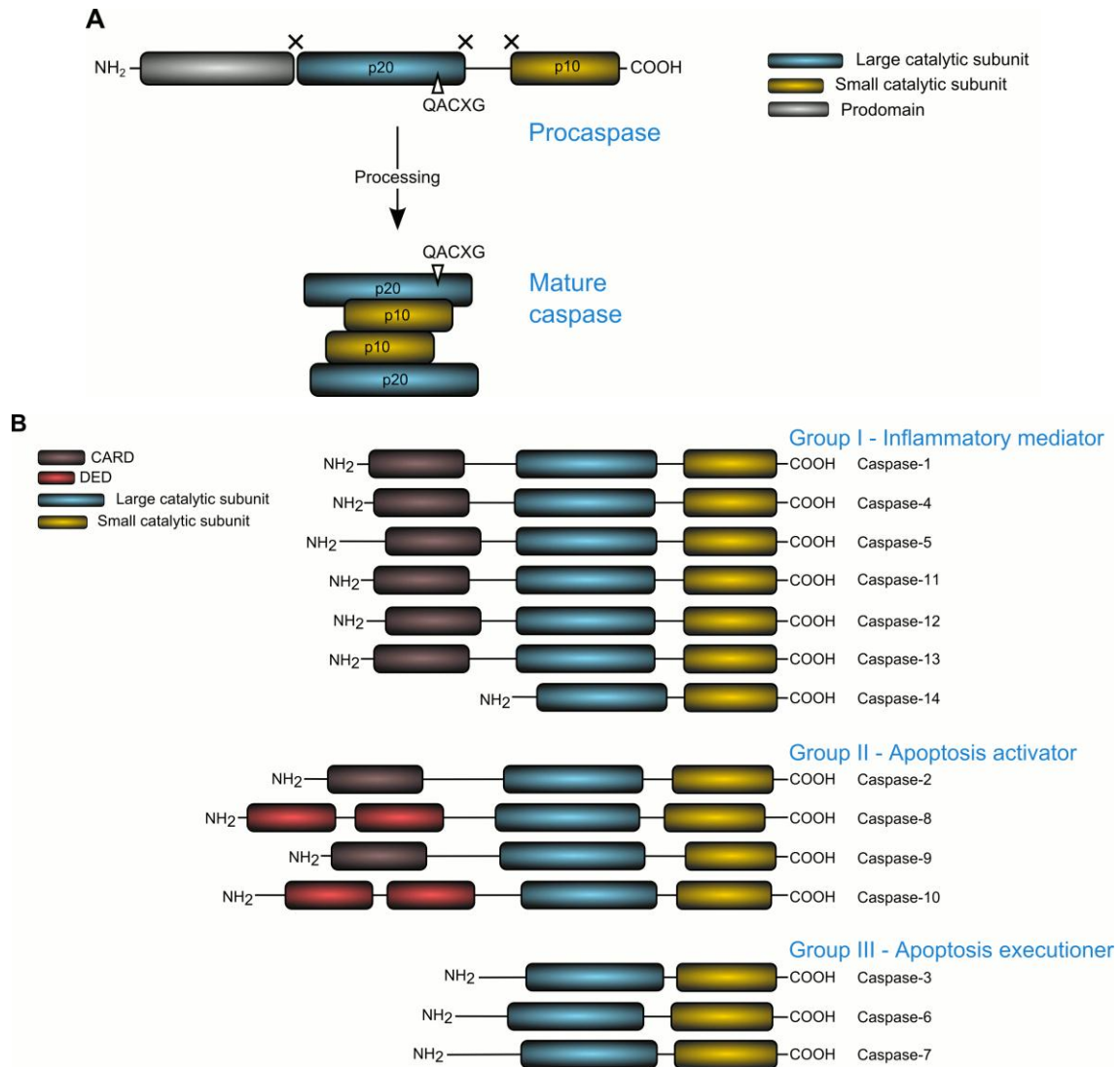


Figure 1. Domain structure and subfamily members of caspase family [48]

(A) Members of the caspase family share some common properties like: aspartate-specific cysteine protease function; have a conservative pentapeptide active site region 'QACXG' (X can be R, Q or D); their precursors are synthesized as zymogens known as pro-caspases. Pro-caspases are capable for autoactivation or also are able to activate other procaspases. The active caspases are heterotetramers, a homodimers of two heterodimers with a large and a small subunit. (B) The caspase family consists of fourteen members and eleven members of this family have been identified in the human genome: caspase-1 to caspase-10, and caspase-14. Based on their homology in amino acid sequences and their function, caspases are divided into three groups: Group I - Inflammatory mediators; Group II - Apoptosis activator caspases; Group III - Executioner caspases. The long prodomain of the activator caspases contains DED is present in the prodomains of procaspase-8 and -10, while the CARD can be found in the prodomains of procaspase -1, -2, -4, -5, -9, -11, -12, -13.

Approximately 400 apoptosis-associated caspase substrates have been predicted and there are likely to be hundreds yet unknown [50]. However, there is still a debate whether caspases are essential for apoptosis or other proteases can replace their function [51-54]. If the caspase activity is experimentally diminished, either through genetic inactivation or by caspase inhibitors, cell death still occurs in response to many proapoptotic triggers and this is taken as evidence that caspases are not required essentially for apoptosis. However, in the majority of these cases the morphological endpoints differ from the common hallmarks of apoptotic cell death [55]. Moreover, caspase inhibition typically converts the phenotype of the dying cell from apoptosis into necrosis [56,57]

1. 2. 2. Secondary necrosis

In multicellular animals, under physiological circumstances apoptosis leads to cell elimination mostly during the embryogenesis and tissue homeostasis. However the apoptotic mode of cell deletion is a “two-cell” process, as it involves other cells that assist the engulfment the apoptotic bodies [58]. Several cell types are able to phagocytose apoptotic cells but mainly macrophages are the prime phagocytes for this task [59]. Engulfment of apoptotic cells is regulated by receptors and bridging molecules on the surface of phagocytic cells that detect molecules, specific for dying cells [60]. Scavengers recognize the dying cells through “eat-me” signals like translocation of PS to the outer leaflet of the lipid bilayer [61]. Besides the “eat-me” signals, “find-me” signals [62,63], as well as absence of “don’t eat-me” signals contribute to the appropriate corpse clearance [64]. When scavenger cells do not operate, the apoptotic pathway progresses until a terminal disintegration of the cells by secondary necrosis [24].

Progression of apoptosis to secondary necrosis can be observed in (i) some physiological situations where apoptotic cells are shed into ducts or into territories topologically outside the organism (like cell death during involution of lactating breast or during autoimmune diseases) [65,66] ii) in case of *mer* gene deficient (phagocyte receptor) knockout mice, which animals have macrophage defects resulting in insufficient clearance of apoptotic cells and as a consequence accumulation of secondary necrotic cells [67]. (iii) extensive secondary necrosis can be observed in

multicellular animals during massive apoptosis that overwhelm the available scavenging capacity [34].

The completion of the apoptotic process in multicellular animals might include an autolytic termination by secondary necrosis, which makes that process self-sufficient leading to self-elimination when scavengers are not available [58]. However the main difference between the two outcomes (i.e. apoptosis and secondary necrosis) is that while apoptosis is non-immunogenic process, secondary necrosis serves to elicit immune response (see more detailed in 2.2.4.).

1. 2. 3. Necrosis

Necrosis or necrotic cell death is morphologically characterized by oncosis, gain in cell volume, swelling of organelles, chromatin clumping, karyolysis, early plasma membrane rupture and subsequent loss of intracellular contents. Historically necrosis was defined in negative fashion: a cell death type without the hallmarks of apoptosis and autophagic vacuolization caused by overwhelming stress. It is known as a harmful process that often associated with pathological cell loss and promotes inflammation.

Indeed, during necrosis, due to the early plasma membrane rupture, necrotic cells can release multiple proinflammatory factors, including heat-shock proteins (such as HSP70, HSP90), histone proteins, high mobility group box proteins (HMGBs) and several other factors (RNA, DNA) which act on different pathogen recognition receptor (PRRs) on immune effector cells to activate inflammatory reactions (see review [68]). These factors function as danger signals, i.e. danger-associated molecular pattern molecules (DAMPs) as they appear in the extracellular space and acts on several immune cells to trigger immune responses.

Necrosis is considered as passive type of cell death which lacks specific biochemical markers, except the presence of early plasma membrane permeabilization. Interestingly, similar inducers can activate the apoptotic program, autophagy or induce necrosis. Just the intensity of the stressors or the duration of the exposure time are different. Physical stressors like irradiation (UV, X-ray, γ), heat or cold, or chemical agents like cytotoxic drugs, lack of nutrients necessary for adenosine triphosphate (ATP) production,

hypoxia, protein accumulation can also trigger different type of cell death included necrosis based on the intensity of the stressor.

Formerly, it was published by others (reviewed in [69]) and also by us [20] that apoptosis can be converted into necrosis. Similarly, the process of autophagy also can be shifted into necrosis via inhibition of the early steps of autophagy [70]. More interestingly we published earlier that necrosis can also be turned into apoptosis [20]. These observations imply that necrosis can also have a programmed mechanism carried out by cascades of activated enzymes. The actual rates of different participating subroutes, the length of induction and the cell type will all influence the final outcome. See below in chapter 2.2.4. and 2.3.3.

1. 2. 4. Necroptosis

A novel, necrotic-like, caspase-independent cell death form has been recently described and termed as necroptosis [12]. Degterev *et al.* demonstrated that stimulation of the extrinsic apoptotic pathway by tumor necrosis factor-alpha (TNF α) or Fas ligand (FASL) under caspase-compromised conditions in certain cell types resulted in a necrotic-like cell death process [12]. This pathway can be hampered by a small molecular weight inhibitor called necrostatin-1 (Nec), which acts by inhibiting the kinase activity of receptor-interacting protein kinase 1 (RIPK1) [71] and by necrosulfonamide (NSA), an inhibitor of mixed lineage kinase domain-like protein (MLKL), substrate of receptor-interacting protein kinase 3 (RIPK3) [72]. As it was published recently one of the targets of MLKL is serine/threonine-protein phosphatase PGAM5, which by its enzymatic activity influences the fusion/fission equilibrium of mitochondria through the regulation of mitochondrial fission factor (DRP1) enzyme activity [73]. Here we use the term necroptosis a type of programmed necrosis which requires the kinase activity of RIPK1 and RIPK3 (receptor-interacting protein kinase 1 and 3) and fulfills under caspase-compromised conditions according to the recommendation of the NCCD [23].

1. 3. Extrinsic cell death pathway and/or survival induction – through TNFR1

1. 3. 1. NF- κ B activation – induction of the survival pathway

The most widely studied pathway leading to necroptosis is triggered by TNF α (see reviews [74,75]), a classical inducer of the extrinsic apoptotic pathway or activator of nuclear factor kappa-B (NF- κ B) survival pathway (Fig. 2). Tumor necrosis factor receptor 1 (TNFR1) upon activation by TNF α undergoes rapid conformational changes. Rearrangement of the intracellular part of TNFR1 provides docking surface for TNF α receptor-associated death domain protein (TRADD) and RIPK1 through their DD. TRADD binding in turn recruits E3 ubiquitin ligase enzymes like the TNFR-associated factor 2 (TRAF2) or the inhibitor of apoptosis protein 1/2 (cIAP1/2), and create the multicomponent membrane-associated structure called complex I [76] (Fig.2).

Polyubiquitylation of RIPK1 via lysine 63 (K63) of ubiquitin attached to the K377 residue of RIPK1 in complex I contributes to the liberation of NF- κ B from its inhibitory complex formed with the inhibitor of κ B (I κ B) protein and leading this way to the activation of the pro-survival pathway [14,77]. During this process, the polyubiquitylated RIPK1 directly recruits the inhibitor of κ B kinase (IKK) protein via the IKK regulatory subunit of NEMO and activates IKK α and β kinases [78]. IKK phosphorylates the NF- κ B inhibitor protein I κ B and targets this protein for degradation by the ubiquitin-proteasome pathway [79]. NF- κ B then liberated and translocated to the nucleus to activate expression of downstream target genes involved in the immune, inflammatory and survival responses [77] (Fig. 2).

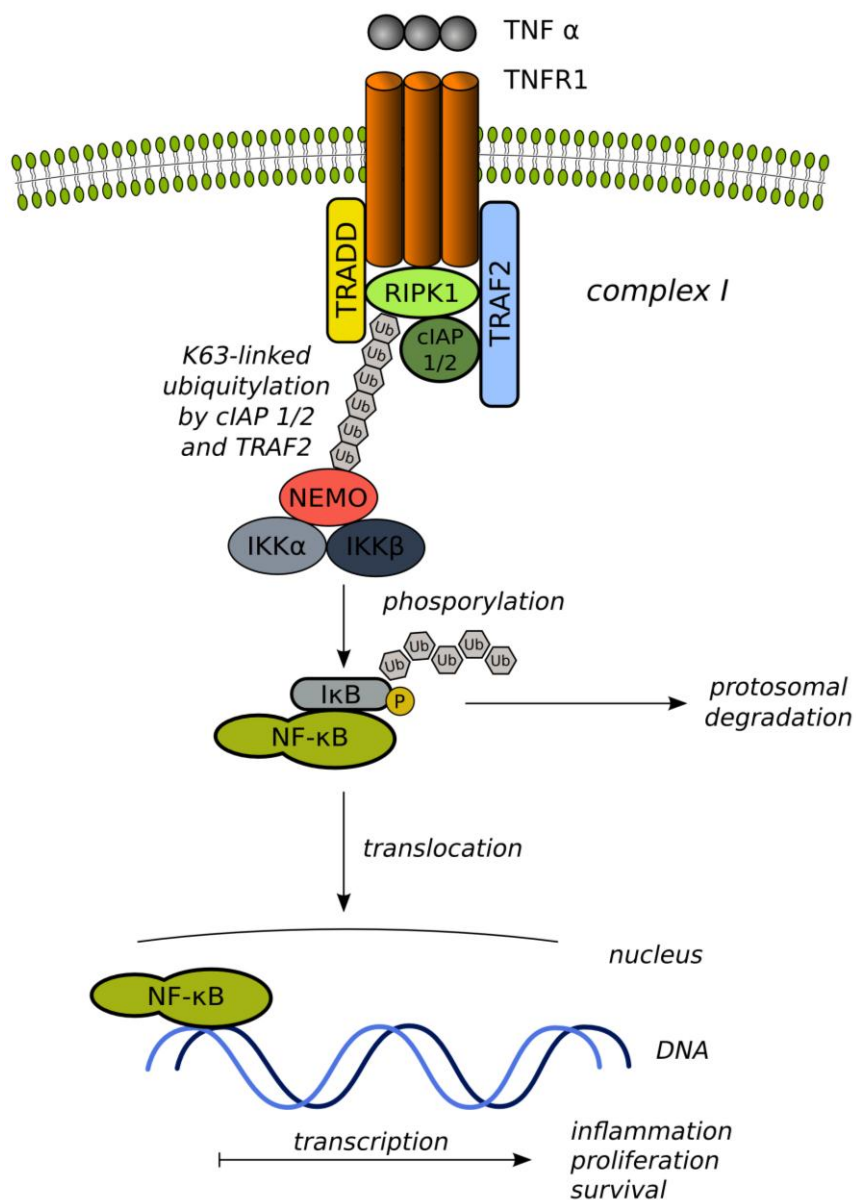


Figure 2. Schematic figure of extrinsic apoptotic signaling pathway induced by TNF α .

TNFR1 upon activation by its ligand (TNF α) trimerises and re-arrange their intracellular part which serves as a platform for the formation of multiprotein signaling complex. TNFR1 signaling complex I is composed of the adapter proteins TRADD, the E3 ligase TRAF2, the death domain-containing RIPK1 and other associated proteins for instance another E3 ligase cIAP1/2. cIAP1/2 and TRAF2 in the complex I ubiquitylate RIPK1 via K63-linked polyubiquitylation. Modified RIPK1 then recruits NEMO, the regulatory subunit of the IKK complex and subsequently activates the IKK α and β . Active IKK complex phosphorylates the I κ B which results in ubiquitylation and dissociation of I κ B from NF- κ B, and eventual degradation of I κ B by the proteasome. Liberated NF- κ B then translocates into the nucleus and activate target genes that are contribute to inflammation, proliferation and cell survival.

1. 3. 2. Apoptosis induction – a route to cell death

As we have seen during the formation of complex I, polyubiquitin chains function not only as protein degradation signal but also provide a platform for the assembly of complex I (Fig. 2). After complex I formation, several other E3 ubiquitin ligases and ubiquitin hydrolases compete to activate or shut down the canonical NF- κ B pathway and reform the polyubiquitin meshwork paving the way to form other macromolecular complexes with different biological functions (Fig. 3). E.g. A20 a dual E3 ligase and hydrolase cleaves off K63-linked polyubiquitin chain from RIPK1 and subsequently marks it for proteasomal degradation through its K48-linked polyubiquitylation [80]. In addition another ubiquitin hydrolase, the ubiquitin carboxyl-terminal hydrolase (CYLD) protein negatively influences the activation of the NF- κ B pathway via removing the K63-linked ubiquitin chain from RIPK1 [13]. The exact details are not known and are targets of intensive research efforts. If the pro-death signal is stronger or lasts longer than the pro-survival signal, the internalized TNFR1 and the deubiquitylated RIPK1 form a new cytoplasmic complex, called complex II (Fig. 3). After dissociation from TNFR1 the DD-s of RIPK1 and TRADD molecules become available to form other complexes with different DD-containing proteins. E.g. Fas-associated death domain protein (FADD) can be adsorbed, leading to subsequent binding of caspase-8 [76]. In the cytosolic complex II the activated caspase-8 then proteolytically cleaves various substrate molecules including RIPK1 and by activating downstream effector caspases the apoptotic cell death is unavoidable (Fig. 3). *In vitro*, in the absence of corpse clearing, apoptosis turns into secondary necrosis.

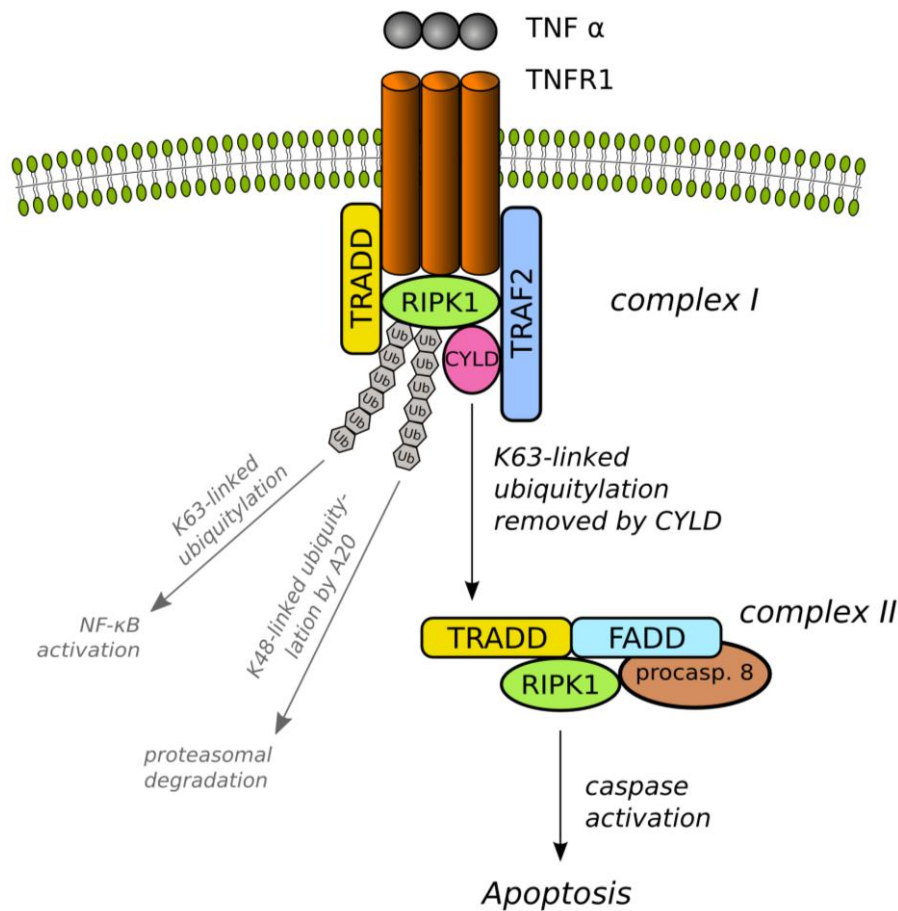


Figure 3. Schematic figure of apoptosis induction via the TNFR1-triggered extrinsic apoptotic signaling pathway.

TNFR1 upon activation by its ligand (TNF α) trimerises and re-arrange their intracellular part which serves as a platform for the formation of multiprotein signaling complex. TNFR1 signaling complex I is composed of the adapter proteins TRADD, the E3 ligase TRAF2, the death domain-containing RIPK1 and other associated proteins for instance another E3 ligase cIAP1/2. cIAP1/2 and TRAF2 in the complex I ubiquitylate RIPK1 via K63-linked polyubiquitylation. In complex I the polyubiquitylated RIPK1 activates the NF- κ B pathway, see detailed in Fig.2. Activation of the NF- κ B pathway is negatively regulated by cIAP inhibitor Smac mimetics and E3 ubiquitin ligases, such as A20 that target TRAF2 and RIPK1 for proteasomal degradation via K48-linked polyubiquitylation. In the meantime the ubiquitin hydrolase CYLD can also remove the K63-linked ubiquitin chain from the RIPK1 similar to A20. Deubiquitylated RIPK1 then serves as a platform to form the cytosolic complex II. Complex II formed with the participation of the deubiquitylated RIPK1, adapter protein FADD and TRADD, and the procaspase-8. In this complex caspase-8 be activated and then proteolytically cleaves various substrate molecules including RIPK1 and by activating downstream effector caspases leads the fulfillment of the apoptotic cell death program.

1. 3. 3. Necroptosis induction

The mechanism how the enzymatic activities of RIP kinases predispose cells to die either by apoptosis or necrosis/necroptosis is intensively studied and explored. Recently the spontaneous formation of a high-molecular-weight complex has been reported by the research groups of Tenev and Feoktistova [81,82]. Core components of this complex, called as Ripoptosome are RIPK1, FADD, and procaspase-8 [81-83] (Fig. 4). Ripoptosome seems to be a death-inducing platform that can direct the cell into apoptosis and necroptosis too. Feoktistova reported that presence of the protease-deficient caspase homolog cellular FLICE-inhibitory protein (cFLIP_L) isoform in the Ripoptosome promotes necroptosis instead of apoptosis [81]. This notion is supported by Chang *et al.* as they published that cFLIP_L can either promote or inhibit apoptosis [84]. In the meantime Tenev reported that presence of cFLIP_L in the Ripoptosome limits the activity of the complex either for apoptosis either for necroptosis induction [82]. Interestingly Ripoptosome assembly can be independent of death receptor activation and mitochondrial pathways, and it is distinct from cytosolic complex II too [82]. Ripoptosome formation requires the kinase activity of RIPK1 and it is negatively regulated by cIAPs [82]. Tenev *et al.* showed that cIAPs and X-linked inhibitor of apoptosis protein (XIAP) directly polyubiquitylate RIPK1 which stimulate the recruitment and activation of various kinases necessary for prosurvival NF- κ B signaling (see chapter 2. 3. 1.) [82]. Additionally cIAPs can also mark RIPK1 for proteasomal degradation by polyubiquitylation [85] (Fig. 4). Not surprisingly IAPs are highly expressed in various tumor cell types and their protein level may have prognostic significance [86]. Consequently depletion of cIAPs and XIAP contributes to the assembly of Ripoptosome and direct the cell to death. During apoptosis, natural IAP antagonists Omi/HtrA2 and Smac/Diablo translocate from the mitochondria to the cytoplasm and through their IAP-binding motif, inactivate IAPs and this way facilitate caspase activation [87]. Based on this fact a novel class of anti-cancer drugs namely Smac mimetics were developed. Smac mimetics facilitate the proteasomal degradation of cIAPs and sensitize various type of tumor cell to death [88].

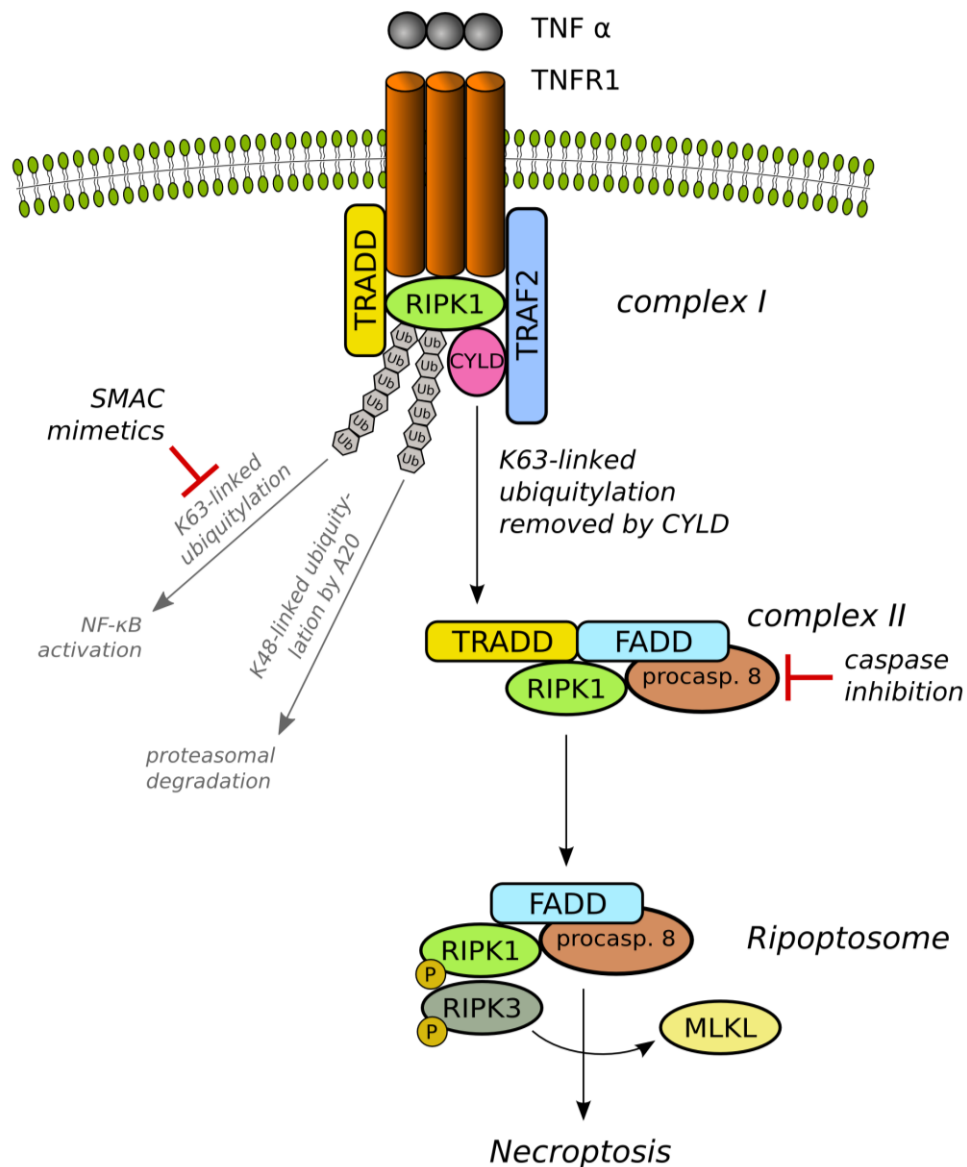


Figure 4. Schematic figure of necroptosis induction via the death receptor TNFR1

In complex I the polyubiquitylated RIPK1 activates the NF- κ B pathway, see detailed in Fig. 2. Deubiquitylated RIPK1 serves as a platform to form the cytosolic complex II with the participation of the adapter protein FADD and TRADD, and the procaspase-8. In the complex II caspase-8 can be activated and trigger apoptosis (see detailed in Fig. 3). In the complex II, if the caspase activation is halted by inhibitor, caspase-8 activation and the subsequent cleavage of RIPK1 are suppressed. Due to arrested caspase activation and the kinase activity of RIPK1, another cytosolic complex, the ripoptosome is established. In the ripoptosome RIPK1 and RIPK3 are phosphorylated and elicit the necroptotic pathway.

RIPK3 contains an N-terminal kinase domain and a C-terminal RIP homotypic interaction motif (RHIM), which mediates its interaction with RIPK1 and therefore can attach to the Ripoptosome [89] (Fig. 4). Under caspase-compromised conditions or in the presence of high level of cFLIP in the Ripoptosome the cleavage of RIPK1 and RIPK3 by caspase-8 is postponed and, as a consequence, kinase activities of RIPK1 and RIPK3 remain active [90]. In 2005, Degterev and colleagues identified a small molecule allosteric inhibitor called Nec which blocks the kinase activity of RIPK1, thereby inhibiting necroptosis but leaving RIPK1-mediated activation of NF- κ B unaffected [12]. The cross-talk between RIPK1 and RIPK3 is not clear yet. Cho *et al.* showed that kinase activity of RIPK3 is responsible for the phosphorylation of RIPK1 that stabilizes their association and initiates pro-necrotic kinase cascade [91] (Fig. 4). Kinase activity of RIPK1 and RIPK3 regulates various mechanisms during necroptosis involving reactive oxygen species (ROS) production, calcium overload, mitochondrial permeability, ATP level of cells and glucose metabolism [14,92].

It was recently published that the adenine nucleotide translocase (ANT), an integral protein of the inner mitochondrial membrane protein which, exchanges mitochondrial ATP with cytosolic adenosine diphosphate (ADP), can be inhibited via RIPK1-dependent way [93]. Inhibition of ANT by RIP1 can be expected to reduce intramitochondrial ADP levels resulting in a reduction of ATP level [93]. On the other hand ANT contributes to the pore formation on the mitochondrial permeability

transition pore complex (PTPC), which is a feature of necroptosis, together with the voltage-dependent anion channel (VDAC) presents on the outer mitochondrial membrane and cyclophilin D (CYPD) localizes in the mitochondrial matrix [94]. Smith and colleagues demonstrated that the CYPD, a core component of the PTPC complex, has to be present in order to observe cardioprotective effect by Nec [95]. This corresponds to results discovering that RIPK1 may alter PTPC formation (see reviews [14,96]).

RIPK3 was published to be involved directly in glucose metabolism related enzyme activation and consequent respiratory burst and ROS generation that characterizes necroptosis [97]. Via allosteric activation of glycogen phosphorylase (PYGL), glutamate–ammonia ligase (GLUL) and glutamate dehydrogenase 1 (GLUD1) RIPK3

contributes to enhance the glycogenolysis, glycolysis and glutaminolysis. Knock down of these enzymes halt the TNF α -induced ROS production and necroptosis under caspase-compromised conditions [97]. In other experimental settings and cell line models non-mitochondrial ROS production by the plasma membrane NADPH oxidase-1 (NOX1) contributes to TNF α -triggered necroptosis [98]. It is possible, that the RIPK1-recruited NOX1-generates ROS, that triggers the subsequent ROS production by the mitochondrial respiratory chain [99].

ROS can react with polyunsaturated fatty acids in cellular membranes and produce reactive aldehydes, which in turn can attack protein and lipid moieties of various membranes, thereby compromising their integrity. Lipid peroxidation mediated destabilization of cellular membranes (including the plasma, lysosomal and ER membranes) results in leakage of proteases or an elevation of cytosolic Ca²⁺ concentrations, two phenomena that participate in necrotic cell death [100].

The further downstream events of necroptosis are less known but intensively studied (see reviews [14,83]). Nowadays, extensive research focuses on the molecular background of necroptosis [81-83,101] and on the identification of necroptosis in physiological [102,103] or pathological [104,105] conditions. Recently MLKL was identified as the target of RIPK3 [72]. MLKL is phosphorylated by RIPK3 and this step seems to be critical for the fulfillment of necroptosis [57,72]. Most recently the mitochondrial protein phosphatase PGAM5 was shown to play role in necroptosis execution [73].

1. 4. Extrinsic cell death and survival induction – through Fas/CD95 and TRAIL receptors

1. 4. 1. Apoptosis and necroptosis induction

In sharp contrast to TNFR1-activated cellular signaling, the binding and activation of tumor necrosis factor-related apoptosis-inducing ligand (TRAIL) and Fas/CD95 receptors through their corresponding cytokine ligands rather promote cell death than the pro-survival of cells. Both TRAIL and FasL-induced apoptosis has crucial role in homeostatic regulation and effector function of the immune system [106,107].

The molecular events involved in TRAIL or FasL-induced apoptosis have been well documented [108]. Upon binding their corresponding ligands Fas/CD95 or TRAIL receptors undergo conformational changes which provides docking surface for FADD, RIPK1, the initiator procaspase-8/-10 and their regulator cFLIP protein (Fig. 5). In this complex, namely death-inducing signaling complex (DISC) the close proximity of procaspase-8 molecules allows the autocatalytic cleavage and formation of active caspase-8 [109]. Activated caspase-8 contributes the induction of apoptosis by initiating a cascade type of activation of downstream effector caspases. Upon receptor internalization the complex translocates from Fas/CD95 or TRAIL receptor and the cytosolic complex II is formed. At this level, based on the RIPK1 kinase activity cell death can be realized via necroptosis or by apoptosis [110] (Fig. 5).

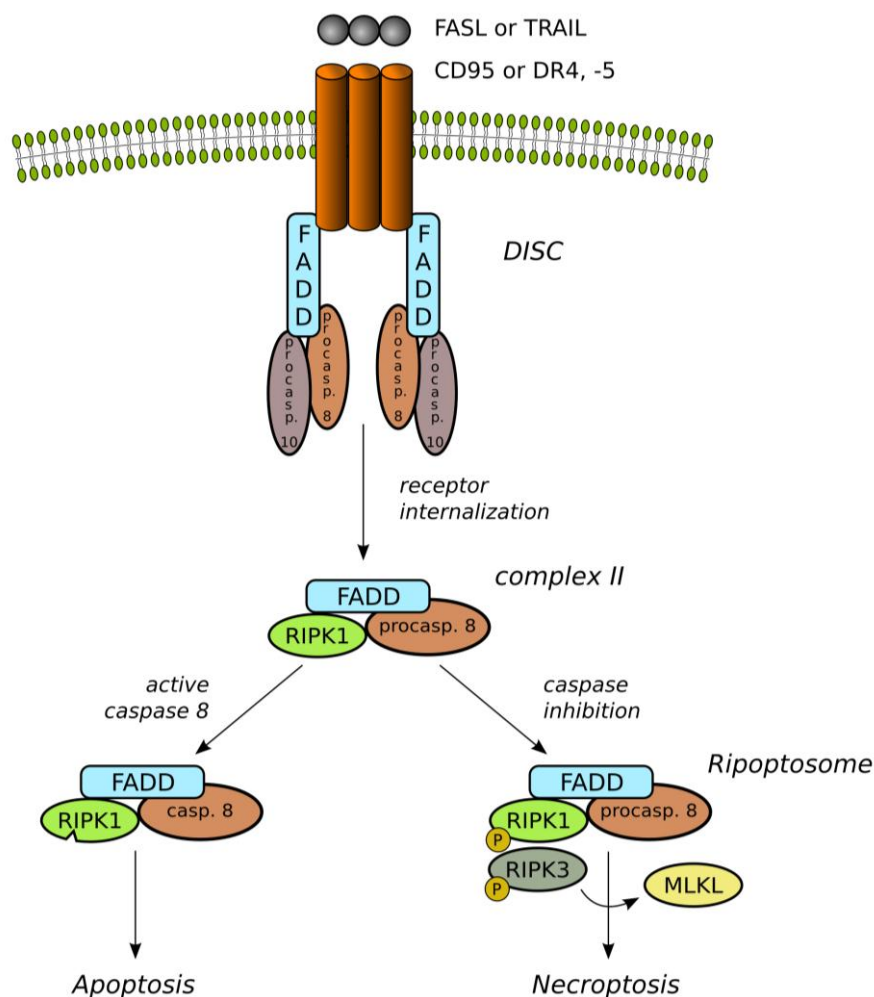


Figure 5. Schematic figure of the extrinsic apoptosis induction via the death receptor DR4/5 and CD95.

In contrast to TNFR1 signaling, the default pathway activated by Fas/CD95 or TRAIL receptors is caspase-8 activation in DISC and induction of apoptosis. Ligation of CD95/FAS or DR4/5 receptor by their ligand FASL and TRAIL respectively cause conformational changes of the death receptors. The re-arrangement of the intracellular parts then serves as a platform for the formation of plasma membrane-associated multiprotein signaling complex called DISC. DISC consists of the death receptor, the adaptor molecule FADD, procaspase-8 and procaspase-10. During the receptor internalization cytosolic complex II is formed together with RIPK1, in which the high local concentration of procaspase-8 is believed to lead to its autoproteolytic cleavage and activation. The active caspase-8 then proteolytically cleaves various substrate molecules including RIPK1 and by activating downstream effector caspases which leads the fulfillment of the apoptotic cell death program. If the caspase activation is halted, the caspase-8 activation and the subsequent cleavage of RIPK1 are suppressed. Due to the kinase activity of RIPK1, another cytosolic complex, the ripoptosome is established. In the ripoptosome RIPK1 and RIPK3 are phosphorylated and elicit the necroptotic pathway.

1. 5. Intrinsic apoptotic pathway

Besides the extrinsic stimuli, initiator procaspases can be activated also by inner death signals like DNA damage, oxidative stress, heat shock, UV radiation, starvation, staurosporine (STS) treatment etc. [111]. The intrinsic apoptotic pathway is characterized by the permeabilization of the mitochondrial outer membrane and as a consequence mitochondrial membrane depolarization, which leads to the cytochrome c and other proteins release from the mitochondrial intermembrane space [112]. In addition to the release of mitochondrial factors the mitochondrial membrane depolarization cause a loss of biochemical homeostasis of the cell: ATP synthesis is inhibited in absence of proton gradient between the intermembrane space and the matrix, and ROS are increasingly generated [113].

This permeabilization is regulated mainly by the B-cell lymphoma 2 (BCL-2) family of proteins which contains both pro- and antiapoptotic proteins [114]. Through their BH3 domains the family members can form hetero- and homodimers. As proposed in their rheostate model, Korsmayer predicted that various stimuli (mentioned above) induce the dimerization of proapoptotic proteins like BCL-2-like protein 4 (BAX), BCL-2 homologous antagonist (BAK) and BCL-2 antagonist of cell death (BAD) which upon their activation are engaged to generate a protein-permeable pore in the mitochondrial outer membrane [115] (Fig. 6). According to the theory the antiapoptotic proteins like BCL-2 and BCL-2-like protein 1 (BCL-X_L) can directly interact with the proapoptotic proteins and consequently inhibit the function of their oligomerization and pore formation [116] (Fig. 6). The mechanism of pore formation is up till now an enigma.

As a consequence of BAX and BAK homo-oligomerized, the formed pore on the outer mitochondrial membrane let leaking out cytochrome c and other mitochondrial proteins (like Smac/Diablo, Omi/HtrA2 and apoptosis-inducing factor (AIF) into the cytosol from the mitochondria intermembrane space [117]. The release of cytochrome c induces the formation of apoptosome which consist of Apaf1, procaspase-9, cytochrome c and ATP or dATP [118] (Fig. 6). In the apoptosome procaspase-9 is activated, which in turn promotes the activation of caspase-3 [119]. Active caspase-3 then leads to the fulfillment of the apoptotic program. This process is further inhibited by XIAP protein, which inhibits the activity of caspase-3, -7, -9 [120]. In parallel Smac/Diablo and

Omi/HtrA2 also released from the mitochondria and interacts with and inactivates the XIAP which therefore forces the caspase activation [121] (Fig. 6).

Another released protein during intrinsic apoptotic pathway is AIF, which has both mitochondrial and nuclear signal sequences and normally located in the mitochondrial intermembrane space. In response to apoptotic stimuli it translocates to the nucleus causing caspase-independent DNA fragmentation and peripheral chromatin condensation, but not oligonucleosomal DNA laddering [122].

It has to be mentioned also that there is an interconnecting link between the extrinsically activated caspase signaling and the mitochondrial pathway via activated caspase-8. BH3 interacting domain death agonist (BID) is cleaved by the active caspase-8 and in its truncated form (tBID) translocates to the mitochondria where it acts similar to other proapoptotic proteins and induce formation of mitochondrial permeabilization pore [123]. With this connection between the extrinsic and intrinsic pathway, cells can multiply and reinforce the extrinsic death signal.

STS a poorly selective wide spectrum inhibitor of protein kinases, is a generally accepted model compound for inducing cell death [124] (Fig. 6). Treatment with STS induces the intrinsic, mitochondrial pathway of apoptosis, activates the BAX protein [125] and promotes its translocation to the mitochondria [126]. Consequently, the outer membrane of the mitochondria becomes permeabilized, allowing the release of proapoptotic proteins such as cytochrome c, Omi/ HtrA2 and AIF [127,128]. Cytochrome c initiates apoptosome formation, activation of caspase-9 and the executioner caspases (-3, -6, -7). Caspases process their selective target proteins, thereby evoking the maturation of the apoptotic morphology [129].

Previously we studied the nature of the switch mechanism between apoptosis and necrosis and investigated the intrinsic apoptotic pathway in STS-treated U937 cells [20]. We [20,130] and others [131] found that STS can provoke necrosis in human cancer cells which was independent of caspase activation. Based on these results we were curious to compare STS-induced necrosis under caspase-compromised conditions and the death ligand-triggered necroptosis in spite of the fact that necroptosis is generally defined as a result of a death receptor-triggered cell death pathway [12].

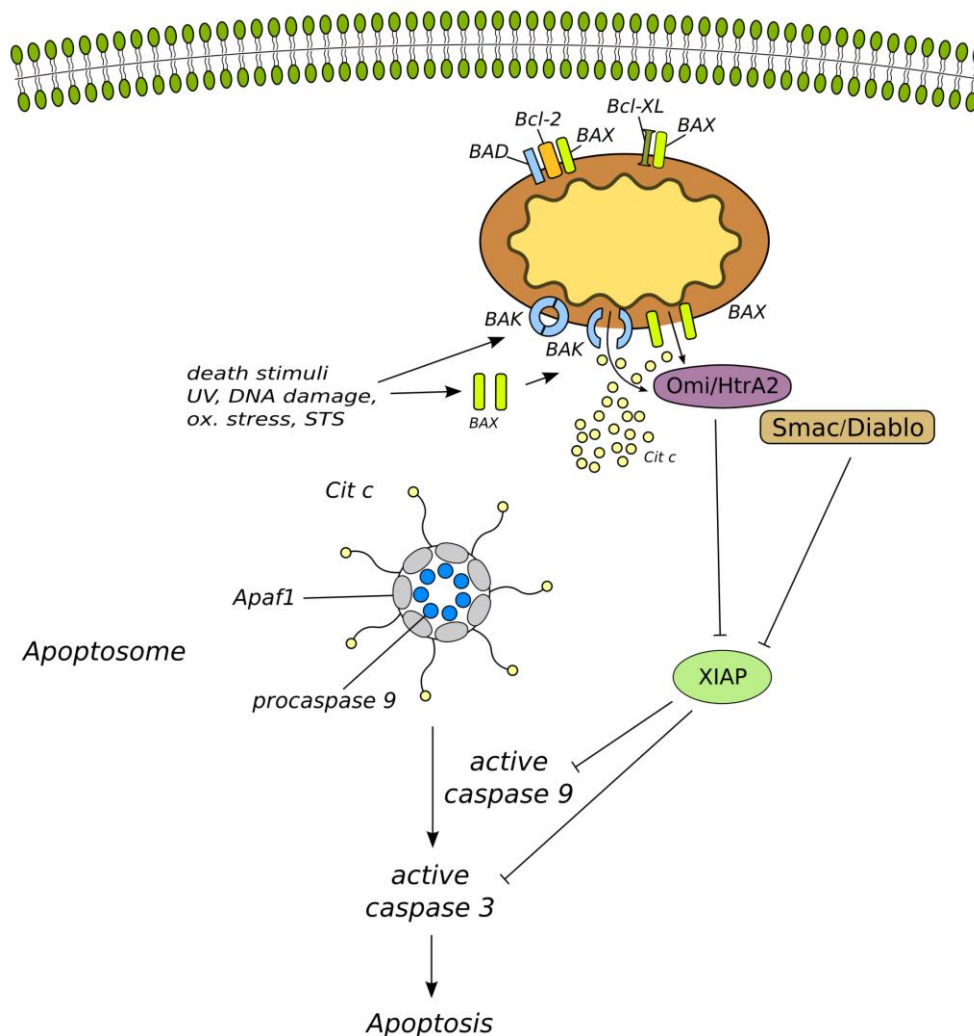


Figure 6. Schematic figure of the intrinsic apoptotic pathway.

The intrinsic apoptotic pathway is initiated by different stimuli mainly represented by like DNA damage, oxidative stress, heat shock, UV radiation etc. The initial events are represented by the activation proapoptotic proteins such as BAX and BAK. These activated cytosolic or mitochondrial membrane-associated proteins are subsequently generate a protein-permeable conduit in the mitochondrial outer membrane. This mitochondrial membrane pore permeable for cytochrome c and other mitochondrial proteins like Smac/Diablo and Omi/HtrA2. The release of cytochrome c contributes to the formation of the so called apoptosome in association with Apaf1 and procaspase-9. In the apoptosome caspase-9 matures and subsequently proteolytically cleaves various substrate molecules, additionally activates the executioner caspase-3 which leads the fulfillment of the apoptotic program. Caspase-3 and -9 activation can be halted by XIAP, however Smac/Diablo and Omi/HtrA2 released from the mitochondria, interact with and inactivate the XIAP, which contributes the fulfillment of the apoptotic pathway. Antiapoptotic BCL-2 proteins negatively influence the mitochondrial membrane pore formation. BCL-2 and BCL-X_L can directly bind and therefore inhibit the function of different pro-apoptotic proteins like BAX and BAD.

1. 6. Further type of programmed necrosis

The cellular events during programmed necrosis are poorly understood. Former studies investigated the role of the lysosomes during necrosis in neurodegenerative diseases. Investigations in both nematodes and mammals confirm the active participation of calpains (calcium-dependent neutral cysteine proteases) and cathepsins (lysosomal aspartyl proteases) in the execution of necrotic cell death [132,133] .

Tavernakis and his colleagues showed that vacuolar H(+)-ATPase, a pump that acidifies lysosomes and other intracellular organelles, is essential for necrotic cell death in *C. elegans* [134]. Cytoplasmic pH drops in dying cells and the intracellular acidification requires the vacuolar H(+)-ATPase, whereas alkalination of endosomal and lysosomal compartments by weak bases protects against necrosis [134].

Calpain proteases are normally requires calcium for activation, whereas cathepsins have a highly acidic pH optimum for full activity [135]. Studies in primates confirmed calpain-mediated disruption of the lysosomal membrane after ischemia [136].

These observations led to the formulation of the “calpain–cathepsin hypothesis,” by Yamashima, which uncover the way of calcium-mediated activation of calpains results in the rupture of lysosomes and leakage of cathepsins that eventually degrade the cell [137].

Formerly we showed that the selective cathepsin-B inhibitor CA-074-OMe (CA) rescued the caspase-independent necrotic and the caspase-dependent apoptotic form of cell death in promyelocytic leukemia (HL60) cells treated by STS [130]. However the applied CA concentration was higher with orders of magnitudes (10 μ M) compared to the concentrations (10 nM) required for the inhibition of cathepsin B protease activity [130]. This result point out that that a non-cathepsin B, currently unknown target of CA can be important in necroptotic cell death.

1. 6. 1. PARP-AIF-mediated programmed necrotic pathway

Besides the death receptor-triggered necroptosis, an other intensively investigated type of programmed necrosis is mediated by poly(ADP-ribose) polymerase (PARP) activation called parthanatos. In response to DNA damage, or exposure of DNA

alkylating agent, like MNNG, the DNA repair PARP-1 protein is activated. Following PARP-1 activation the consequent poly(ADP-ribose) (PAR) accumulation and/or the ATP/Nicotinamide adenine dinucleotide (NAD) pool depletion leads to the release of the AIF from the mitochondrial intermembrane space. Cytosolic AIF then enter to the nucleus and perform caspase-independent, large-scale DNA fragmentation. The mechanism requires calpains but not cathepsins or caspases [138].

AIF-deficient harlequin mutant mice are protected against several necrotic stimuli, including ischaemia–reperfusion injury of the brain [139]. Similarly, pharmacological and genetic inhibition of PARP-1 has consistent cytoprotective effects [140].

Further question is the demarcation of different types of programmed necrosis. Surprisingly, it was published that c-Jun N-terminal kinase (JNK), especially JNK1, but not the other members of mitogen-activated protein kinase family, is required for PARP-1-induced mitochondrial dysfunction, AIF translocation, and subsequent cell death [141]. Moreover this group showed that knockouts of RIPK1 and TRAF2 of mouse embryonic fibroblast (MEF) cells caused a resistance to PARP-1-induced cell death [141].

It means that it is possible that RIPK1 plays role as central molecule of the execution and fulfillment of programmed necrosis, and different types of programmed necrosis are emerged at the level of RIPK1.

1. 7. Physiological and pathological aspects of programmed necrotic cell death

1. 7. 1. Physiological aspects

Apoptosis was described as a regulated cell death form which participates in normal tissue homeostasis during the embryogenesis of different organisms, especially in the genetic control of cell elimination during development of *C. elegans*. This early description of apoptosis may had influenced researchers to focus on the programmed cell death and at the same time neglect the other modalities of cell death already known [1,2].

At the same time some arguments suggested that apoptosis is not the solely form of cell death responsible for unwanted cell elimination during embryogenesis or physiological tissue renewal. For example interdigital membrane elimination provides a representative evidence for the role of apoptosis in tissue sculpting during embryonic development. Contrarily to this Yoshida *et al.* reported that a delayed but apparently normal interdigital membrane removal exists in *apaf1*^{-/-} mutant mice embryos, where the apoptosome can not be formed [142].

In other cases, necrotic-like cell demise was observed under conditions where the apoptotic machinery was blocked. For instance, in *BAK*^{-/-} and *BAX*^{-/-} double mutant mice various defects of apoptotic process were observed: the syndactyly phenotype, excess cells accumulation in the central nervous system and finally most embryos died at or just before birth. Some of the littermates of the dying *BAK*^{-/-} and *BAX*^{-/-} mice could survive and lived until adulthood [143,144]. Similarly, in the protist *Dictyostelium discoideum* stalk cells showed autophagy-like cell death when treated with differentiation-inducing factor (DIF-1) under condition of starvation. Inactivation of autophagy-related 1 homolog gene (*atg1*) shifted the process to a classical necrotic-like cell death [145]. Based on this results necrosis is a candidate process as a back-up mechanism which can substitute the defective apoptotic pathway. On the other hand, necrosis was also observed during normal mammalian tissue homeostasis as a programmed event. For instance, the human large intestine crypts contain necrotic colonocytes [15], or in human growth plate during late pubertal fusing, chondrocytes showed necrotic phenotype [16]. Moreover, disappearance of linker cells in *C. elegans* at a well defined time point during development is essential for future fertility. Abraham *et al.* reported that caspases and other apoptosis-associated gene products do not participate in the loss of linker cells and indeed, the dying linker cells showed necrotic morphology [12,17,18]. For more details see reviews of Kroemer, McCall and Thompson [35,37,146]. However, the above-mentioned reports are based mostly on morphological observations, therefore further investigations would be preferable, to evaluate the type of cell death.

This context raises the question of evolutionary appearance and potential hierarchy of different cell death modalities. Golstein and Kroemer discussed the redundancy of cell

death mechanisms and hypothesized that an evolutionary ancestral cell death – resembling necrosis – was overridden by evolutionary younger, more elaborate processes, likely autophagy and apoptosis. Cell death types emerging later in evolution may turn into the major dominant form of cell death while masking the ancestral one, but which can resurface as back-up mechanism when the other cell death pathways are blocked [69].

It is tempting to speculate how necroptosis is related to other cell death modalities and what physiological role it might have. It is conceivable that necroptosis compared to necrosis is a relatively new evolutionary mechanism, an alternative programmed cell death that serves as a back-up process when apoptosis is abrogated. Hitomi *et al.* in a murine genome-wide siRNA screen for genes involved in zVAD.fmk (zVAD) induced necroptosis in L929 cell line have found that some genes required for necroptosis had increased expression in macrophages, dendritic cells and natural killer (NK) cells, while another gene cluster was upregulated in B and T lymphocytes connecting necroptosis to the immunological processes [13]. Another interaction between the necroptotic process and the immune-response has also been shown [91]. Viruses are known to frequently express antiapoptotic proteins to control the lifespan of their (Vertebrate) host in order to avoid cell death until their replication cycle is finished [147]. As Cho *et al.* have shown that in vaccinia virus infected T cell, when the apoptotic process was abrogated by caspase inhibitors, the RIP3K directed necroptotic cell death became dominant [91]. Accordingly, necroptosis might be an evolutionary response of host cells to avoid the pathogen-induced apoptosis inhibition. Moreover, further benefit of the necrotic cell demise in a multicellular organism might be that necrosis/necroptosis leads to a proinflammatory response. The release of the intracellular content can provoke the immune response, which serves not only as a warning system, indicating the internal or external hazardous conditions, but also initiating the immune response. This observation raises the clinical benefits of necroptosis induction in antiviral therapy.

To study the phylogenetics of necroptosis, the Inparanoid, a comprehensive database of eukaryotic orthologs was used and results have shown that RIP1 and RIP3 kinases are characteristic to Vertebrates. However, a human RIP1 kinase homolog can be found in an annelid worm (*Capitella sp.*), and proteins similar to the human RIP3 kinase is

present in the chordate *Ciona savignyi*, the amoeba *Dictyostelium discoideum*, and in the smallest free-living unicellular eukaryote, *Ostreococcus tauri* [148]. The connection of those these proteins to cell death pathways are unknown and their homology might be explained by prior exon shuffling process. Based on the above mentioned facts necroptosis may be an important stage in the arms race where vertebrates are constantly participating, evolving and learning how to cope with viral invasion.

The above mentioned evidences namely that certain cell types can initiate their own death via necrosis, apparently refute the bias that the term necrosis solely refers to accidental, uncontrolled event.

1. 7. 2. Pathological aspects

Necrosis has for a very long time been described as a direct cause or as a simultaneously occurring phenomenon of cell death in many cases of human diseases, such as neurodegenerative diseases with necrotic outcome [26], pancreatic adiponecrosis [27], trauma [28], ischemia-reperfusion in myocardial infarction [29], in cerebral infarction [30], bacterial infection [31,32] or in tumor malignancies [33,34]. However, having the preconception that this type of cell death is random and unregulated, researchers have regarded its harmful effects inevitable. Undoubtedly, overwhelming stress induces necrosis that can not be impeded, it is still worthwhile to examine if there is an activated signaling pathway behind the focal necrotic morphology that at least partially can be hampered. For instance following ischemia in the brain [149] and myocardial tissues [150] an increase in inflammatory cytokines production, including TNF α might occur and resulting in accompanying necroptosis.

Using Nec Degtrev *et al.* investigated the *in vivo* participation of necroptosis in a murine model of ischemia-reperfusion [12]. As it was reported the area of the infarct and the neurological score due to middle cerebral artery occlusion was significantly reduced by intracerebroventricular administration of 7-Cl-Nec in a wide therapeutic window [12]. On the other hand, Whalen *et al.* hypothesized that Nec would reduce histopathological appearance of cell death and improve functional outcome in a controlled cortical impact (CCI) model of traumatic brain injury (TBI) in mice [151]. As they reported, short- and long-term Nec treatment attenuated the plasmamembrane

damage and moderated the motor and cognitive deficits compared to untreated littermates after CCI. In similar experiments Nec failed to adjust the outcomes the caspase-mediated apoptosis which also operates in TBI [28]. Moreover, pretreatment with Nec significantly reduced the microglial activation and neutrophil influx 48 hours after CCI. These results underline the possible involvement of necroptosis in acute brain injury and underscore the applicability of Nec in reducing posttraumatic lesion and inflammation [151].

Additional contribution of necroptosis in neurodegenerative diseases was published recently. N-Methyl-D-aspartate (NMDA) exposure through ionotropic glutamate receptor induced excitotoxicity in primary rat cortical cell cultures could be partially reduced by Nec, shown by cell viability assays and lactate dehydrogenase (LDH) leakage. It was also reported by the authors that the elevated intracellular Ca^{++} level may contribute to NMDA induced necroptosis [152].

Oxidative glutamate toxicity, also called as oxytosis is characterized by glutathione (GSH) depletion, increased reactive oxygen species production, calcium influx and caspase-independence that could be prevented by antioxidants [153]. Further study showed that Nec could attenuate non-receptor mediated glutamate toxicity in a mouse hippocampal cell line (HT22) and not only blocked the nuclear translocation of AIF but an increase in the GSH level and a decrease of ROS production were also observed [154]. The inhibition of AIF transport to the nucleus by Nec raises the question whether is there a connection between RIP1 kinase activity and AIF transport, thus PAR plays any role in the necroptotic process. These questions need further experimental answers [155].

In another study Kim *et al.* characterized arachidonic acid- (AA) induced cell death in oligodendrocyte precursors [156]. The authors previously demonstrated that AA-induced cell death was lipoxygenase- (LOX) dependent and mediated by elevated ROS level and JNK activation, but it was independent from caspase activation. Authors confirmed that AA-induced cytotoxicity was markedly prevented by an antioxidant butylated hydroxyanisole (BHA), or a 12-LOX specific inhibitor or by Nec. Moreover, Nec markedly prevented cell death via blocking ROS production and JNK activation. The authors hypothesized that deubiquitylation of RIP1 kinase is upregulated by

oxidative stress contributing to necroptosis. This is supported by the notion that Nec also blocked oxidative cell death that had been induced by glutathione-depleting agents. This and previously mentioned findings underline the possibility of the receptor-independent role of RIP1 kinase in oxidative stress.

Peroxynitrite formed from nitric oxide (NO) and superoxide are among the most damaging nitrosative agents. In rat pulmonary endothelial cells the superoxide formed as a by-product of mitochondrial respiration in sufficient amount to generate peroxynitrite in the presence of NO. Peroxynitrite inhibited mitochondrial complex I via S-nitrosation of NDUF8 (a protein presents in complex I), which limited electron entry into the mitochondrial electron transport chain and led to endothelial dysfunction. NO-induced necrotic cell death could be prevented by overexpression of superoxide dismutase (MnSOD) or inhibition of RIP1 kinase by Nec. The level of RIP3 kinase was elevated by NO treatment and was colocalized to mitochondria. These results further support the role of RIP1 and RIP3 kinase in receptor independent NO-induced necroptosis [157].

Smith and colleagues tested the protective effect of Nec on animal cardiomyocyte cell lines and in different *in vivo* murine models in case of heart and brain ischemia reperfusion injury [158]. They concluded that Nec could reduce the infarct size and was protective against ischemia reperfusion injury in the myocardium. In their subsequent paper they demonstrated that the CYPD, a core component of MOMP, has to be present in order to observe cardioprotective effect by Nec [95]. In wild-type mice Nec efficiently reduced infarct size *in vivo* when administered intravenously during reperfusion but it failed to produce a similar effect in CYPD^{-/-} mice due to its resistance for MOMP formation ability [95]. This corresponds to results discovering that RIPK1 may alter MOMP formation [93].

It was recently shown that cell death induced by sitosterol, a plant sterol, differs from the cholesterol induced cell death modality in isolated murine macrophages [159].

Cholesterol triggers a caspase-, acyl-CoA:cholesterol acyltransferase- (ACAT), C/EBP homologous protein- (CHOP) and JNK-dependent apoptosis via endoplasmic reticulum stress. In contrast, sitosterol, which differs from cholesterol in a single ethyl group, initiates a caspase-independent, p38-dependent process which could be

completely blocked by Nec and moderately by autophagy inhibitors. The authors hypothesized that in sitosterolemia the accumulating sitosterol may lead to accelerated macrophage death resembling necroptosis, coupled with inefficient phagocytic clearance. This contributes to a faster progression of plaque necrosis, disruption and thrombo-occlusive vascular events which are common symptoms in sitosterolemia [159].

A potential anticancer drug shikonin, a naphthoquinone isolated from *Lithospermum erythrorhizon* was found to induce necroptosis in MCF-7 adenocarcinoma and HEK293 embryonic kidney cells. Nec effectively inhibited the shikonin-induced loss of plasmamembrane integrity, mitochondrial depolarization, elevation of ROS level, and formation of autophagoc vacuoles. Interestingly, the shikonin triggered necroptosis showed faster kinetics compared to the TNF α -induced one reported by Degterev *et al.* This phenomenon can be explained by direct activation of necroptosis in case of shikonin, compared to the effect of TNF α which induces first apoptotic cell death and which later turns into necroptosis in presence of caspase inhibitor [160].

The induction of cell death is a double edged sword. While in the case of neurological disorders prevention of cell death is in the focus of therapeutically approaches, in case of cancer cells the elimination of excess cell growth is in the frontline. Deregulated apoptosis is a hallmark of cancer [161]. A decrease in the sensitivity to apoptosis induction is an important stage of carcinogenesis, elevated level of antiapoptotic proteins (BCL-2, BCL-X_L, cFLIP, IAPs, heat shock proteins) or reduced expression or mutations of proapoptotic proteins (P53, Apaf1, BAX, BAD, caspases, death ligands, death receptors) provide the means for that [161]. Therefore it became an attractive option in theory to trigger different cell death pathway to kill tumor cells. Several apoptosis inducer are successfully applied in the anticancer therapy [162,163]. However acquired drug resistance due to high ABC transporter expression in tumors is the result of poor outcome in clinical practice. Therefore finding necroptosis-inducing drugs which are not targets of multi-drug resistant ATP binding cassette (MDR-ABC) transporters would have high clinical relevance.

Necroptosis as being a back-up mechanism of apoptosis may represent a new perspective in anticancer therapy. Recently published data showed that in glucocorticoid

resistant acute lymphoblastic leukemia (ALL) cells can be resensitized by obatolax – antagonist of BCL-2 family – via autophagy dependent necroptotic cell death [105]. Thus, activation of autophagy is required to induce necroptosis. Involvement of RIP1 kinase, CYLD and autophagy-related proteins indicate a direct link between the necroptotic and autophagocytic network [105].

It was shown that in acute myeloid leukemia (AML) a granulocyte-macrophage colony stimulating factor (GM-CSF)-fused diphtheria toxin construct initiates simultaneously apoptosis and necroptosis [104]. Cell death induced by diphtheria toxin alone in three AML cell lines were similar to the cycloheximide-triggered apoptosis which was moderately inhibited by zVAD or Nec. These results indicate the role of RIP1 kinase in diphtheria toxin-induced cell death and may signify the contribution of a freshly synthesized protein in necroptosis.

As it was discussed above, necroptosis, as an alternative form of programmed necrosis might be an alternative form of cell death under physiological and pathological conditions activated by various stimuli. Growing body of evidences provide a more and more detailed picture from the underlying molecular mechanisms of the cell death process, however up till now, many questions remain unresolved.

2. Objectives

Previously we studied the nature of the switch mechanism between apoptosis and necrosis and investigated the intrinsic apoptotic pathway in STS-treated U937 cells [20]. STS is a generally accepted inducer of intrinsic apoptotic pathway and it is a wide spectrum inhibitor of protein kinases [164]. STS initiates apoptosis by enhancing mitochondrial permeability transition [128,165]. In absence of clearing mechanism, apoptotic cell death process is followed by secondary necrosis, an uncontrolled disruption of the plasma membrane. Earlier, we [20,130] and others [131] found that STS could provoke necrosis in caspase-compromised cancer cells. We were interested to examine the role of necroptosis in the same necrotic process, in spite of the fact that necroptosis is generally defined as a result of a death receptor-triggered cell death pathway [12].

We aimed to characterize the STS-induced necrosis in U937 cell line. We were curious about the role of RIPK1, MLKL, PARP-1 and the effect of lysosomal enzyme inhibitor CA in STS-triggered necrosis to differentiate secondary necrosis and necroptosis [130]. We also focused on the TRAIL-induced necroptotic type of cell death that might has high clinical relevance because of the known ability of TRAIL cytokine to induce apoptosis in a variety of human cancer cell lines while leaving most of normal cells unaffected [166]. We concluded that both TRAIL and STS can induce at least partially necroptosis which can be completely hampered by CA but not by the PARP inhibitor PJ-34.

3. Methods

3. 1. Materials

Staurosporine (STS), PARP inhibitor (PJ-34), geldanamycin (GA), 3-methyladenine (MA), RNase A, propidium iodide (PI), DiOC₆(3), acridine orange (AO), Hoechst 33258 and cell culture products were purchased from Sigma-Aldrich (St. Louis, MO, USA). hr-TRAIL (114-281 aa) (TRAIL) was prepared as described earlier [167]. z-Val-DL-Asp-fluoromethylketone (zVD) and CA-074-OMe (CA) were purchased from Bachem (Bubendorf, Switzerland). Necrostatin-1 (Nec) was obtained from Calbiochem (Darmstadt, Germany). Antibody against PARP-1 was ordered from Cell Signaling Technology, (Danvers, MA), (#9542), against RIPK1 from Becton Dickinson (Budapest, Hungary), (610458) and against GAPDH from Santa Cruz (Heidelberg, Germany, (D-6) sc-166545). Necrosulfonamide (NSA) was a kindly gift of Professor Xiaodong Wang (Beijing, China).

3. 2. Cell culture

U937 promonocytic cell line was purchased from ATCC. Cells were cultured in RPMI 1640 medium, supplemented with 10 % heat inactivated fetal bovine serum, 2 mM L-glutamine and 100 µg/mL penicillin and 100 units/ml streptomycin at 37 °C in a 5% CO₂ containing, humidified incubator. Cells were regularly tested for the presence of certain human CD antigens: CD45 (+); CD33 (+); CD13 (+); CD34 (-); CD14 (-); CD4 (-). Fluorochrome-labeled antibodies were purchased from Becton-Dickinson (Franklin Lakes, NJ USA). For treatments, cells were distributed into 48-well suspension plates (Greiner), 0.5 mL into each well at a cell density of 3 x 10⁵ cells/mL or 5 x 10⁵ cells/mL, 60 minutes before drug treatment. Then zVD (10 µM) was added with or without together other drugs as described above started 1 hr (Nec, CA, NSA, PJ) or 4 hrs (GA) before STS (1 µM) or TRAIL (50 ng/mL) addition. Duration of drug treatments varied between 4-24 hours.

3. 3. Detection of the cell death-associated functional changes by flow cytometry

Data collection was carried out using FACScan flow cytometer (Becton Dickinson) see hereinafter, and analysis of the results was performed by WINLIST software (VERITY Software House, Topsham, USA). The following standard light filters were applied to fluorescence channels: FL1: 530/30 nm; FL2: 585/42 nm; FL3: 650LP. Analysis was performed on the amplitude (height, H) of the fluorescence signal in log scale. A doublet discrimination panel was set on FL2 channel for the detection of FL2A (area) and FL2W (width) of the fluorescence signals are shown in linear scale.

3. 3. 1. Assay of PI uptake of native cells representing the damage of plasma membrane

An increase in the permeability of the cell membrane is a characteristic signal for the early phase of necrosis and can be detected using flow cytometry. Treated or non-treated cells were stained directly by adding 0.5 mL PBS containing 5 mM glucose and 10 µg/mL PI to each well, and incubated for a further 15 minutes at 37 °C in the CO₂ incubator. Necrotic (PI positive) cells usually lost light scatter intensity therefore they mixed up with debris in the [FSC, SSC] two-dimensional parameter diagram. For gating necrotic cells out of debris we applied [FSC, FL3H] diagram where necrotic cells contained high amount of DNA could be separated from debris containing significantly lower DNA content. Gated cells were analyzed on FL2H log scale histograms, where the population with low fluorescence intensity represents the PI negative population, while the population displaying high fluorescence represents the membrane ruptured PI positive cells (Fig. 7). Data were presented as percentage of cells. In certain experiments, samples were co-labeled with DiOC₆(3) or Annexin V-FITC together with PI labelling and used for analysis PI uptake.

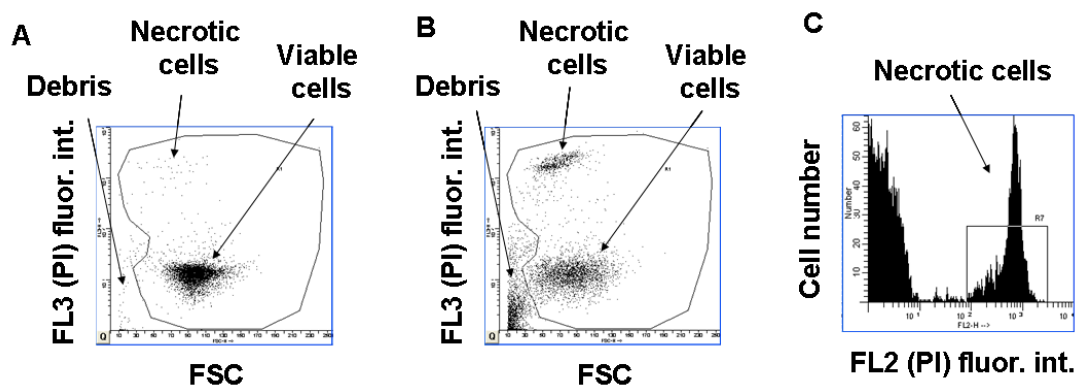
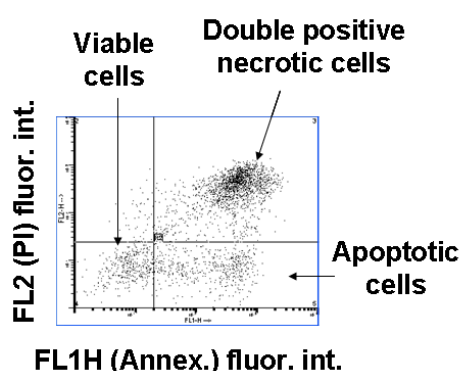


Figure 7. Assay of PI uptake representing the damage of plasma membrane.

For gating necrotic cells out of debris we applied [FSC, FL3H] diagram. U937 cells were treated with (A) solvent or (B) STS (1 μ M) for 20 hrs. Gated STS-treated cells were analyzed on (C) FL2H log scale histograms.

3. 3. 2. Characterization of PS distribution in the plasma membrane by flow cytometric analysis of Annexin V-FITC and PI double-labeled cells

The assay was performed according to the suggestions of the vendor (Alexis Biochemicals, Lausen, Switzerland). Briefly, cells in suspension cultures were stained with an equal volume of PBS, containing 5 mM glucose and 10 μ g/mL PI, directly in the tissue culture wells for 10 minutes at 37 $^{\circ}$ C. After centrifugation (300 \times g/ 2 min), cells were suspended in 400 μ L binding buffer (10 mM HEPES, 140 mM NaCl, 2.5 mM CaCl₂) and stained with 5 μ L AnnexinV-FITC for 10 minutes in dark. Thereafter an additional 400 μ L of binding buffer, containing 1 μ g/mL PI was add to the samples and FACS analysis was carried out immediately. The [FSC, FL3H] diagram was applied for gating and the gated cells were analyzed in [FL1H, FL2H] log scale two dimensional diagram (Fig. 8). Auto-fluorescence of the cells was positioned in first decade, and compensation for FITC fluorescence in the FL2 channel was applied. Data were

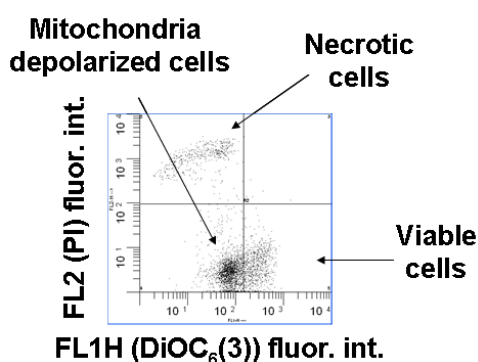


presented as percentage of cells in the marked regions of the diagram.

Figure 8. Characterization of PS distribution in the plasma membrane by flow cytometric analysis of Annexin V-FITC and PI double-labeled cells.

3. 3. 3. Changes of mitochondrial transmembrane potential were characterized by the DiOC₆(3) uptake method

Samples were prepared for the measurements according to Darzynkiewicz and Bender [168], with minor modifications. Pre-treated cells were stained with an equal volume of PBS containing 5 mM glucose, 10 nM DiOC₆(3) and 10 µg/mL PI directly in the wells and incubated further for 15 minutes at 37 °C and analyzed without further washing

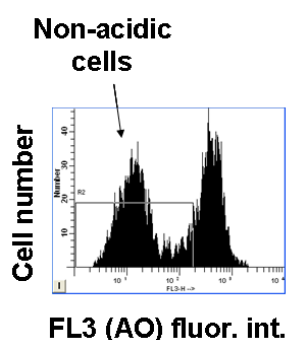


steps by FACS. Fluorescent signals of the cells were gated in [FSC, FL3H] diagram, analyzed on [FL1H, FL2H] log scale two dimensional diagram (Fig. 9). The data were presented as fluorescence intensity of the whole gated cell population. High $\Delta\Psi$, but PI negative cells were considered as functioning mitochondria-containing, surviving population of cells.

Figure 9. Characterization of changes of mitochondrial transmembrane potential by flow cytometric analysis of DiOC₆(3) and PI double-labeled cells.

3. 3. 4. Functioning lysosomal compartments are characterized by the red fluorescence of acridine orange emitted in the acidic environment of lysosomes

Treated cells were stained with an equal volume of PBS containing 5 mM glucose and 5 µg/mL AO directly in the wells and incubated for a further 15 minutes at 37 °C. The

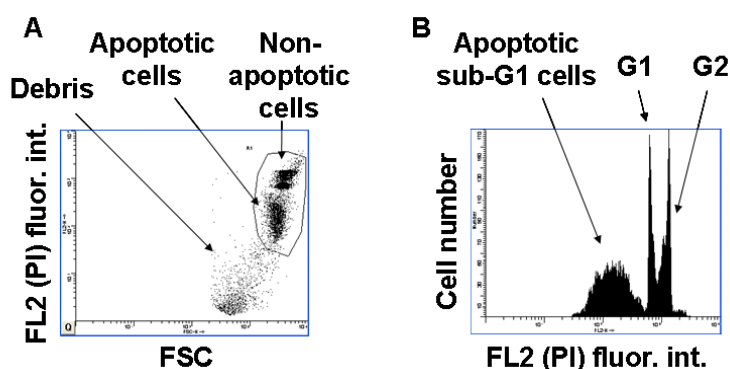


pelleted cells (300 x g/ 2 minutes) were resuspended in 1 mL of 5 mM glucose containing PBS and analyzed by FACS immediately. Cells were gated in [FL1H, FL3H] diagram for discriminating cells with high DNA content from debris with low amount of DNA. The gated populations were analyzed on FL3H log scale histograms and the data were presented as fluorescence intensity of the whole population (Fig. 10).

Figure 10. Assay of AO uptake representing the acidic environment of lysosomes.

3. 3. 5. Determination of oligonucleosomal DNA fragmentation by the measurement of sub-G1 population of cells

Apoptosis was characterized by measuring the sub-G1 pool of cells as an indication of DNA fragmentation. Samples were prepared according to Gong *et al.* [169]. Briefly, treated cells were pelleted (300 x g/ 2 min) and the cells were suspended in 1 mL 70% ethanol (-20 °C), and were fixed at room temperature for a half an hour. The ethanol-fixed cells were sedimented again and their broken, oligonucleosomal sized DNA content were extracted by treating the cells with 750 µL of extraction buffer containing 200 mM Na₂HPO₄/citric acid (pH=7.8) buffer supplemented with 10 µg/mL RNase A, for 15 minutes. The DNA remaining inside the permeabilized cells were stained with 5 µg/mL of PI for at least 10 minutes before FACS analysis. Cells were gated in [FSC,



FL2H] diagram for discriminating debris and analyzed on FL2H log scale histogram as percentage of cells in the marked, sub-G1 region (Fig. 11).

Figure 11. Determination of oligonucleosomal DNA fragmentation by the measurement of sub-G1 population of cells.

For gating cells out of debris we applied [FSC, FL2H] diagram. U937 cells were treated with (A) STS (1 µM) for 8 hrs. Gated cells were analyzed on (C) FL2H log scale histograms.

3. 3. 6. Representation of side scatter change and DNA fragmentation

Cells were fixed, stained with PI and gated according to the sub-G1 technique. The gated populations were analyzed on the (SSC, FL2H) diagrams marked regions as (SSCnorm, DNA_{low}) for apoptotic cells, (SSC_{low}, DNA_{norm}) for necrotic cells and (SSC_{low}, DNA_{low}) for cells with a mixed, atypical phenotype and percentage of cells in this regions were presented (Fig. 12).

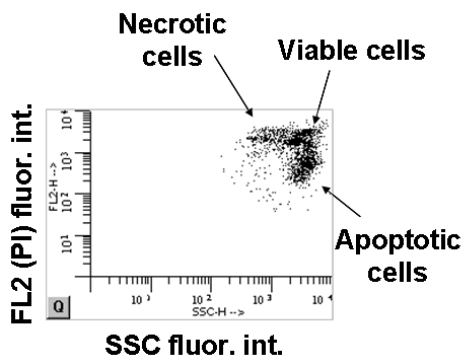


Figure 12. Representation of side scatter change and DNA fragmentation.

3. 4. Agarose gel electrophoresis

DNA fragmentation was analyzed as described earlier [170]. Briefly, U937 cells (one million cells per sample) were treated for 20 hrs as indicated at the legends of figures. Then cells were collected, washed with PBS and resuspended in 300 μ l of a solution, containing 10 mM Tris-HCl, pH 7.5, 1 mM EDTA, 0.15 M NaCl, 1% SDS supplemented with 0.2 mg/ml of proteinase K and incubated overnight at 37 °C. Samples were phenol-chloroform extracted once and their DNA content were precipitated in ethanol, pelleted and redissolved in 50 μ l of TE buffer containing 0.2 mg/mL DNase free RNase A and incubated for an hour at 37°C. DNA was electrophoresed in 1.5% agarose gel in TBA buffer, stained with ethidium bromide (EtBr) and DNA was detected under UV light.

3. 5. Light microscopic studies

Cytospin preparations (10^5 cells) were fixed in methanol, stained with hematoxylin-eosin, were dehydrated with subsequent extractions with ethanol, acetone and xilol. The morphological changes of apoptosis were studied by light microscopy at 400x magnification. Cells were categorized according to the recommendations of Kroemer *et al.* [171] as follows: stage I apoptotic cells have moderately condensed nuclei (including smooth nuclei too); stage II apoptotic cells have full blown nuclear condensation (pyknosis) and formation of nuclear apoptotic bodies (karyorrhexis). Necrosis was characterized by cell swelling, blurred plasma membrane, chromatin clumping and dissolution of chromatin matter (karyolysis). Ghost cells with washed out cytoplasmic contents were identified as being in the late necrotic stage.

3. 6. Fluorescent microscopic studies

Treated U937 cells were pelleted (300 x g / 3 min) and were stained with 2 μ M Hoechst dye (332581) in 1 mL 5 mM glucose containing PBS to distinguish between apoptotic and necrotic cells. After an incubation for 30 minutes at 37 °C, cells were pelleted (300 x g / 3 minutes) again and resuspended in 10 μ L of 5 mM glucose and 10 μ M PI containing PBS and were immediately photographed under a fluorescence microscope (Nikon Eclipse E 400, Japan) at 400x magnification using a SPOT Jr Camera. Excitation wavelength of 330-380 nm was applied for Hoechst dye and 450-490 nm for PI. Apoptotic cells were identified on the basis of morphologic changes in their nuclear assembly by observing chromatin condensation and fragment staining by the Hoechst dye. Secondary necrotic cell were identified based on positive staining with PI and apoptotic nuclear morphology with Hoechst dye. In each case at least four microscopic fields were photographed randomly. The experiments were repeated at least twice.

3. 7. Western blot representation of PARP-1 and RIPK1 cleavage

Western blot analysis of the proteolytic degradation of PARP-1 and RIPK1 was carried as published [172]. U937 cells were treated as indicated at the legends of figures.. After treatment cells were collected, washed with PBS and resuspended in 50 μ l of Laemmli sample buffer. After boiling the samples their 20 μ l aliquots were electrophoresed in a 10% SDS-PAGE gel and blotted onto nitrocellulose. After blocking membranes with 3% milk in PBS overnight, specific antibodies against PARP-1 (#9542, Cell Signaling Technology) or RIPK1 (BD 610458) were added, incubated for 3 hours and membranes were washed exhaustively with 1% milk containing PBS (25 ml of each washing step) and with PBS twice. Blots were incubated with HPO labeled second antibodies for two hours, washed as described above. Proteins were visualized by ECL. After immunodetection of RIPK1 protein levels in cells, blots were stripped and reprobed with an anti GAPDH antibody (Santa Cruz, (D-6) sc-166545). The intensities of GAPDH bands served as loading controls.

3. 8. DEVD-ase activity assay

Aliquots of cells (5×10^5 cells/mL) incubated for different durations of time with drugs were withdrawn centrifuged and washed with PBS twice ($300 \times g$ / 2 minutes) and finally were suspended in 100 μ l of caspase buffer (50 mM HEPES (pH=7.4), 100 mM NaCl, 0.1% (w/v) CHAPS, 10% (w/v) sucrose and 10 mM DTT. After transferring samples into wells of 96-well plates, Triton X-100 (final concentration of 0.2 %) were added, and cell lysis was completed by repeated up and down pipetting of the cells. Caspase substrate z-DEVD-AMC (20 μ M) was admixed, and fluorescence intensities of the liberated 7-amino-4-methylcoumarin (AMC) were recorded for 15 minutes in Fluoroskan Ascent fluorescence plate reader (Thermo Fisher Scientific, Waltman MA, USA). Excitation wavelength was 380 nm and emission was measured at 445 nm. Protease activity was expressed as the slope of the AMC fluorescence curves.

3. 9. Statistics

Statistical analysis and significance of differences in comparable values were calculated by applying Student's t-probe (two tailed, two sample unequal variance) and the indicated significance of differences in the graphs are: $P < 0.05$ (*); $P < 0.01$ (**); $P < 0.001$ (***). In the legends of the figures “n” indicates the number of the independent experiments.

4. Results

4. 1. TRAIL induces necroptosis in U937 cell line in the presence of a caspase inhibitor

To build a reliable model system, first, we tested the classical death ligand-induced necroptosis with TRAIL cytokine. TRAIL is known to induce apoptosis in a wide variety of tumor cells [173,174] and necroptosis in Jurkat cells [175]. We selected U937 monocytic cell line which was shown to undergo necroptosis induced by TNF α in the presence of a caspase inhibitor [12].

We found U937 cells sensitive to TRAIL cytokine treatment. Light microscopic studies of hematoxylin-eosin stained samples confirmed that TRAIL treatment generated apoptotic nuclear DNA condensation (Fig. 13A) together with nucleosomal DNA fragmentation revealed by flow cytometric sub-G1 assay method (Fig. 13B). These changes resulted in apoptotic PARP-1 fragmentation (Fig. 13C) due to caspase-3 activation (Fig. 13D). Finally, signs of secondary necrosis occurred when cells turn permeable for propidium iodide (PI) (Fig. 13E, F).

When cells were pre-treated with the pan-caspase inhibitor z-VD.fmk (zVD) one hour before TRAIL treatment, the executioner caspase activation was prevented (Fig. 13D), therefore PARP-1 processing was inhibited (Fig. 13C). Apoptotic type oligonucleosomal DNA fragmentation diminished, however, the high molecular weight fragmentation of DNA appeared resembling necrosis [176,177] (Fig. 13B) and DNA condensation was evaded (Fig. 13A). Instead of apoptotic morphology, dying cells were swelling and showing a “ghost-like” morphology resembling necrosis (Fig. 13A). Plasma membrane rupture detected and quantified by PI uptake revealed that the number of PI positive cells in caspase inhibitor-sensitized U937 cells upon TRAIL treatment were increasing compared to cells treated with TRAIL alone (Fig. 13E, F). In the presence of RIPK1 inhibitor Nec (10 μ M), PI uptake was reduced only marginally in caspase-competent (secondary necrotic) cells, while it was completely reduced in caspase-compromised cells after TRAIL treatment (Fig. 13E, F).

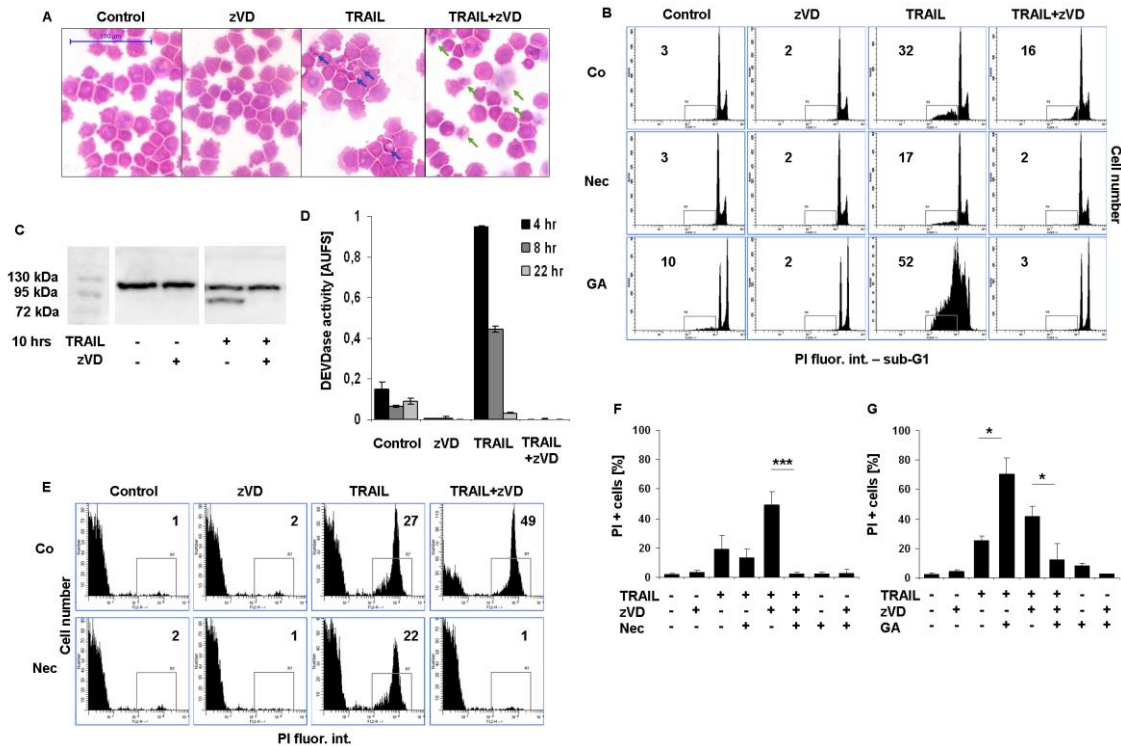


Figure 13. TRAIL induces necroptosis in the presence of caspase inhibitor.

TRAIL-induced cell death in U937 cells. Cells were treated as indicated for 20 hrs. (A) Cytospins were stained with hematoxylin-eosin. Blue arrows show the apoptotic, green ones the necrotic cells (400x) (representative of $n=2$). Scale bar on the first subfigure applies to all the figures in the panel. (B) Representative histograms of PI stained, ethanol-fixed U937 cells, detected by flow cytometry (sub-G1 technique). Inserted values indicate the percentage of cells in the marked regions. U937 cells were exposed to 50 ng/mL TRAIL in the presence or absence of zVD (5 μ M) and Nec (10 μ M) or GA (1 μ M) for 20 hrs ($n=3$). (C) Western blot analysis of fragmented PARP-1 protein. Full length PARP-1 is 116 kDa, cleaved PARP-1 fragment is 89 kDa (representative of $n=2$). (D) TRAIL-induced caspase activity in U937 cells. U937 cells were exposed to 50 ng/mL TRAIL in the presence or absence of zVD (5 μ M) for the indicated period of time. The ordinate shows the slope of the measured DEVDase activity curves of a representative experiment carried out in triplicates. (E) FACS analysis of treated cells. Plasma membrane integrity was analyzed after PI staining of cells. Inserted values on histograms show the percentage of the marked population (representative of $n=7$). (F-G) Nec and GA protected U937 cells from TRAIL+zVD-induced necroptosis. U937 cells were exposed to 50 ng/mL TRAIL in the presence or absence of zVD (5 μ M) and (F) Nec (10 μ M) or (G) GA (1 μ M) for 20 hrs. PI stained cells were analyzed for membrane permeability. Percentages of PI positive cells were determined ($n=7$ for Nec and $n=4$ for GA). Values are mean \pm SD. *, $P < 0.05$, **, $P < 0.01$ and ***, $P < 0.001$ calculated by Student's t-probe.

To further confirm the role of RIPK1 activity in TRAIL-induced necroptotic or secondary necrotic cell death processes we studied the effect of geldanamycin (GA, 1 μ M). GA, an inhibitor of the heat shock protein 90 kDa (HSP90) [178], was known to downregulate the protein level of RIPK1 [179] and therefore was expected to halt necroptosis. Indeed, GA pre-treatment (4 hrs) significantly reduced the extent of TRAIL-induced necroptosis detected by PI uptake (Fig. 13G). At the same time GA enhanced the extent of TRAIL-induced apoptosis (Fig. 13B), possibly via downregulating the NF- κ B signaling pathway [180]. Furthermore GA caused cell cycle inhibition in G2 phase (Fig. 13B). Secondary necrosis (Fig. 13G) was also increased in line with the elevation of DNA fragmentation (Fig. 13B).

These results indicate that in the presence of caspase inhibitor, TRAIL-exposed U937 cells undergo necroptosis instead of apoptosis, moreover TRAIL-triggered necroptosis can be suspended both by Nec and GA.

4. 2. STS induces primary necrosis in the presence of a caspase inhibitor

Earlier, we found that STS alone induced caspase 3-like DEVDase activity after 2 hrs, accompanied by small scale DNA fragmentation detected by flow cytometry as sub-G1 cells (Fig. 14A). Plasma membrane damage occurred only several hours later, possibly as a sign of secondary necrosis (PI+ cells) detected by PI staining. In the presence of caspase inhibitor zVAD, STS did not evoke DEVDase activity for up to 15 hrs (Fig. 14B). Meanwhile, we could detect a gradually increasing number of sub-G1 cells and PI-positive cells after 5 hrs of treatment (Fig. 14B).

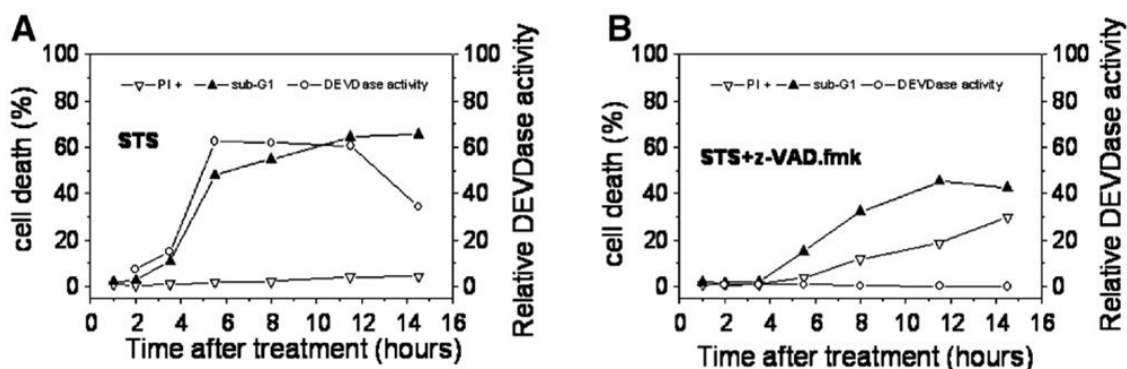


Figure 14. STS induced apoptotic and necrotic cell death forms in caspase-compromised cells after shorter (5 hrs) and prolonged (15 hrs) treatment.

U937 cells were exposed to STS (1 μ M) in the presence or absence of zVAD (50 μ M) or DMSO as vehicle. Time kinetics of cell death (sub-G1: cells with fragmented DNA; PI+: cells with plasma membrane damage) and effector caspase (DEVDase) activity (detected with z-DEVD.amc fluorogenic substrate) in samples exposed to (A) STS or (B) STS+zVAD (n=2).

To further study the STS-evoked necrosis we applied the caspase inhibitor zVD-fmk. (zVD) instead of zVAD, due to its better solubility and selectivity for caspases, and its lower IC₅₀ value than zVAD [181]. We found that in the presence of zVD, STS triggered mainly plasma membrane damage after shorter incubation time (8-12 hrs) (Fig. 15A, B) meanwhile we could detect both sub-G1 and PI-positive population after prolonged treatment (20 hrs) (Fig. 15C, D). While the STS-evoked DEVDase activity was completely halted by zVD, that is correspond with the effect of zVAD (Fig. 15E). The discrepancy with the sub-G1 population can be attributed to the different properties of the two applied caspase inhibitor.

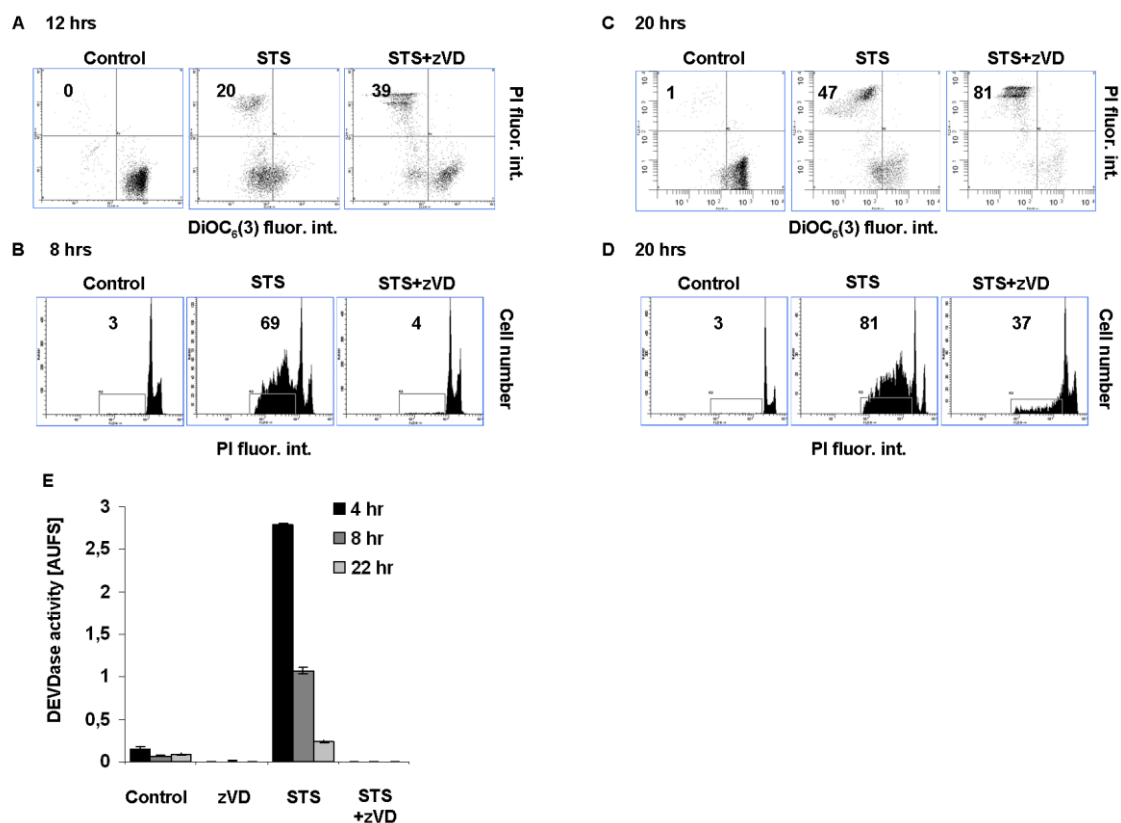


Figure 15. STS induced necrotic cell death form in caspase-compromised cells after shorter (8 hrs) incubation time.

U937 cells were exposed to STS (1 μ M) in the presence or absence of zVD (5 μ M) for 8, 12 or 20 hrs. (A, C) The mitochondrial transmembrane potential and plasma membrane integrity is shown in representative dot plots of DiOC₆(3) and PI stained, unfixed cells. The values indicate the percentage of cells in the marked regions (n=5 and n=13 respectively). (B, D) Representative histograms of PI stained, ethanol-fixed U937 cells detected by flow cytometry (sub-G1 technique). The numbers indicate the percentage of cells in the marked regions (n=5 and n=13 respectively). (E) STS-induced caspase (DEVDase) activity in U937 cells. The ordinate shows the slope of the measured DEVDase activity curves of a representative experiment carried out in triplicates.

Next we tested the effect of the RIPK1 inhibitor under caspase-compromised conditions. Nec concentration dependently abrogated the necrosis confirmed by the reduced ratio of PI positive cells (Fig. 16A). At the applied concentration Nec (10 μ M) and GA (1 μ M) arrested the necrosis after 8, 12 hrs of incubation time confirmed by flow cytometry and by fluorescent microscopic studies using Hoechst dye and PI double staining technique (Fig. 16B, C, D, E). Inhibition of Hsp90 activity by GA is known to

induce cell cycle arrest in G1 as well as in G2/M phases [182]. We assessed and found that the two functions of GA (modulation of the cell death and the cell cycle) were similarly affected by GA dilutions, confirming that both functions are related to inhibition of Hsp90.

After prolonged (20 hrs) treatment the STS and zVD-triggered plasma membrane rupture was diminished only partially by Nec (Fig. 16F, G, H) or GA (Fig. 16I).

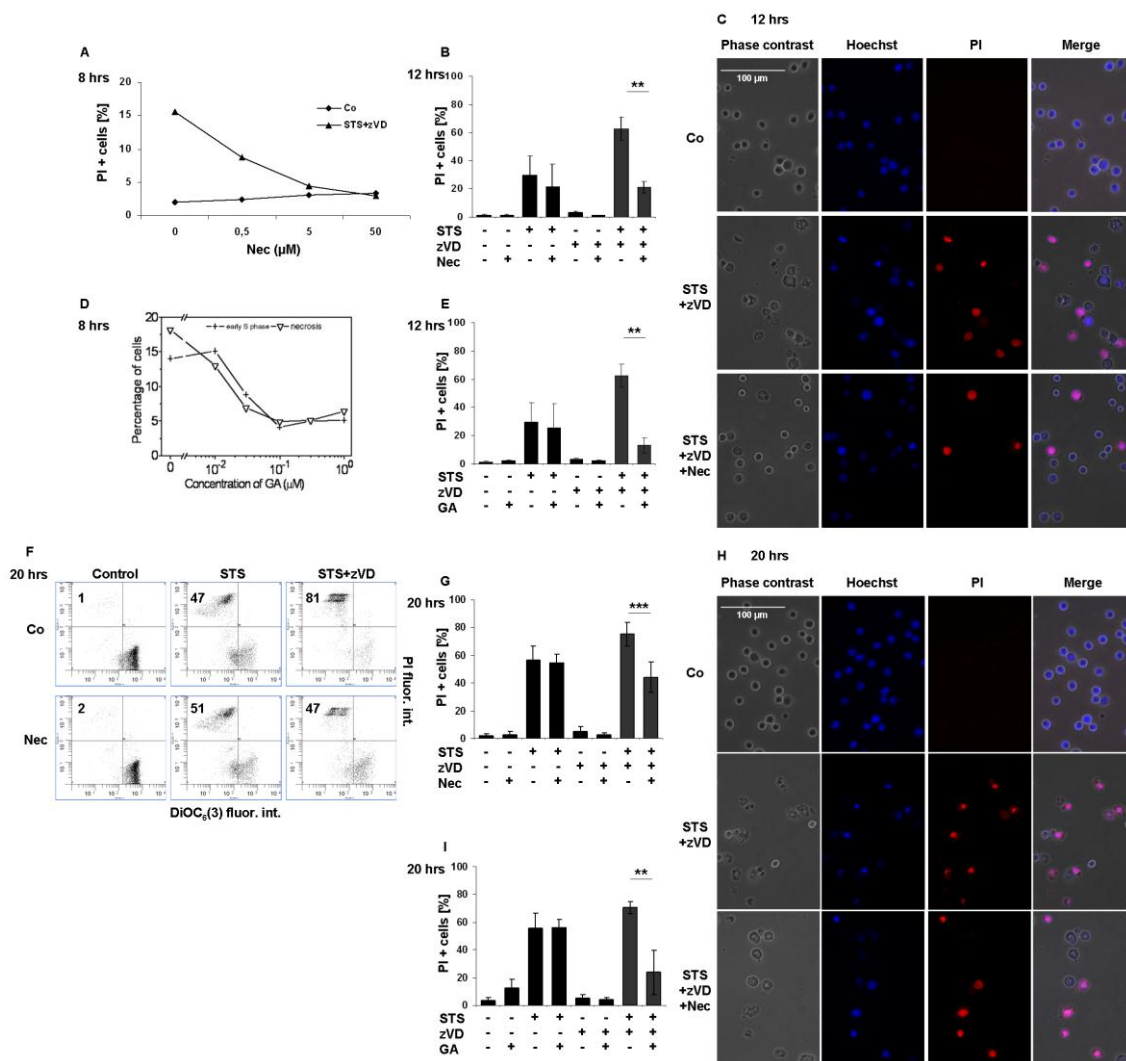


Figure 16. STS induces primary necrosis in the presence of caspase inhibitor.

(A) Nec reduced the STS-induced necroptosis in a concentration-dependent manner after 8 hrs incubation time – representative experiment. Cells were exposed to STS (1 µM) and varying concentrations of Nec (0-50 µM) in the presence of zVD (5 µM) for 8 hrs. Percentage of PI positive cells was determined. (B-C) Nec (10 µM) significantly inhibited the STS-triggered necrois. Cells were exposed to STS (1 µM) in the presence or absence of zVD (5 µM) and Nec (10 µM) for 12 hrs. Percentage of PI positive cells was determined by flow cytometry (B) (n=13) and by Hoechst/PI double staining technique (C) (representative of n=2), (400x). Scale bar on the first subfigure applies to all the figures in the panel. (D-E) GA (1 µM) also significantly inhibited the STS-triggered necrosis. (D) Cells were pre-treated with varying concentration of GA, then exposed to STS+zVAD (50 µM). Cell cycle distribution was determined by flow cytometry and absolute percentage of cells of early S phase was plotted (–x–). Percentage of PI positive cells was determined by flow cytometry as necrosis (open down triangles). Representative of two independent experiments is presented. (E) Cells were exposed to STS (1 µM) in the presence or absence of zVD (5 µM) for 12 hrs.

Percentage of PI positive cells was determined by flow cytometry (n=4). (F) Nec (10 μ M) arrested the STS-induced (1 μ M) necroptosis in the presence of zVD (5 μ M) after 20 hrs incubation. The mitochondrial transmembrane potential and plasma membrane integrity is shown in representative dot plots of DiOC₆(3) and PI stained, unfixed cells. The values indicate the percentage of cells in the marked regions (n=13). (G-I) Nec (10 μ M) (G, H) and GA (1 μ M) (I) partially inhibited the STS-triggered necroptosis. Cells were exposed to STS (1 μ M) in the presence or absence of zVD (5 μ M) for 20 hrs. Percentage of PI positive cells was determined by flow cytometric analysis (G, I) (n=13 for Nec and n=4 for GA), and by Hoechst/PI double staining technique (H) (n=2). Scale bar on the first subfigure applies to all the figures in the panel. Values are mean \pm SD. *, P < 0.05, **, P < 0.01 and ***, P < 0.001 calculated by Student's t-probe.

Furthermore, Nec unaffected the caspase-mediated DNA fragmentation and condensation either after shorter (8, 12 hrs) (Fig. 17A, B) or after longer incubation time (20 hrs) (Fig. 17C, D). GA affected only moderately the DNA fragmentation (Fig. 17E) delaying the appearance of the shorter nucleosomal fragments (Fig. 17F). The STS-induced secondary necrosis, the final stage of cell death, was affected by neither Nec (Fig. 16G) nor GA (Fig. 16I)

Concerning the apoptotic parameters, zVD prevented the executioner caspase activation (Fig. 15E). It is worth to mention that the proportion of sub-G1 cells was reduced both by Nec (Fig. 17D) and by GA (Fig. 17E) after prolonged STS treatment in the presence of zVD. However this observed reduction correlated well with the reduced ratio of the number of PI positive cells (Fig. 16G, I). This correlation denotes that the number of sub-G1 DNA containing cells observed when STS and the caspase inhibitor were applied, is unequal with the classical fragmented DNA containing population obtained after STS treatment alone. STS and zVD-exposed samples showed high molecular weight DNA fragments confirmed by agarose gel electrophoresis, accompanied with low molecular weight DNA fragments that are primarily smear-like, opposite to apoptotic DNA fragmentation and typical to necrosis [176,177]. STS treatment resulted in nucleosomal DNA ladder fragmentation trimmed by postmortem DNase activity (Fig. 17F).

These results indicate that STS-induced apoptosis in U937 cells ensued by secondary necrosis, while under caspase-compromised conditions STS induced primary necrosis that is partially inhibitable by Nec and GA, two drugs affecting RIPK1 activity.

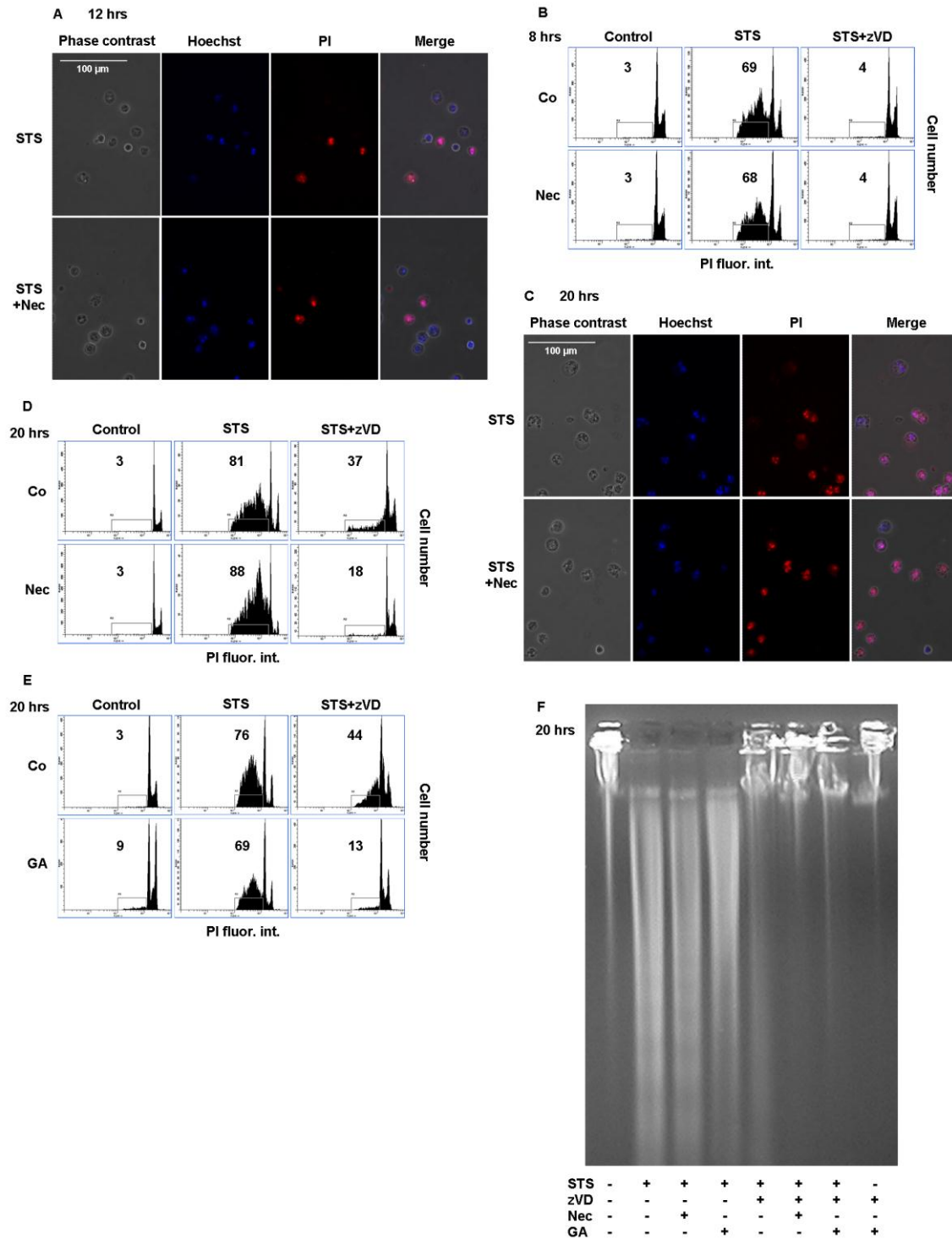


Figure 17. STS induces necrotic type DNA degradation in the presence of caspase inhibitor.

STS induced DNA fragmentation. U937 cells were treated with STS (1 μ M) in the presence of zVD (5 μ M) for 12 hrs or 20 hrs. Cells were pre-treated with Nec (10 μ M, 1 hr) or GA (1 μ M, 4 hrs). (A, C) Representative fluorescent microscopic images (400x) of Hoechst/PI double stained U937 cells (n=2). Scale bar on the first subfigure applies to all the figures in the panel. (B, D, E) Representative histograms of PI stained,

ethanol-fixed cells detected by flow cytometry (sub-G1 technique) (n=3 for 8 hrs with Nec, n=13 for 20 hrs with Nec and n=4 for 20 hrs with GA treatments). Inserted values indicate the percentage of cells in the marked regions. (F) STS-induced DNA fragmentation. Agarose gel electrophoresis was performed to detect the DNA ladder formation. Cells were treated as indicated for 20 hrs (representative of n=2).

4. 3. STS and TRAIL induce RIPK1 and MLKL-dependent necroptosis

To confirm the role of RIPK1 in the STS-induced necroptosis, we tested the proteolytic degradation of RIPK1 in U937 cell line by Western blot analysis. STS-triggered caspase activation led to RIPK1 processing (Fig. 18A). Full length RIPK1 (~75 kDa) was proteolytically cleaved by caspase-8 during STS-induced apoptosis [183]. The cleavage at the carboxyl group of aspartic acid residue (at amino acid position of 324) resulted in two fragments, a shorter N-terminal part which contains the kinase domain (~37 kDa) and a longer C-terminal fragment with the RHIM and death domain (~39 kDa) [184]. Processing of RIPK1 was highly inhibited in the presence of the caspase inhibitor zVD (Fig. 18A).

To further study the molecular components involved in STS-triggered necroptotic pathway under caspase-compromised conditions we investigated the role of MLKL. Cells were treated with various concentrations of NSA, an inhibitor of MLKL [72]. NSA reduced the ratio of PI positive cells in a concentration-dependent fashion independently of the way of cell death trigger (either TRAIL or STS) under caspase-compromised condition (Fig. 18B). Complete inhibition was observed at NSA concentration of 0.5 μ M, the same concentration as reported by Sun *et al.* [72]. NSA at the applied concentration arrested both the TRAIL and STS-triggered necrosis, confirmed by PI uptake measurements (Fig. 18C) and also by Hoechst/PI double staining method (Fig. 18D).

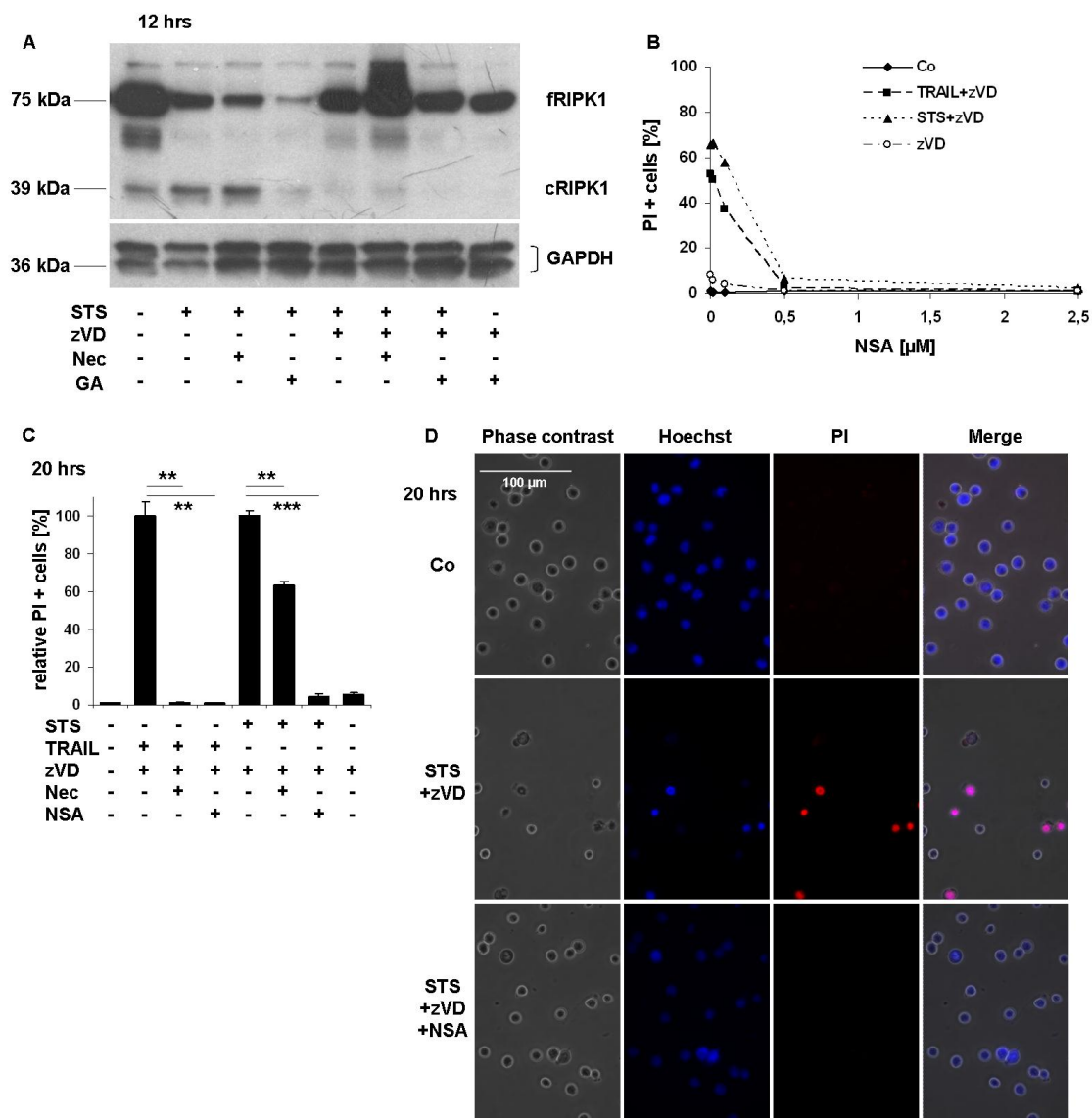


Figure 18. STS induces RIPK1 and MLKL-dependent necroptosis.

(A) zVD hampered RIPK1 fragmentation triggered by STS for 12 hrs. Western blot analysis was performed for the detection of RIPK1 protein level and presence of cleaved fragment due to caspase activity (representative of $n=2$). (B) NSA reduced TRAIL and STS-induced necroptosis in a concentration-dependent manner after 20 hrs incubation time – representative experiment. U937 cells were exposed to STS ($1 \mu\text{M}$) and TRAIL (50 ng/mL) and varying concentrations of NSA (0 – $2.5 \mu\text{M}$) in the presence of zVD ($5 \mu\text{M}$) for 20 hrs. Percentage of PI positive cells was determined. (C–D) NSA ($0.5 \mu\text{M}$) significantly hampered both the TRAIL and STS-triggered necroptosis. (C) Relative percentage of PI positive cells was determined by FACS analysis ($n=3$). Values are mean \pm SD. *, $P < 0.05$, **, $P < 0.01$ and ***, $P < 0.001$ calculated by Student's *t*-probe. (D) Morphological signs of apoptosis and necrosis are shown in representative fluorescent microscopic images ($400\times$) of Hoechst/PI double stained U937 cells ($n=2$). Scale bar on the first subfigure applies to all the figures in the panel.

Meanwhile NSA failed to reverse the STS-evoked DNA fragmentation (Fig. 19A, B) or prevent secondary necrosis (Fig. 19B). Earlier, searching discriminative properties of cell death forms, we observed that unfixed, PI-positive necrotic cells showed not only the well-known loss of forward scatter (FSC) property, but also considerable loss of side scatter (SSC) property detected by flow cytometry, after STS treatment of caspase compromised cells [20]. Interestingly, after ethanol fixation and PI-staining, this population of cells reserved the properties of diminished SSC, while DNA content of these cells was the same as non-dead (ND) (or untreated) cells with fully retained DNA content (SSC_{low}, DNA_{norm}). The percentage of this (SSC_{low}, DNA_{norm}) population in fixed samples correlated well with the percentage of the PI-positive population in vitally PI-stained samples (Fig. 19C). As Fig. 19D shows NSA arrested the appearance of the necrotic (SSC_{low}, DNA_{norm}) population both for TRAIL and STS-treatment. Meanwhile NSA failed to reverse TRAIL or STS-evoked apoptosis (SSC_{norm}, DNA_{low}). Note that however Nec could completely arrest the appearance of the SSC_{low}, DNA_{norm} population for TRAIL+zVD treatment, it was just partial effective in case of STS+zVD treatment. This can be addressed to the STS-induced divergence pathways in the presence of caspase inhibitor.

These results confirmed the crucial role of RIPK1 and MLKL in STS and TRAIL-induced necrosis under caspase-compromised conditions. Therefore we can consider the observed necrosis in U937 cells as necroptosis.

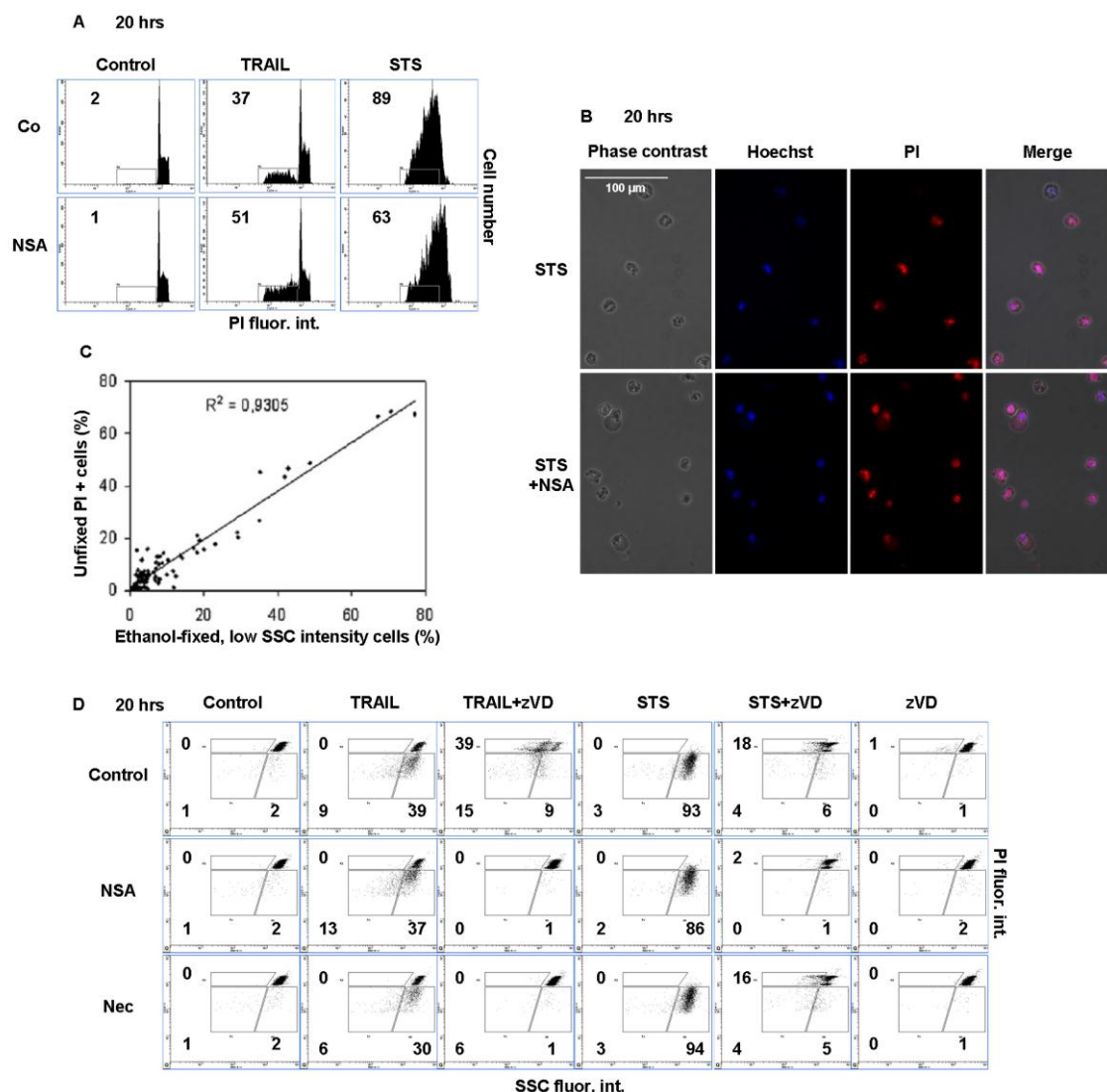


Figure 19. TRAIL and STS induce MLKL-independent DNA fragmentation and secondary necrosis.

(A) Representative histograms of PI stained, ethanol-fixed U937 cells detected by flow cytometry (sub-G1 technique). Inserted values indicate the percentage of cells in the marked regions. U937 cells were exposed to TRAIL (50 ng/mL) or STS (1 μ M) and NSA (0.5 μ M) for 20 hrs (n=3). (B) Morphological signs of apoptosis and necrosis are shown in representative fluorescent microscopic images (400x) of Hoechst/PI double stained U937 cells (representative of n=2). Scale bar on the first subfigure applies to all the figures in the panel. (C) Correlation between absolute percentage of PI+ cells in unfixed samples and SSC low intensity cells in ethanol fixed samples. (D) Representative dot plots of PI-stained ethanol-fixed U937 cells detected by flow cytometry (SSC, DNA content representation). Cells were exposed to TRAIL (50 ng/mL) or STS (1 μ M) and NSA (0.5 μ M) or Nec (10 μ M) for 20 hrs (n=3). Inserted values on representative dot plots show the percentage of the marked population.

4. 4. 3-MA inhibits STS-induced necroptosis

Degtarev *et al.* have shown that autophagy is a common downstream consequence of necroptosis and acts as a repair and energy production process, but inhibition of autophagy has no effect on necroptosis [12]. On the contrary, Bonapace *et al.* reported that inhibition of autophagy blocked the necroptotic process [105].

To test the contribution of autophagy to the STS-induced necroptotic process we studied the effect of 3-methyladenine (MA). MA is known to inhibit autophagy by blocking autophagosome formation via inhibition of type III phosphatidylinositol 3-kinases [185]. We applied increased concentration of MA to test its inhibitory effect (Fig. 20A). We could detect only partial inhibition of MA either at 10 mM final concentration on STS+zVD-induced necroptosis, meanwhile MA was failed to adjust STS-triggered apoptotic pathway (Fig. 20A). In comparison to the effect of Nec, we also detected a partial protection of plasma membrane integrity under our standard assay conditions when MA was applied in 10 mM concentration (Fig. 20B). The combination of Nec with MA resulted in an additive protection and no synergism was observed indicating that necroptosis and autophagic cell death are presumably two independent cell death pathways when cell death is induced by STS+zVD in U937 cells (Fig. 20B). Considering that under the same conditions CA provided complete protection we surmised that the bifurcation point of the necroptotic and autophagic pathway has to be downstream from the site of action of CA.

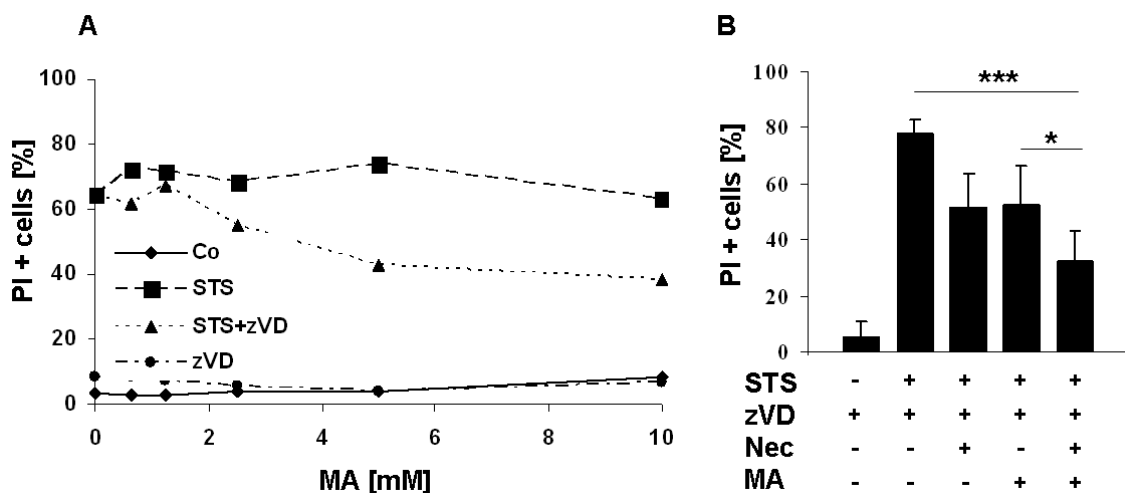


Figure 20. Effect of MA and Nec on STS-induced plasma membrane damage.

(A) MA reduced STS-induced necroptosis after 20 hrs incubation time – representative experiment. U937 cells were exposed to STS (1 μ M) and varying concentrations of MA in the presence of zVD (5 μ M) for 20 hrs. Percentage of PI positive cells was determined. (B) U937 cells were treated with STS (1 μ M) in the presence of zVD (5 μ M) for 20 hrs. Nec (10 μ M) and MA (10 mM) were added 1 hr before the addition of STS. Percentage of PI positive cells was determined. Values are mean \pm SD. *, P <0.05, **, P < 0.01 and ***, P <0.001 calculated by Student's t-probe (two tailed, two sample unequal variance).

4. 5. CA inhibits both the TRAIL and STS-induced necroptosis in the presence of a caspase inhibitor

Previously we found that CA, an inhibitor of cysteine cathepsins, rescued the caspase-independent necrotic form of cell death of promyelocytic leukemia cells treated by STS [130]. In this study we tested whether CA (10 μ M) treatment might promote the survival of U937 cells dying under necroptotic conditions.

Interestingly CA almost completely hampered the TRAIL-induced necroptotic cell death measured by plasma membrane rupture (Fig. 21A). Moreover, CA was comprehensive inhibitor of STS-triggered necroptosis too (Fig. 21B). In case of both inducers, CA abolished the ratio of PI positive cells in a concentration-dependent manner (Fig. 21C, D). IC₅₀ amount was approximately at 5 μ M in both cases (Fig. 21C, D). To further characterize the effect of CA on the necroptotic pathway and to compare to the inhibitory activities of Nec and GA, its action on different cellular compartments were investigated. Time course detection of mitochondrial membrane depolarization was carried out by flow cytometric analysis of DiOC₆(3) stained STS+zVD-treated U937 cells. Our results confirmed that a continuous, time-dependent reduction of mitochondrial membrane integrity happens in the cell population (Fig. 21E). While Nec prevented partially the cells to loose their mitochondrial membrane potential for STS-treatment, CA provided nearly complete protection under caspase activity arrested conditions (Fig. 21E). Furthermore Nec completely inhibited the appearance of AnnexinV and PI double positive cell population after TRAIL and zVD co-treatment (Fig. 21F).

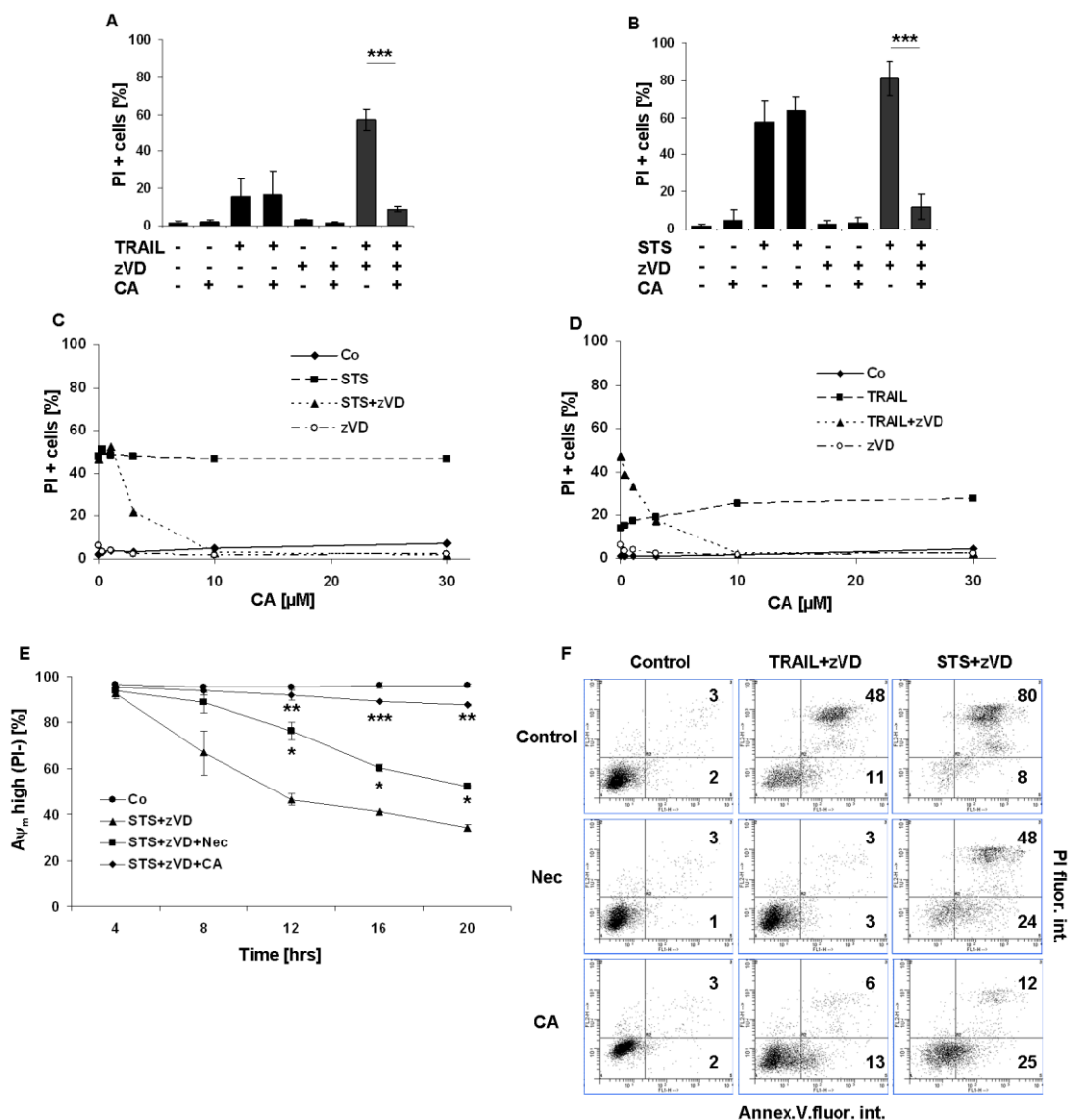


Figure 21. CA inhibits either the TRAIL or STS-induced necroptosis in presence of caspase inhibitor.

U937 cells were treated either with STS (1 μM) or with TRAIL (50 ng/mL) in the presence or absence of zVD (5 μM) for 20 hrs. Nec (10 μM) or CA (10 μM) were added 1 hr before cell death was induced. (A-B) CA (10 μM) considerably inhibited the (A) TRAIL (n=4) or (B) STS-triggered necroptosis (n=3). Percentage of PI positive cells was determined. (C-D) CA reduced the ratio of PI positive cells for (C) STS+zVD or (D) TRAIL+zVD treatment for 20 hrs in a concentration-dependent manner, representative experiments. (E) Time course analysis of cells with depolarized mitochondria is shown after DiOC₆(3) staining of, unfixed cells for STS treatment combined with the indicated inhibitors (n=2). Values are mean \pm SD. *, P < 0.05, **, P < 0.01 and ***, P < 0.001 calculated by Student's t-probe. (F) PS distribution in the plasma membrane is shown in representative dot plots of Annexin V-FITC and PI

stained, unfixed cells analyzed by flow cytometry. The values indicate the percentage of cells in the marked regions (n=2).

In case of STS treatment, the depletion was just partial (Fig. 21F) in concordance with the earlier mentioned PI positivity results (Fig 10F, G). Contrarily, the effect of CA treatment on the reduction of PS translocation and plasma membrane rupture was complete (Fig. 21F). Similarly, the complete arrest of CA on plasma membrane rupture was detected by PI uptake (Fig. 21A, B) and by Hoechst/PI double staining technique for STS (Fig. 22A) or TRAIL (data not shown) treated U937 cells in the presence of zVD. Moreover the loss of lysosomal acidity induced either by STS (Fig. 22B, C) or TRAIL (Fig. 22D) treatment under necroptosis inducing conditions was remarkably withheld by CA pretreatment. Additionally CA could significantly prevent the loss of mitochondrial membrane depolarization in both cases of STS (Fig. 21E, 22E, F) and TRAIL (Fig. 22E) treatment in the presence of the caspase inhibitor zVD.

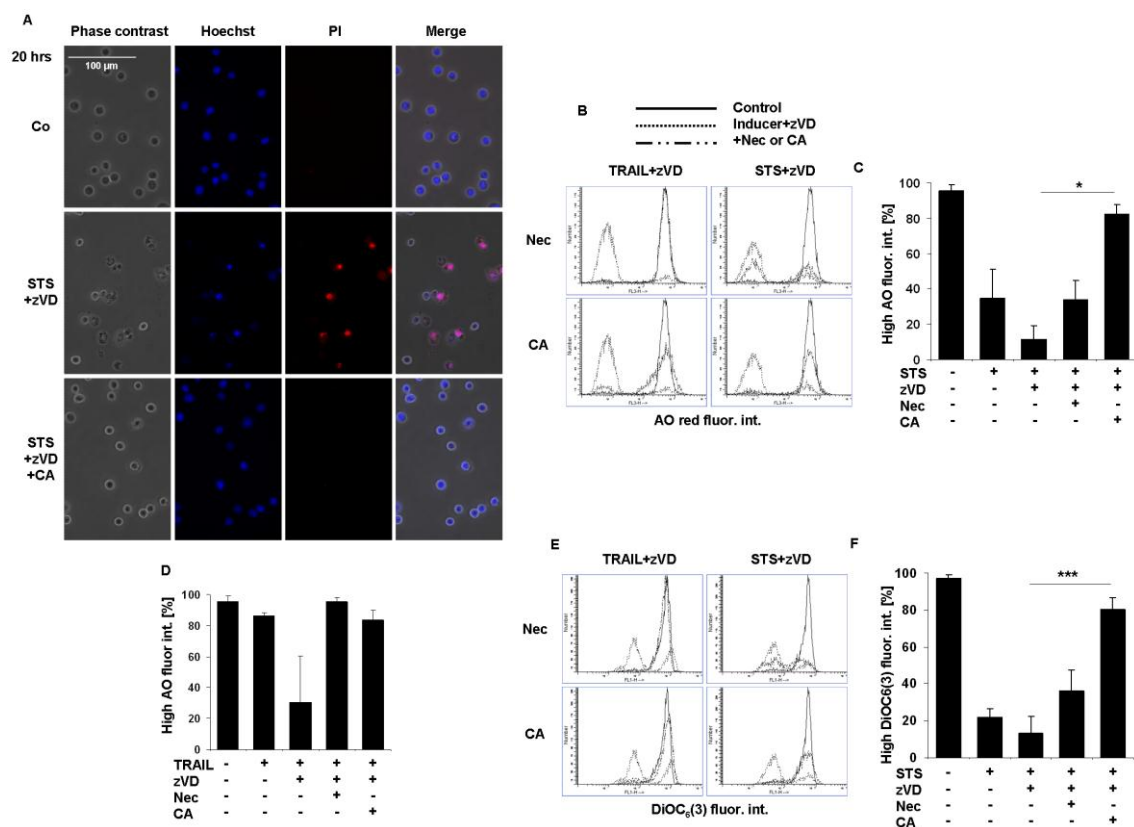


Figure 22. CA inhibits either the TRAIL or STS-induced necroptosis in presence of caspase inhibitor.

U937 cells were treated either with STS (1 μ M) or with TRAIL (50 ng/mL) in the presence or absence of zVD (5 μ M) for 20 hrs. Nec (10 μ M) or CA (10 μ M) were added 1 hr before cell death was induced. (A) Morphological signs of apoptosis and necrosis are shown in representative fluorescent microscopic images (400x) of Hoechst/PI double stained U937 cells (n=2). Scale bar on the first subfigure applies to all the figures in the panel. (B) Distribution of cells with various volumes of acidic compartments (endo-lysosomes) is shown in representative overlay histograms of AO stained cells analyzed by flow cytometry. (C) Column diagram of percentage of cells with high AO red fluorescence intensity (n=2). (D) Column diagram of percentage of cells with high AO fluorescence intensity (n=2). (E) Distribution of cells with various mitochondrial transmembrane potential is shown in representative overlay histograms of DiOC₆(3) stained cells analyzed by flow cytometry. (F) Column diagram of percentage of cells with high DiOC₆(3) fluorescence intensity (n=3). Values are mean \pm SD. *, P < 0.05, **, P < 0.01 and ***, P < 0.001 calculated by Student's t-probe.

Compared to the aforementioned effects of CA, Nec was only partially effective inhibitor of all the measured cellular functions in STS-triggered necroptosis (Fig. 21E, F, Fig. 22B, C, E, F). On the other hand Nec completely diminished the TRAIL-induced necroptosis (Fig. 21F, Fig. 22B, D, E, Fig. 23A). The observed apoptotic parameters: the invariable percentage of the sub-G1 cell population (Fig. 23B, C, D) and the presence of ladder type DNA degradation observed in agarose gels (Fig. 23E) proved that CA had no effect on caspase-dependent apoptosis or on the ensuing secondary necrosis (Fig. 21A, B) in TRAIL or STS-exposed cells. Moreover, the absence of proteolytic degradation of RIPK1 also confirmed the avoidance of apoptosis (Fig. 23F).

From these data we surmised that CA, similarly to NSA is also an effective inhibitor of the necroptotic pathway induced by STS in the presence of caspase inhibitor. While Nec and GA withheld only the early phase of STS-induced necroptosis in U937 cells.

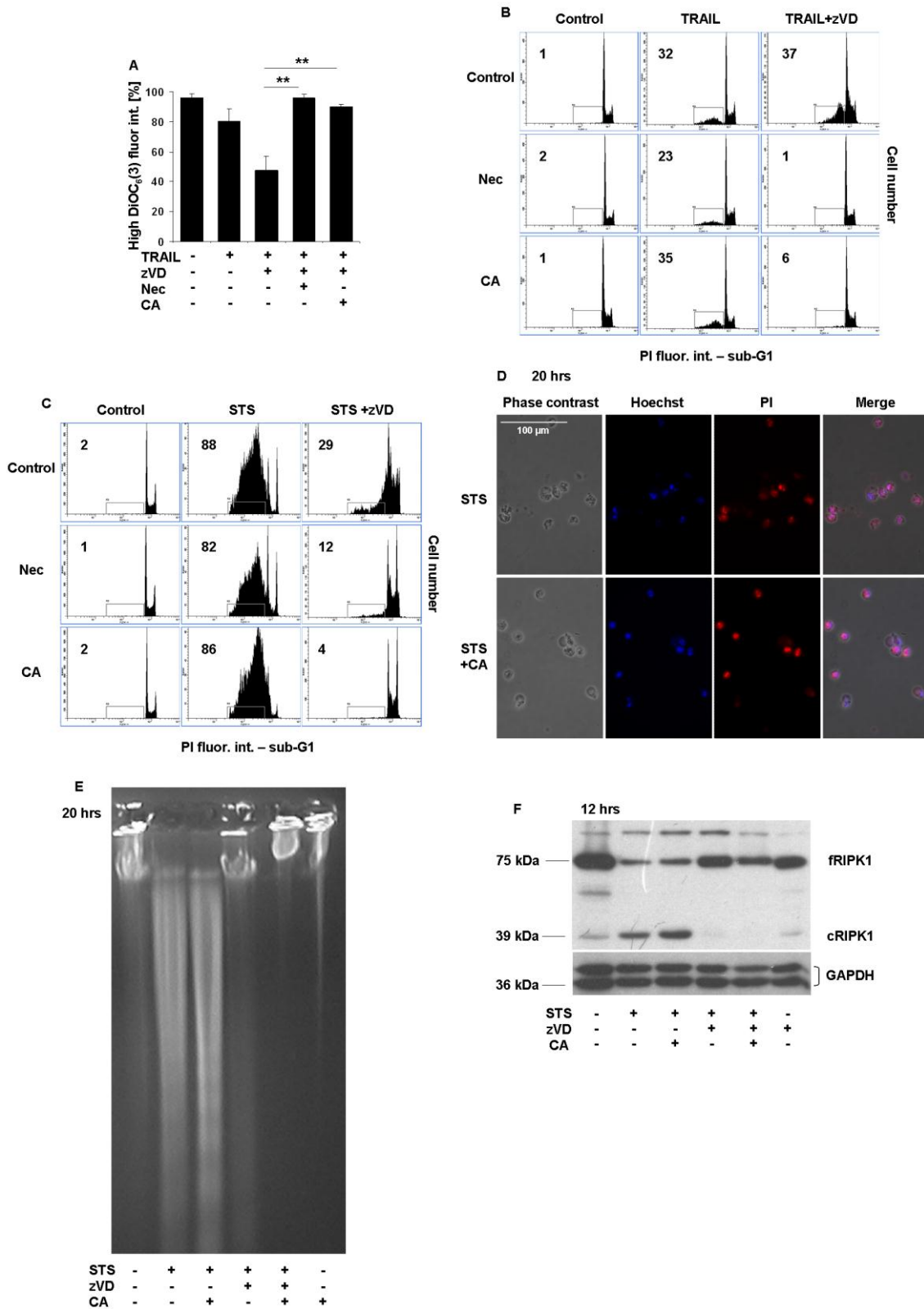


Figure 23. CA inhibits both the TRAIL and STS-induced necroptosis in the presence of caspase inhibitor.

U937 cells were treated either with STS (1 μ M) or with TRAIL (50 ng/mL) in the presence or absence of zVD (5 μ M) for 20 hrs. Nec (10 μ M) or CA (10 μ M) were added 1 hr before cell death was induced. (A) Column diagram of percentage of cells with high DiOC₆(3) fluorescence intensity (n=4). (B-C) Representative histograms of PI stained, ethanol-fixed U937 cells detected by flow cytometry (sub-G1 technique). The numbers indicate the percentage of cells in the marked regions (n=3 for STS and n=4 for TRAIL). Values are mean \pm SD. *, P <0.05, **, P < 0.01 and ***, P <0.001 calculated by Student's t-probe. (G-H) STS-induced DNA fragmentation and condensation. (D) Hoechst/PI double staining (400x) and (E) agarose gel electrophoresis was performed with samples treated as indicated for 20 hrs (representative of n=2). Scale bar on the first subfigure applies to all the figures in the panel. (F) zVD treatment prevents RIPK1 fragmentation triggered by STS. Western blot analysis was performed for the detection of RIPK1 protein level and presence of cleaved fragment due to caspase activity (representative of n=2).

4. 6. PJ-34 does not arrest either the TRAIL or STS-induced necroptosis in the presence of a caspase inhibitor

Participation of PARP-1 enzyme is well documented at several forms of cell death processes [36]. Applying PARP inhibitor reduces the rate of PARP activation and slows down the exhaustion of NAD and ATP pools, therefore generally shifts the cell death process towards apoptosis and prevents necrosis [74].

In our experimental system we tested the effect of PARP-1 enzyme inhibitor PJ-34 on the necroptotic cell death pathway. Major differences in the necroptotic process were not observed in the presence of the inhibitor. In STS or in TRAIL-treated and caspase-inhibited U937 cells PJ-34 did not influence the changes observed in mitochondrial transmembrane potentials (Fig. 24A, Fig. 24B), in PI permeability of cells (Fig. 24C, D), in the acidity of lysosomes (Fig. 24E, F) or in the PS distribution in the plasma membrane (Fig. 24G, data not shown). Furthermore, neither the caspase-dependent nor the caspase-independent STS or TRAIL-induced apoptotic DNA fragmentation was abolished by the applied PARP-1 inhibitor (Fig. 24H, I).

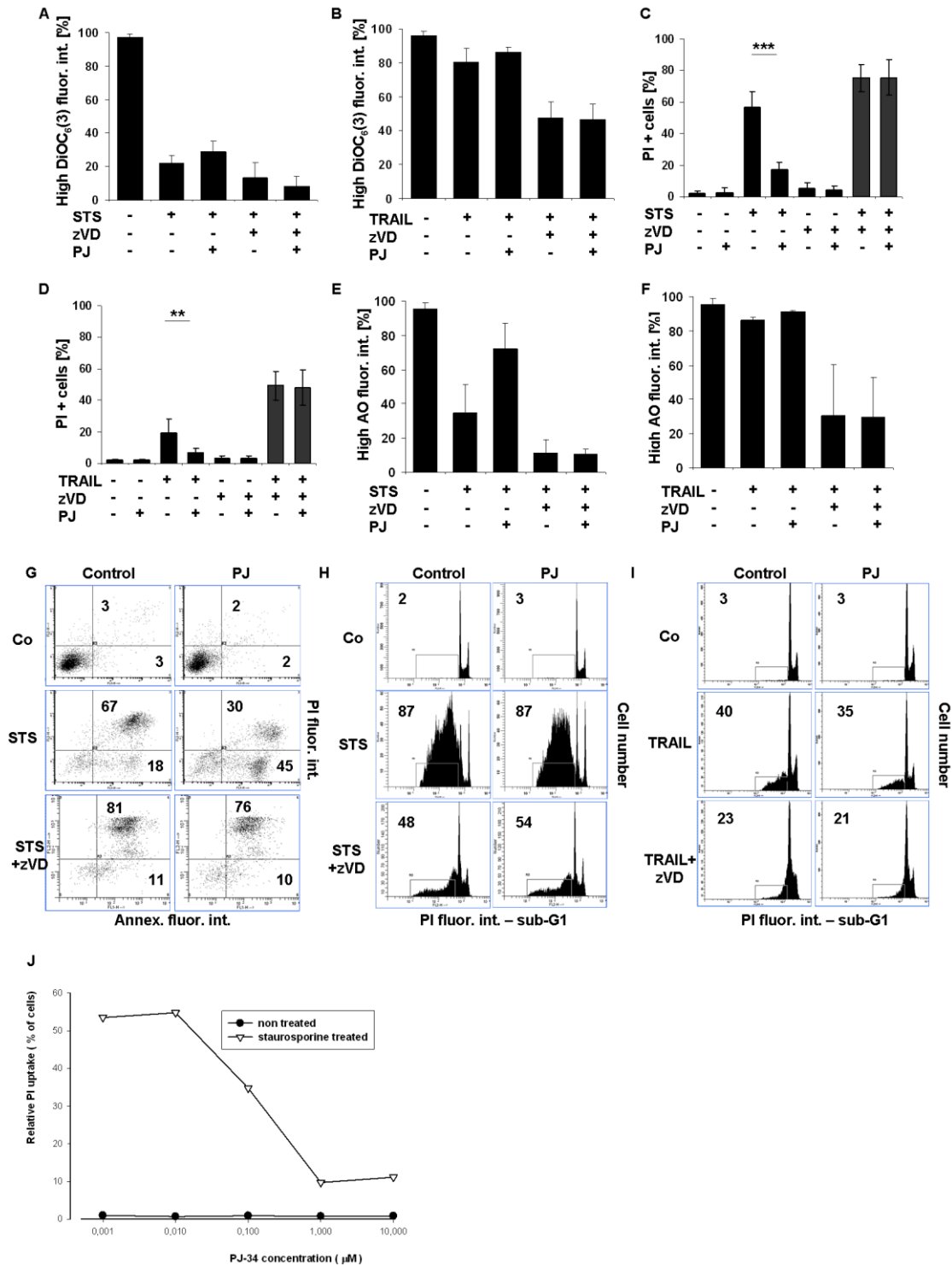


Figure 24. PJ3-4 does not arrest either the TRAIL or STS-induced necroptosis in presence of caspase inhibitor.

U937 cells were treated either with STS (1 μM) or with TRAIL (50 ng/mL) in the presence or absence of zVD (5 μM) for 20 hrs. PJ-34 (1 μM) was added 1 hr before cell death was induced. (A) Column diagram of percentage of cells with high DiOC₆(3) fluorescence intensity (n=3). (B) Column diagram of percentage of cells with high

DiOC₆(3) fluorescence intensity (n=4). (C-D) PJ-34 (1 μ M) considerably inhibited the (C) STS (n=8) or (D) TRAIL-triggered (n=8) secondary necrosis but not the necroptosis. Percentage of PI positive cells was determined. Values are mean \pm SD. *, P < 0.05, **, P < 0.01 and ***, P < 0.001 calculated by Student's t-probe. (E) Column diagram of percentage of cells with high AO fluorescence intensity (n=2). (F) Column diagram of percentage of cells with high AO red fluorescence intensity (n=2). (G) Dot plot distribution of cells stained with Annexin V-FITC and PI analyzed by flow cytometry. The values indicate the percentage of cells in the marked regions (representative of n=2). (H) Representative histograms of distribution of PI stained, ethanol-fixed (sub-G1) cells were analyzed by flow cytometry (n=8). (I) Representative histograms of PI stained, ethanol-fixed cells detected by flow cytometry (sub-G1 technique). The numbers indicate the percentage of cells in the marked regions (n=8). The numbers indicate the percentage of cells in the marked regions. (J) PJ-34 concentration dependently reduced the proportion of PI positive cells for STS treatment for 20 hrs – representative experiment.

At the same time the secondary necrotic cell death process was postponed by PJ-34 in a concentration-dependent manner. This effect was confirmed by the observed intact plasma membrane integrity both under STS (Fig. 24C, J) and TRAIL-induced (Fig. 24D) conditions where the enzyme activity of PARP-1 was increased in the absence of the inhibitor (unpublished results). In addition, the loss of lysosomal acidity was notably reduced by PJ-34 during prolonged treatment of U937 cells with STS (Fig. 24E) and this effect, although with much less extent was observed after TRAIL treatment as well (Fig. 24F).

Contrary to the necrotic process, in cases of STS or TRAIL-induced apoptosis PJ-34 showed only marginal effect on the cell death process. The hallmarks of apoptosis including PS distribution (Fig. 24G, data not shown), loss of mitochondrial transmembrane potential (Fig. 24A, Fig. 24B) and the DNA fragmentation (Fig. 24H, I) were not influenced by PJ-34. Note, that in Fig. 24G most STS-treated cells are Annexin and PI positive while in the presence of PJ-31 more than half of the cells were not stained with PI indicated that PJ-34 prevented postapoptotic membrane disruption.

These results indicate that PJ-34 could only delay the secondary necrosis, but was unable to prevent the caspase-dependent apoptosis. Our results show that the enzymatic activity of PARP-1 directly or indirectly influences the process of secondary necrosis but is dispensable in necroptosis at least in TRAIL and STS-treated U937 cells.

5. Discussion

We analyzed different aspects of cell death modalities in TRAIL and STS-treated monocytic U937 cells by using known inhibitors of the apoptotic, necrotic and necroptotic processes. We have found that under caspase-compromised conditions necroptosis can be triggered both by TRAIL and STS, which compounds are classical inducers of the extrinsic and intrinsic apoptotic pathways respectively. Necroptosis could be arrested by the MLKL inhibitor NSA, by the RIPK1 inhibitor Nec, by the HSP90 inhibitor GA and by the cathepsin B inhibitor CA. On the other hand PJ-34, a PARP-1 inhibitor did not affect the necroptotic pathway, but effectively arrested the progress of secondary necrosis ensued the caspase-mediated apoptosis, at least in U937 cell line.

First, we built up a model system to study the classical death ligand-triggered necroptosis. We selected TRAIL cytokine as inducer of cell death which compound is a promising anticancer agent. Although, it was investigated as a potent and selective apoptosis inducing agent in malignant cells [166], its effect on the necroptotic process was not known in detail. In U937 human monocytic cell line TRAIL induced apoptotic cell death with a moderate intensity, characterized by caspase activation, PARP-1 cleavage and ladder type DNA degradation. After extended periods of TRAIL treatment, apoptosis was followed by a secondary necrotic process. Applying zVD pan-caspase inhibitor together with TRAIL, turned the apoptotic process into a necroptotic cell death form that was arrested by Nec, and none of the signs of apoptosis or that of secondary necrosis were observed even after 20 hours of treatment. These results are in concordance with recent publications [71,175]. After confirming that U937 cells can show apoptotic, necroptotic or secondary necrotic phenotypes upon TRAIL treatment, we started to study the effect of inhibitors influencing certain segments of cell death pathways.

Next, we tested the effect of GA, an inhibitor of the ATP-ase activity of the chaperone protein HSP90. Our former results showed that the two effect of GA namely modulation of the cell death and the cell cycle were related to the inhibition of HSP90 [20]. Based on the results of GA dilution on STS+zVAD-treated sample, we selected the most effective 1 μ M concentration for further experiments.

U937 cells were pre-treated with GA (4 hrs) or Nec (1 hr) both in the absence and presence of zVD before TRAIL administration, and the changes of biochemical events were recorded. Nec or GA prevented the rupture of plasma membrane, due to the inhibition of RIPK1 kinase activity by Nec and partial downregulation of RIPK1 protein level by GA in line with the literature [175,186]. Nec did not affect the extent of TRAIL-induced apoptosis or secondary necrosis in the presence of caspase activation. However, GA administration increased the ratio of apoptotic U937 cells possibly by decreasing the RIPK1-dependent NF- κ B activation [179]. Previously RIPK1 was described to serve as an adapter surface having critical role in the activation of apoptotic and in NF- κ B pathways, where its kinase activity is dispensable [187-189]. Contrarily, kinase activities of RIPK1 and RIPK3 are crucial for necroptosis [71,91,190].

Previously we published that STS induced necrosis in U937 cells where caspase activities were halted by a broad spectrum caspase inhibitor zVAD [20]. Detection of early plasma membrane rupture, morphological characteristics and the absence of caspase activities were considered as important signs of necrotic cell death. In the following study we asked if the STS-induced cell death measured in the absence of caspase activities can be considered as necroptosis.

To further study the caspase-compromised cell death forms provoked by STS we applied the selective caspase inhibitor zVD.fmk instead of the formerly used pan-caspase inhibitor zVAD.fmk. zVD.fmk is a dipeptide caspase inhibitor which is selective for caspases and has no activity against noncaspase proteases, such as cathepsin B, calpain I [181]. Moreover zVD.fmk was shown to have lower IC₅₀ value than zVAD and it is more soluble in water than tripeptide-based caspase inhibitors [181].

We detected that the STS-induced, caspase activity-independent necrotic-like cell death was also withheld by Nec and GA pre-treatments. This inhibitory action was almost complete after 12 hours and was partial but still significant if the incubation time was longer (20 hrs). The inhibitory effect of GA was more potent than that of Nec during STS-evoked necroptosis; however, the difference was not significant. This might be the consequence of the inhibition of HSP90 and degradation or loss of function of various other proteins than RIPK1. E.g. the autophagocytic protein Beclin-1 was shown to form

complex with HSP90 [191]. Parallel processes of necroptosis and autophagy might be inhibited by GA while Nec arrests only the former one.

Earlier we found that GA in presence of zVAD slightly increased the STS-induced, caspase activity-independent cell proportion with fragmented DNA, meanwhile in presence of zVD, this effect was not observed. This discrepancy can be solved by the different physical and chemical properties of zVAD and zVD [181].

The reason of the incomplete inhibition of Nec or GA observed after extended periods of treatments with STS and zVD might be connected to alternatively activated cell death pathways (e.g. autophagy).

Degterev *et al.* showed that autophagy is a common downstream consequence of necroptosis and acts as a scavenger process of cellular debris [12]. On the contrary, Bonapace *et al.* reported that inhibition of autophagy blocked the necroptotic process too [105]. We found that in STS-treated caspase-compromised conditions MA partially decreased plasma membrane rupture similar to Nec. Combined treatment beyond 8 hours with Nec and MA elicited two distinct pathway progress, one can be blocked by Nec the other by MA. It was also conceivable that these two inhibitors halted the same pathway at different points, and their effect was additive but not synergistic. Our observation coincides with that of Degterev *et al.* who investigated the effect of MA in TNF α treated L929 or Jurkat cells in the presence of the caspase inhibitor z-VAD.fmk [12]. These different observations might be due to the different sets of available proteins in different cell types. Autophagy may play role parallel or sequential to necroptosis after treatments with STS and zVD, as MA partially (like Nec) inhibited the PI staining in U937 cells.

RIPK1 was processed in the STS-induced apoptosis that was dominantly inhibited by the caspase inhibitor zVD. The size of the fragment is in accordance with the caspase-8-mediated cleavage of RIPK1 [192]. As the STS-triggered necroptosis could proceed only in the presence of caspase inhibition, the absence of RIPK1 degradation also supports its role in the STS-evoked necroptosis. In a recent publication STS was shown to induce cell death in cultured rat cortical astrocytes, that can be arrested by 100 μ M Nec [193]. However in a former publication Cho *et al.* demonstrated that Nec can inhibit necrosis in a RIPK1-independent manner in L929 cell line at around 20-50 μ M

Nec concentration when cell death was induced by TNF α administration. Thus, care should be taken when results obtained with this inhibitor are interpreted [101]. To reflect on this, throughout our experiments we used lower concentration of Nec (namely 10 μ M).

To further investigate the possible members of the STS-provoked necroptosis we tested the involvement of MLKL in the process. Our results show that both the TRAIL and the STS-induced necroptosis were prevented by NSA. This observation suggests that not only RIPK1 but MLKL are also involved in the STS-triggered necroptotic pathway. As Nec provides only a partial inhibition while NSA results in full protection we propose the hypothesis that STS acts through two parallel pathways which are equally dependent on MLKL.

Presence of NSA strongly inhibits the occurrence of the decreased SSC cell population for STS plus zVD treatment. Compared to this Nec failed to alter the percentage of the reduced SSC cell population under the same conditions. It might mean that STS+zVD treatment activates parallel signaling pathways and while NSA inhibits both the homogenization of the cytosol and the rupture of the plasma membrane, Nec can hamper only the plasma membrane rupture.

How STS induces necroptosis is rather enigmatic. Death receptor-independent assembly of Ripoptosome is a recently proposed model [83]. This process is controlled by endogenous inhibitors of apoptosis proteins (cIAPs) and the XIAP as they can directly ubiquitylate the components of Ripoptosome [82]. Tenev *et al.* found that during etoposide-induced genotoxic stress the levels of cIAPs and XIAP decreased causing the spontaneous formation of the Ripoptosome [82]. Conceivably during STS-induced necroptosis the cIAP and XIAP level also decrease and therefore the formation of Ripoptosome can occur. This notion is supported by former publications revealing that STS decreases the level of XIAP in leukemia cells [194] and in MCF-7 cells [195].

Previously, cathepsin B, a ubiquitous lysosomal cysteine protease was shown to be a component of TNF α -induced cell death pathway [196]. In the absence of caspase activity cathepsins were shown to process cellular proteins leading either to apoptosis [197] or necrosis [198]. We previously discussed that CA, the methylated variant of a highly specific inhibitor of cathepsin B [199] abrogated the necrotic cell in caspase-

inhibited leukemia cells, independently from its inhibitory effect on cathepsin B [130]. In this study we demonstrated that CA stabilized the acidic pH of the lysosomal compartment, prevented the membrane potential loss of mitochondria and finally the rupture of plasma membrane. This indicates that the target of CA is functionally located upstream of the lysosomal breakdown and the mitochondrial depolarization [130]. Van den Berghe and his colleagues recently found that CA significantly blocked TNF α -induced necroptosis [200]. Our results with TRAIL and STS demonstrated that CA completely abrogated necroptosis at 10 μ M concentration in the caspase-inhibited U937 cells. However, this CA concentration was higher with orders compared to concentration required for inhibition of cathepsin B protease activity [130,201]. Thus the effective target of CA in necroptosis remains to be determined.

Participation of PARP and the effect of PARP inhibitor on the prevention or during the induction of cell death are very much cell type dependent. Inhibition of PARP activity might prevent cell death via preventing the exhaustion of a cell's ATP and NAD pools or by inhibiting the transfer of AIF from mitochondria to cell nuclei. In U937 cells, PARP inhibitor did not influence either the apoptotic or the necroptotic cell death pathways induced either by TRAIL or STS, but were able to postpone the secondary necrotic process. It is also worth mentioning that PJ-34 is active site inhibitor of PARP-1 and PARP-2 [202]. Using siRNA gene ablation screen it was shown that PARP-2 is involved in the necroptotic process [13]. It is possible that not the enzymatic activity of PARP-2 but an adapter function is involved in the cell death process, only its presence as a protein is needed as a building block of a signaling protein complex.

6. Conclusions

We proved that TRAIL, a death receptor ligand cytokine, which generally induces apoptotic cell death through the extrinsic pathway, under caspase-compromised conditions triggers necroptosis in U937 cells.

We have also shown that STS, a kinase inhibitor compound which generally induces apoptosis through the intrinsic pathway can also induce necroptosis under caspase-deprived conditions.

Our results show that both TRAIL and the STS-provoked necroptosis were prevented by NSA. This observation suggests that not only RIPK1 but MLKL are also involved in the STS-triggered necroptotic pathway. As Nec provides only a partial inhibition while NSA results in full protection we propose the hypothesis that STS acts through parallel pathways which equally depend on MLKL.

We proved that in parallel of the STS-induced necroptotic process autophagy is also activated, and shown to be partially blocked by the (type III) PI3K inhibitor MA. The combination of Nec with MA resulted in an additive protection of cell death and no synergism was observed indicating that necroptosis and autophagic cell death are presumably two independent cell death pathways.

We have shown that CA inhibits the necroptotic cell death in U937 cells induced by either TRAIL or STS. Note that while the inhibitory potential of Nec and GA is only partial, CA treatment of cells provide complete protection upon STS treatment. These results point out that a non-cathepsin B, currently unknown target of CA can pharmacologically be important in necroptotic cell death.

Moreover, we showed that in U937 cells neither apoptosis nor necroptosis was influenced by PJ-34, a specific inhibitor of PARP-1 and PARP-2. On the other hand, while the secondary necrosis of U937 cells was significantly postponed by PJ-34, it was not affected by Nec, GA or CA at all. If these results will be proved in other cancer cell

lines, clinical application of PARP inhibitors might control the tumor lysis syndrome, where the intracellular content spilling out from the abruptly dying large number of cells poisons the whole body.

The flow chart shown in Fig. 25 summarizes the hypothetical places of actions, where the drugs used in the current study inhibit the STS or TRAIL-induced cell death pathways in U937 cells. We hope that the presented results will contribute to the better understanding of the molecular background of necroptosis and propagate research on CA to find novel drug candidates against necroptotic cell death.

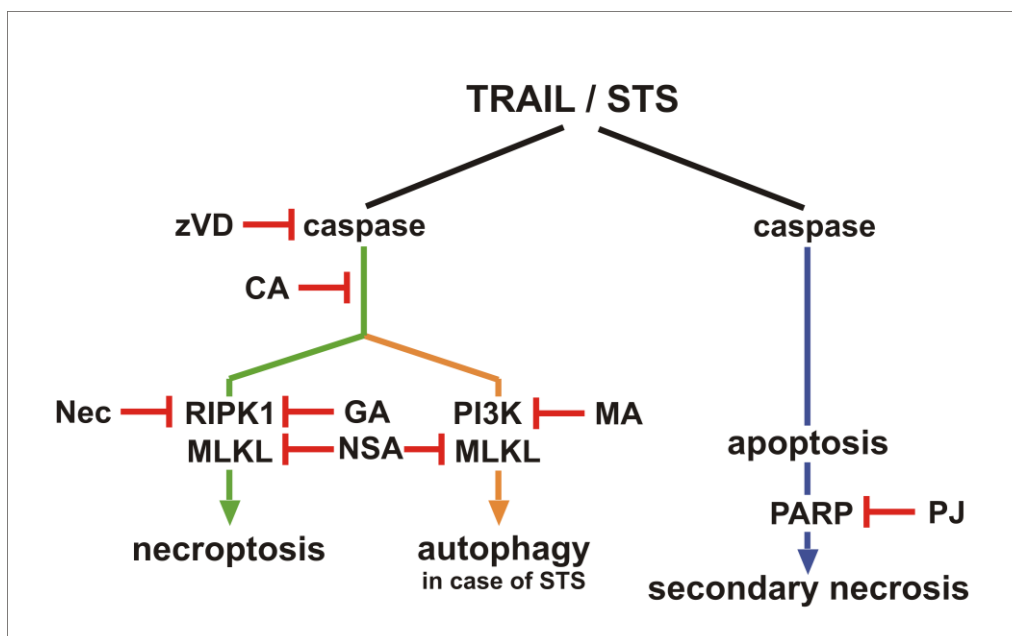


Figure 25. Schematic diagram about the action of inhibitors on TRAIL and staurosporine- induced cell death pathways.

Both TRAIL and STS triggered necroptosis in caspase depleted U937 cells upon prolonged incubation time. RIPK1 inhibitors Nec and GA could completely inhibit the TRAIL-evoked necroptosis, but had partial inhibitory potential to the STS-provoked process. Contrarily CA and NSA abolished both the TRAIL and STS-induced necroptosis. In absence of caspase inhibitor TRAIL and STS induced apoptosis which is followed by secondary necrosis. PJ-34 delayed the necrotic plasma membrane disruption during secondary necrosis, but failed to inhibit necroptosis.

7. Summary

Apoptosis is considered to be the dominant form of cell death *in vivo* and can be induced both through the extrinsic and the intrinsic pathways under various physiological, pathological and experimental conditions. *In vitro* and *in vivo*, in absence of corpse clearing, apoptosis turns into secondary necrosis. Necrosis was thought to be an uncontrolled process for a long time but evidences recently have revealed that necrosis can also occur in a regulated manner. Necroptosis, a type of programmed necrosis which requires the kinase activity of RIPK1 and RIPK3 (receptor-interacting protein kinase 1 and 3) and fulfills under caspase-compromised conditions. Our aim was to compare if the kinase inhibitor staurosporine-induced necrotic signaling pathway differs from the TRAIL (TNF-related apoptosis-inducing ligand)-induced one.

Here we report that both TRAIL, the extrinsic death stimulus and staurosporine, the classical inducer of intrinsic apoptotic pathway can trigger necroptosis in U937 cell line when caspase activity is inhibited. We applied known inhibitors to characterize the contributing proteins of the necroptotic process and their effect on cell viability was detected. We found that both the TRAIL and staurosporine induced necroptotic pathway that was completely or at least partially arrested (respectively) by necrostatin, the inhibitor of RIPK1 kinase activity or by geldanamycin, the inhibitor of HSP90 which is a chaperon of RIPK1 folding. Interestingly, CA-074-OMe, an inhibitor of cysteine cathepsins and necrosulfonamide, inhibitor of MLKL (mixed lineage kinase domain-like protein) completely hampered both the staurosporine- and TRAIL-triggered necroptosis. We proved that in parallel of the staurosporine-induced necroptotic process autophagy is also activated, and shown to be partially blocked by the (type III) PI3K inhibitor 3-methyladenine. We also confirmed that the PJ-34-inhibited enzymatic activity of PARP-1 (poly(ADP-ribose) polymerase-1) was dispensable in the necroptotic process, but it contributed to the disruption of plasma membrane during secondary necrosis ensued either the TRAIL- or the staurosporine-induced apoptosis.

In conclusion we provide evidences that staurosporine, the typical drug of initiating the intrinsic, mitochondrial apoptosis pathway can activate also a necroptotic pathway in U937 cells under caspase-compromised conditions. Furthermore we shed light on a

promising, yet unknown target of CA action in the signaling pathway of necroptosis. Finally we have shown that PARP-1 enzyme does not participate in the process of necroptosis but has crucial role in secondary necrosis. If these results will be proved in other cancer cell lines, clinical application of PARP inhibitors might help to interfere with tumor lysis syndrome.

8. Összefoglaló

In vivo az apoptózist tekintjük domináns sejthalál formának, mely egyaránt aktiválható a külső- és belső jelútvonalon fiziológiás és patológiás körülmények között is. In vivo és in vitro az apoptotikus sejtek eltakarításának hiányában a folyamat másodlagos nekrozisba torkollik. A nekrozist korábban szabályozatlan folyamatnak tekintették, de mára számos eredmény igazolja, hogy a nekrozis regulált módon is megvalósulhat. A nekroptózis a szabályozott nekrozis egyik formája, mely RIPK1 és RIPK3 (receptor-interacting protein kinase 1 és 3) fehérjék aktivitásának függvényében, kaszpázgátolt körülmények között jön létre. Azt kívántuk feltárni, hogy a staurosporin proteinkinázgátló által aktivált nekrozis jelpályák eltérnek-e a TRAIL (TNF-related apoptosis-inducing ligand) citokinnel aktiválhatóktól.

Vizsgálataink során igazoltuk, hogy a külső apoptotikus jelutat indukáló TRAIL mellett a staurosporin is - mely az apoptózis belső, mitokondriális jelútjának aktivátora - nekroptózist indukál kaszpáz aktivitás hiányában, U937 sejtvonalon. Ismert gátlószereket alkalmaztunk, annak érdekében, hogy azonosítani tudjuk a jelútvonalban résztvevő fehérjéket és azok szerepét a sejtelhalás szignálkaskádjában.

Eredményeink szerint i.) a TRAIL és a staurosporin indukálta nekroptózis jelútvonala teljesen, illetve részben gátolható a RIPK1 inhibitorának (necrostatin) és a HSP90 chaperon fehérje gátlószereének (geldanamycin) alkalmazásával; ii.) a ketepszingátló CA-074-OMe és az MLKL (mixed lineage kinase domain-like protein) inhibitor necrosulfonamide teljes mértékben megakadályozta a nekroptotikus jelkaskád lefutását; iii.) a staurosporin indukálta nekroptózis mellett autofágiás folyamat is zajlik, mely a (III-as típusú) PI3K (phosphatidylinositol 3-kinase) inhibitorával (3-methyladenin) felfüggeszthető; iv.) a PJ-34 okozta PARP-1 (poly(ADP-ribose) polymerase-1) gátlás nem befolyásolta sem a TRAIL, sem a staurosporin indukálta apoptózist és nekroptózist; v.) a PARP-1 aktivitása viszont hozzájárul a sejthártya felszakadásához a másodlagos nekrozis során.

Eredményeink rámutatnak arra, hogy 1.) ha más daganatsejteken is igazolódik az eredményünk, akkor a PARP-1 enzim gátlása esetleg alkalmas lehet a tumor lízis szindróma kialakulásának a kivédésében. 2.) A CA-074-OMe alkalmazásával

ravilágítottunk egy ma még ismeretlen target fehérjére, mely fontos szerepet tölt be a nekroptózis szignálkaskádjában.

9. Bibliography

1. Kerr JF, Wyllie AH, Currie AR (1972) Apoptosis: a basic biological phenomenon with wide-ranging implications in tissue kinetics. *British Journal of Cancer* 26: 239-257.
2. Metzstein MM, Stanfield GM, Horvitz HR (1998) Genetics of programmed cell death in *C. elegans*: Past, present and future. *Trends in Genetics* 14: 410-416.
3. Clarke PGH (1990) Developmental cell death: Morphological diversity and multiple mechanisms. *Anatomy and Embryology* 181: 195-213.
4. Déas O, Dumont C, MacFarlane M, Rouleau M, Hebib C, Harper F, Hirsch F, Charpentier B, Cohen GM, Senik A (1998) Caspase-independent cell death induced by anti-CD2 or staurosporine in activated human peripheral T lymphocytes. *Journal of Immunology* 161: 3375-3383.
5. Amin F, Bowen ID, Szegedi Z, Mihalik R, Szende B (2000) Apoptotic and non-apoptotic modes of programmed cell death in MCF-7 human breast carcinoma cells. *Cell Biology International* 24: 253-260.
6. Szende B, Keri G, Szegedi Z, Benedeczky I, Csikos A, Orfi L, Gazit A (1995) Tyrphostin induces non-apoptotic programmed cell death in colon tumor cells. *1995* 19: 903-911.
7. Majno G, Joris I (1995) Apoptosis, oncosis, and necrosis: An overview of cell death. *American Journal of Pathology* 146: 3-15.
8. Lemasters JJ (1999) V. Necrapoptosis and the mitochondrial permeability transition: shared pathways to necrosis and apoptosis. *The American journal of physiology* 276.
9. Li M, Beg AA (2000) Induction of necrotic-like cell death by tumor necrosis factor alpha and caspase inhibitors: Novel mechanism for killing virus-infected cells. *Journal of Virology* 74: 7470-7477.
10. Sperandio S, De Belle I, Bredesen DE (2000) An alternative, nonapoptotic form of programmed cell death. *Proceedings of the National Academy of Sciences of the United States of America* 97: 14376-14381.
11. Borst P, Rottenberg S (2004) Cancer cell death by programmed necrosis? *Drug Resistance Updates* 7: 321-324.

12. Degterev A, Huang Z, Boyce M, Li Y, Jagtap P, Mizushima N, Cuny GD, Mitchison TJ, Moskowitz MA, Yuan J (2005) Chemical inhibitor of nonapoptotic cell death with therapeutic potential for ischemic brain injury. *Nature chemical biology* 1: 112-119.
13. Hitomi J, Christofferson DE, Ng A, Yao J, Degterev A, Xavier RJ, Yuan J (2008) Identification of a Molecular Signaling Network that Regulates a Cellular Necrotic Cell Death Pathway. *Cell* 135: 1311-1323.
14. Vandenabeele P, Galluzzi L, Vanden Berghe T, Kroemer G (2010) Molecular mechanisms of necroptosis: An ordered cellular explosion. *Nature Reviews Molecular Cell Biology* 11: 700-714.
15. Barkla DH, Gibson PR (1999) The fate of epithelial cells in the human large intestine. *Pathology* 31: 230-238.
16. Emons J, Chagin AS, Hultenby K, Zhivotovsky B, Wit JM, Karperien M, Sävendahl L (2009) Epiphyseal fusion in the human growth plate does not involve classical apoptosis. *Pediatric Research* 66: 654-659.
17. Abraham MC, Lu Y, Shaham S (2007) A Morphologically Conserved Nonapoptotic Program Promotes Linker Cell Death in *Caenorhabditis elegans*. *Developmental Cell* 12: 73-86.
18. Kumar A, Rothman J (2007) Cell Death: Hook, Line and Linker. *Current Biology* 17.
19. Kroemer G, El-Deiry WS, Golstein P, Peter ME, Vaux D, Vandenabeele P, Zhivotovsky B, Blagosklonny MV, Malorni W, Knight RA, Piacentini M, Nagata S, Melino G (2005) Classification of cell death: Recommendations of the Nomenclature Committee on Cell Death. *Cell Death and Differentiation* 12: 1463-1467.
20. Imre G, Dunai Z, Petak I, Mihalik R (2007) Cystein cathepsin and Hsp90 activities determine the balance between apoptotic and necrotic cell death pathways in caspase-compromised U937 cells. *Biochimica et Biophysica Acta - Molecular Cell Research* 1773: 1546-1557.
21. Casares N, Pequignot MO, Tesniere A, Ghiringhelli F, Roux S, Chaput N, Schmitt E, Hamai A, Hervas-Stubbs S, Obeid M, Coutant F, Metivier D, Pichard E, Aucoeur P, Pierron G, Garrido C, Zitvogel L, Kroemer G (2005) Caspase-

- dependent immunogenicity of doxorubicin-induced tumor cell death. *Journal of Experimental Medicine* 202: 1691-1701.
22. Kroemer G, Galluzzi L, Vandenabeele P, Abrams J, Alnemri ES, Baehrecke EH, Blagosklonny MV, El-Deiry WS, Golstein P, Green DR, Hengartner M, Knight RA, Kumar S, Lipton SA, Malorni W, Nunez G, Peter ME, Tschopp J, Yuan J, Piacentini M, Zhivotovsky B, Melino G (2009) Classification of cell death: Recommendations of the Nomenclature Committee on Cell Death 2009. *Cell Death and Differentiation* 16: 3-11.
23. Galluzzi L, Vitale I, Abrams JM, Alnemri ES, Baehrecke EH, Blagosklonny MV, Dawson TM, Dawson VL, El-Deiry WS, Fulda S, Gottlieb E, Green DR, Hengartner MO, Kepp O, Knight RA, Kumar S, Lipton SA, Lu X, Madeo F, Malorni W, Mehlen P, Nunez G, Peter ME, Piacentini M, Rubinsztein DC, Shi Y, Simon HU, Vandenabeele P, White E, Yuan J, Zhivotovsky B, Melino G, Kroemer G (2012) Molecular definitions of cell death subroutines: Recommendations of the Nomenclature Committee on Cell Death 2012. *Cell Death and Differentiation* 19: 107-120.
24. Wyllie AH, Kerr JFR, Currie AR (1980) Cell death: The significance of apoptosis. *International Review of Cytology* VOL. 68: 251-306.
25. Silva MT Secondary necrosis: The natural outcome of the complete apoptotic program. *FEBS Letters* 584: 4491-4499.
26. Yuan J (2009) Neuroprotective strategies targeting apoptotic and necrotic cell death for stroke. *Apoptosis* 14: 469-477.
27. Mareninova OA, Sung KF, Hong P, Lugea A, Pandol SJ, Gukovsky I, Gukovskaya AS (2006) Cell death in pancreatitis: Caspases protect from necrotizing pancreatitis. *Journal of Biological Chemistry* 281: 3370-3381.
28. Zhang X, Chen Y, Jenkins LW, Kochanek PM, Clark RSB (2005) Bench-to-bedside review: Apoptosis/programmed cell death triggered by traumatic brain injury. *Critical Care* 9: 66-75.
29. McCully JD, Wakiyama H, Hsieh YJ, Jones M, Levitsky S (2004) Differential contribution of necrosis and apoptosis in myocardial ischemia-reperfusion injury. *American Journal of Physiology - Heart and Circulatory Physiology* 286: H1923-H1935.

30. West T, Atzeva M, Holtzman DM (2006) Caspase-3 deficiency during development increases vulnerability to hypoxic-ischemic injury through caspase-3-independent pathways. *Neurobiology of Disease* 22: 523-537.
31. Beattie G, Siriwardena A (2000) Bacterial infection and extent of necrosis are determinants of organ failure in patients with acute necrotizing pancreatitis. *The British Journal of Surgery* 87: 250.
32. Lancerotto L, Tocco I, Salmaso R, Vindigni V, Bassetto F (2012) Necrotizing fasciitis: classification, diagnosis, and management. *The Journal of Trauma Acute Care Surgery* 72: 560-566.
33. Fokas E, McKenna WG, Muschel RJ (2012) The impact of tumor microenvironment on cancer treatment and its modulation by direct and indirect antivascular strategies. *Cancer Metastasis Review* 31: 823-842.
34. Cairo MS, Bishop M (2004) Tumour lysis syndrome: New therapeutic strategies and classification. *British Journal of Haematology* 127: 3-11.
35. McCall K (2010) Genetic control of necrosis-another type of programmed cell death. *Current Opinion in Cell Biology* 22: 882-888.
36. Zong WX, Ditsworth D, Bauer DE, Wang ZQ, Thompson CB (2004) Alkylating DNA damage stimulates a regulated form of necrotic cell death. *Genes and Development* 18: 1272-1282.
37. Zong WX, Thompson CB (2006) Necrotic death as a cell fate. *Genes and Development* 20: 1-15.
38. Christofferson DE, Yuan J (2010) Necroptosis as an alternative form of programmed cell death. *Current Opinion in Cell Biology* 22: 263-268.
39. Fixsen W, Sternberg P, Ellis H, Horvitz R (1985) Genes that affect cell fates during the development of *Caenorhabditis elegans*. *Cold Spring Harbor symposia on quantitative biology* 50: 99-104.
40. Cecconi F (1999) Apaf1 and the apoptotic machinery. *Cell Death and Differentiation* 6: 1087-1098.
41. Richardson H, Kumar S (2002) Death to flies: *Drosophila* as a model system to study programmed cell death. *Journal of Immunological Methods* 265: 21-28.
42. Thornberry NA, Lazebnik Y (1998) Caspases: Enemies within. *Science* 281: 1312-1316.

43. Cohen GM (1997) Caspases: The executioners of apoptosis. *Biochemical Journal* 326: 1-16.
44. Walker NP, Talanian RV, Brady KD, Dang LC, Bump NJ, Ferez CR, Franklin S, Ghayur T, Hackett MC, Hammill LD (1994) Crystal structure of the cysteine protease interleukin-1 beta-converting enzyme: a (p20/p10)₂ homodimer. *Cell* 78: 343-352.
45. Rotonda J, Nicholson DW, Fazil KM, Gallant M, Gareau Y, Labelle M, Peterson EP, Rasper DM, Ruel R, Vaillancourt JP, Thornberry NA, Becker JW (1996) The three-dimensional structure of apopain/CPP32, a key mediator of apoptosis. *Nature Structural Biology* 3: 619-625.
46. Earnshaw WC, Martins LM, Kaufmann SH (1999) Mammalian caspases: structure, activation, substrates, and functions during apoptosis. *Annual Review of Biochemistry* 68: 383-424.
47. Fesik SW (2000) Insights into programmed cell through structural biology. *Cell* 103: 273-282.
48. Lavrik IN, Golks A, Krammer PH (2005) Caspase: Pharmacological manipulation of cell death. *Journal of Clinical Investigation* 115: 2665-2672.
49. Ashkenazi A, Dixit VM (1998) Death receptors: Signaling and modulation. *Science* 281: 1305-1308.
50. Luthi AU, Martin SJ (2007) The CASBAH: A searchable database of caspase substrates. *Cell Death and Differentiation* 14: 641-650.
51. Leist M, Jaattela M (2001) Triggering of apoptosis by cathepsins. *Cell Death and Differentiation* 8: 324-326.
52. Egger L, Schneider J, Rheme C, Tapernoux M, Hacki J, Borner C (2003) Serine proteases mediate apoptosis-like cell death and phagocytosis under caspase-inhibiting conditions. *Cell Death and Differentiation* 10: 1188-1203.
53. Yuan J, Kroemer G Alternative cell death mechanisms in development and beyond. *Genes and Development* 24: 2592-2602.
54. Chipuk JE, Green DR (2005) Do inducers of apoptosis trigger caspase-independent cell death? *Nature Reviews Molecular Cell Biology* 6: 268-275.
55. Kroemer G, Martin SJ (2005) Caspase-independent cell death. *Nature Medicine* 11: 725-730.

56. Kitanaka C, Kuchino Y (1999) Caspase-independent programmed cell death with necrotic morphology. *Cell Death and Differentiation* 6: 508-515.
57. Dunai ZA, Imre G, Barna G, Korcsmaros T, Petak I, Bauer PI, Mihalik R (2012) Staurosporine induces necroptotic cell death under caspase-compromised conditions in U937 cells. *PLoS ONE* 7.
58. Silva MT (2010) Secondary necrosis: The natural outcome of the complete apoptotic program. *FEBS Letters* 584: 4491-4499.
59. Henson PM, Hume DA (2006) Apoptotic cell removal in development and tissue homeostasis. *Trends in Immunology* 27: 244-250.
60. Krysko DV, D'Herde K, Vandenabeele P (2006) Clearance of apoptotic and necrotic cells and its immunological consequences. *Apoptosis* 11: 1709-1726.
61. Erwig LP, Henson PM (2008) Clearance of apoptotic cells by phagocytes. *Cell Death and Differentiation* 15: 243-250.
62. Lauber K, Bohn E, Krober SM, Xiao YJ, Blumenthal SG, Lindemann RK, Marini P, Wiedig C, Zobywalski A, Baksh S, Xu Y, Autenrieth IB, Schulze-Osthoff K, Belka C, Stuhler G, Wesselborg S (2003) Apoptotic cells induce migration of phagocytes via caspase-3-mediated release of a lipid attraction signal. *Cell* 113: 717-730.
63. Elliott MR, Chekeni FB, Trampont PC, Lazarowski ER, Kadl A, Walk SF, Park D, Woodson RI, Ostankovich M, Sharma P, Lysiak JJ, Harden TK, Leitinger N, Ravichandran KS (2009) Nucleotides released by apoptotic cells act as a find-me signal to promote phagocytic clearance. *Nature* 461: 282-286.
64. Brown S, Heinisch I, Ross E, Shaw K, Buckley CO, Savill J (2002) Apoptosis disables CD31-mediated cell detachment from phagocytes promoting binding and engulfment. *Nature* 418: 200-203.
65. Walker NI, Bennett RE, Kerr JF (1989) Cell death by apoptosis during involution of the lactating breast in mice and rats. *The American Journal of Pathology* 135: 19-32.
66. Silva MT, Do Vale A, Dos Santos NMN (2008) Secondary necrosis in multicellular animals: An outcome of apoptosis with pathogenic implications. *Apoptosis* 13: 463-482.

67. Scott RS, McMahon EJ, Pop SM, Reap EA, Caricchio R, Cohen PL, Shelton Earp H, Matsushima GK (2001) Phagocytosis and clearance of apoptotic cells is mediated by MER. *Nature* 411: 207-211.
68. Zitvogel L, Kepp O, Kroemer G (2010) Decoding Cell Death Signals in Inflammation and Immunity. *Cell* 140: 798-804.
69. Golstein P, Kroemer G (2005) Redundant cell death mechanisms as relics and backups. *Cell Death and Differentiation* 12: 1490-1496.
70. Yu L, Alva A, Su H, Dutt P, Freundt E, Welsh S, Baehrecke EH, Lenardo MJ (2004) Regulation of an ATG7-beclin 1 program of autophaglic cell death by caspase-8. *Science* 304: 1500-1502.
71. Degterev A, Hitomi J, Gernscheid M, Ch'en IL, Korkina O, Teng X, Abbott D, Cuny GD, Yuan C, Wagner G, Hedrick SM, Gerber SA, Lugovskoy A, Yuan J (2008) Identification of RIP1 kinase as a specific cellular target of necrostatins. *Nature Chemical Biology* 4: 313-321.
72. Sun L, Wang H, Wang Z, He S, Chen S, Liao D, Wang L, Yan J, Liu W, Lei X, Wang X (2011) Mixed lineage kinase domain-like protein mediates necrosis signaling downstream of RIP3 kinase. *Cell* 148: 213-227.
73. Wang Z, Jiang H, Chen S, Du F, Wang X (2012) The mitochondrial phosphatase PGAM5 functions at the convergence point of multiple necrotic death pathways. *Cell* 148: 228-243.
74. Andera L (2009) Signaling activated by the death receptors of the TNFR family. *Biomedical Papers* 153: 173-180.
75. Dunai Z, Bauer PI, Mihalik R (2011) Necroptosis: Biochemical, physiological and pathological aspects. *Pathology and Oncology Research* 17: 791-800.
76. Micheau O, Tschopp J (2003) Induction of TNF receptor I-mediated apoptosis via two sequential signaling complexes. *Cell* 114: 181-190.
77. Chen ZJ (2005) Ubiquitin signalling in the NF- κ B pathway. *Nature Cell Biology* 7: 758-765.
78. Wang C, Deng L, Hong M, Akkaraju GR, Inoue JI, Chen ZJ (2001) TAK1 is a ubiquitin-dependent kinase of MKK and IKK. *Nature* 412: 346-351.
79. Lee TH, Shank J, Cusson N, Kelliher MA (2004) The kinase activity of Rip1 is not required for tumor necrosis factor- α -induced I κ B kinase or p38 MAP kinase

- activation or for the ubiquitination of Rip1 by Traf2. *Journal of Biological Chemistry* 279: 33185-33191.
80. Wartz IE, O'Rourke KM, Zhou H, Eby M, Aravind L, Seshagiri S, Wu P, Wiesmann C, Baker R, Boone DL, Ma A, Koonin EV, Dixit VM (2004) De-ubiquitination and ubiquitin ligase domains of A20 downregulate NF- κ B signalling. *Nature* 430: 694-699.
 81. Feoktistova M, Geserick P, Kellert B, Dimitrova D, Langlais C, Hupe M, Cain K, MacFarlane M, HÄcker G, Leverkus M (2011) CIAPs Block Ripoptosome Formation, a RIP1/Caspase-8 Containing Intracellular Cell Death Complex Differentially Regulated by cFLIP Isoforms. *Molecular Cell* 43: 449-463.
 82. Tenev T, Bianchi K, Darding M, Broemer M, Langlais C, Wallberg F, Zachariou A, Lopez J, MacFarlane M, Cain K, Meier P (2011) The Ripoptosome, a Signaling Platform that Assembles in Response to Genotoxic Stress and Loss of IAPs. *Molecular Cell* 43: 689.
 83. Imre G, Larisch S, Rajalingam K (2011) Ripoptosome: A novel IAP-regulated cell death-signalling platform. *Journal of Molecular Cell Biology* 3: 324-326.
 84. Chang DW, Xing Z, Pan Y, Algeciras-Schimnich A, Barnhart BC, Yaish-Ohad S, Peter ME, Yang X (2002) c-FLIP(L) is a dual function regulator for caspase-8 activation and CD95-mediated apoptosis. *EMBO Journal* 21: 3704-3714.
 85. Vucic D, Dixit VM, Wertz IE (2011) Ubiquitylation in apoptosis: A post-translational modification at the edge of life and death. *Nature Reviews Molecular Cell Biology* 12: 439-452.
 86. Tamm I, Kornblau SM, Segall H, Krajewski S, Welsh K, Kitada S, Scudiero DA, Tudor G, Qui YH, Monks A, Andreeff M, Reed JC (2000) Expression and prognostic significance of IAP-family genes in human cancers and myeloid leukemias. *Clinical Cancer Research* 6: 1796-1803.
 87. Vaux DL, Silke J (2003) Mammalian mitochondrial IAP binding proteins. *Biochemical and Biophysical Research Communications* 304: 499-504.
 88. Varfolomeev E, Blankenship JW, Wayson SM, Fedorova AV, Kayagaki N, Garg P, Zobel K, Dynek JN, Elliott LO, Wallweber HJA, Flygare JA, Fairbrother WJ, Deshayes K, Dixit VM, Vucic D (2007) IAP Antagonists Induce

- Autoubiquitination of c-IAPs, NF- κ B Activation, and TNF α -Dependent Apoptosis. *Cell* 131: 669-681.
89. Sun X, Yin J, Starovasnik MA, Fairbrother WJ, Dixit VM (2002) Identification of a novel homotypic interaction motif required for the phosphorylation of receptor-interacting protein (RIP) by RIP3. *Journal of Biological Chemistry* 277: 9505-9511.
90. Galluzzi L, Kepp O, Kroemer G (2009) RIP kinases initiate programmed necrosis. *Journal of molecular cell biology* 1: 8-10.
91. Cho Y, Challa S, Moquin D, Genga R, Ray TD, Guildford M, Chan FKM (2009) Phosphorylation-Driven Assembly of the RIP1-RIP3 Complex Regulates Programmed Necrosis and Virus-Induced Inflammation. *Cell* 137: 1112-1123.
92. Vanlangenakker N, Vanden Berghe T, Krysko DV, Festjens N, Vandenabeele P (2008) Molecular mechanisms and pathophysiology of necrotic cell death. *Current Molecular Medicine* 8: 207-220.
93. Temkin V, Huang Q, Liu H, Osada H, Pope RM (2006) Inhibition of ADP/ATP exchange in receptor-interacting protein-mediated necrosis. *Molecular and Cellular Biology* 26: 2215-2225.
94. Nakagawa T, Shimizu S, Watanabe T, Yamaguchi O, Otsu K, Yamagata H, Inohara H, Kubo T, Tsujimoto Y (2005) Cyclophilin D-dependent mitochondrial permeability transition regulates some necrotic but not apoptotic cell death. *Nature* 434: 652-658.
95. Lim SY, Davidson SM, Mocanu MM, Yellon DM, Smith CCT (2007) The cardioprotective effect of necrostatin requires the cyclophilin-D component of the mitochondrial permeability transition pore. *Cardiovascular Drugs and Therapy* 21: 467-469.
96. Kroemer G, Galluzzi L, Brenner C (2007) Mitochondrial membrane permeabilization in cell death. *Physiological Reviews* 87: 99-163.
97. Zhang DW, Shao J, Lin J, Zhang N, Lu BJ, Lin SC, Dong MQ, Han J (2009) RIP3, an energy metabolism regulator that switches TNF-induced cell death from apoptosis to necrosis. *Science* 325: 332-336.

98. Kim YS, Morgan MJ, Choksi S, Liu Zg (2007) TNF-Induced Activation of the Nox1 NADPH Oxidase and Its Role in the Induction of Necrotic Cell Death. *Molecular Cell* 26: 675-687.
99. Morgan MJ, Kim YS, Liu ZG (2008) TNF α and reactive oxygen species in necrotic cell death. *Cell Research* 18: 343-349.
100. Orrenius S, Gogvadze V, Zhivotovsky B (2007) Mitochondrial oxidative stress: Implications for cell death. In: Cho AK, editor. *Annual Review of Pharmacology and Toxicology*. pp. 143-183.
101. Cho Y, McQuade T, Zhang H, Zhang J, Chan FKM (2011) RIP1-dependent and independent effects of necrostatin-1 in necrosis and T cell activation. *PLoS ONE* 6: e23209.
102. Peter ME (2011) Programmed cell death: Apoptosis meets necrosis. *Nature* 471: 310-312.
103. Zhang H, Zhou X, McQuade T, Li J, Chan FKM, Zhang J (2011) Functional complementation between FADD and RIP1 in embryos and lymphocytes. *Nature* 471: 373-377.
104. Horita H, Frankel AE, Thorburn A (2008) Acute myeloid leukemia-targeted toxin activates both apoptotic and necroptotic death mechanisms. *PLoS ONE* 3.
105. Bonapace L, Bornhauser BC, Schmitz M, Cario G, Ziegler U, Niggli FK, Schafer BW, Schrappe M, Stanulla M, Bourquin JP (2010) Induction of autophagy-dependent necroptosis is required for childhood acute lymphoblastic leukemia cells to overcome glucocorticoid resistance. *Journal of Clinical Investigation* 120: 1310-1323.
106. Falschlehner C, Schaefer U, Walczak H (2009) Following TRAIL's path in the immune system. *Immunology* 127: 145-154.
107. Strasser A, Jost PJ, Nagata S (2009) The Many Roles of FAS Receptor Signaling in the Immune System. *Immunity* 30: 180-192.
108. Ashkenazi A (2002) Targeting death and decoy receptors of the tumour-necrosis factor superfamily. *Nature Reviews Cancer* 2: 420-430.
109. Boatright KM, Renatus M, Scott FL, Sperandio S, Shin H, Pedersen IM, Ricci JE, Edris WA, Sutherlin DP, Green DR, Salvesen GS (2003) A unified model for apical caspase activation. *Molecular Cell* 11: 529-541.

110. Vanlangenakker N, Vanden Berghe T, Vandenabeele P (2012) Many stimuli pull the necrotic trigger, an overview. *Cell Death and Differentiation* 19: 75-86.
111. Wang X (2001) The expanding role of mitochondria in apoptosis. *Genes and Development* 15: 2922-2933.
112. Green DR, Kroemer G (2004) The pathophysiology of mitochondrial cell death. *Science* 305: 626-629.
113. Kroemer G (1999) Mitochondrial control of apoptosis: An overview. *Biochemical Society Symposium*. pp. 1-15.
114. Desagher S, Martinou JC (2000) Mitochondria as the central control point of apoptosis. *Trends in Cell Biology* 10: 369-377.
115. Korsmeyer SJ, Shutter JR, Veis DJ, Merry DE, Oltvai ZN (1993) Bcl-2/Bax: A rheostat that regulates an anti-oxidant pathway and cell death. *Seminars in Cancer Biology* 4: 327-332.
116. Yip KW, Reed JC (2008) Bcl-2 family proteins and cancer. *Oncogene* 27: 6398-6406.
117. Nechushtan A, Smith CL, Lamensdorf I, Yoon SH, Youle RJ (2001) Bax and Bak coalesce into novel mitochondria-associated clusters during apoptosis. *Journal of Cell Biology* 153: 1265-1276.
118. Acehan D, Jiang X, Morgan DG, Heuser JE, Wang X, Akey CW (2002) Three-dimensional structure of the apoptosome: Implications for assembly, procaspase-9 binding, and activation. *Molecular Cell* 9: 423-432.
119. Jiang X, Wang X (2000) Cytochrome c promotes caspase-9 activation by inducing nucleotide binding to Apaf-1. *Journal of Biological Chemistry* 275: 31199-31203.
120. Salvesen GS, Duckett CS (2002) IAP proteins: Blocking the road to death's door. *Nature Reviews Molecular Cell Biology* 3: 401-410.
121. van Loo G, Saelens X, van Gurp M, MacFarlane M, Martin SJ, Vandenabeele P (2002) The role of mitochondrial factors in apoptosis: A Russian roulette with more than one bullet. *Cell Death and Differentiation* 9: 1031-1042.
122. Susin SA, Lorenzo HK, Zamzami N, Marzo I, Snow BE, Brothers GM, Mangion J, Jacotot E, Costantini P, Loeffler M, Larochette N, Goodlett DR, Aebersold R,

- Siderovski DP, Penninger JM, Kroemer G (1999) Molecular characterization of mitochondrial apoptosis-inducing factor. *Nature* 397: 441-446.
123. Luo X, Budihardjo I, Zou H, Slaughter C, Wang X (1998) Bid, a Bcl2 interacting protein, mediates cytochrome c release from mitochondria in response to activation of cell surface death receptors. *Cell* 94: 481-490.
124. Tamaoki T, Nomoto H, Takahashi I (1986) Staurosporine, a potent inhibitor of phospholipid/Ca⁺⁺ dependent protein kinase. *Biochemical and Biophysical Research Communications* 135: 397-402.
125. Zong WX, Lindsten T, Ross AJ, MacGregor GR, Thompson CB (2001) BH3-only proteins that bind pro-survival Bcl-2 family members fail to induce apoptosis in the absence of Bax and Bak. *Genes and Development* 15: 1481-1486.
126. Tafani M, Cohn JA, Karpinich NO, Rothman RJ, Russo MA, Farber JL (2002) Regulation of intracellular pH mediates Bax activation in HeLa cells treated with staurosporine or tumor necrosis factor-alpha. *Journal of Biological Chemistry* 277: 49569-49576.
127. Scarlett JL, Sheard PW, Hughes G, Ledgerwood EC, Ku HH, Murphy MP (2000) Changes in mitochondrial membrane potential during staurosporine-induced apoptosis in Jurkat cells. *FEBS Letters* 475: 267-272.
128. Tafani M, Minchenko DA, Serroni A, Farber JL (2001) Induction of the mitochondrial permeability transition mediates the killing of HeLa cells by staurosporine. *Cancer Research* 61: 2459-2466.
129. Zou H, Li Y, Liu X, Wang X (1999) An APAf-1 - cytochrome C multimeric complex is a functional apoptosome that activates procaspase-9. *Journal of Biological Chemistry* 274: 11549-11556.
130. Mihalik R, Imre G, Petak I, Szende B, Kopper L (2004) Cathepsin B-independent abrogation of cell death by CA-074-OMe upstream of lysosomal breakdown [1]. *Cell Death and Differentiation* 11: 1357-1360.
131. Cummings BS, Kinsey GR, Bolchoz LJC, Schnellmann RG (2004) Identification of caspase-independent apoptosis in epithelial and cancer cells. *Journal of Pharmacology and Experimental Therapeutics* 310: 126-134.

132. Syntichaki P, Xu K, Driscoll M, Tavernarakis N (2002) Specific aspartyl and calpain proteases are required for neurodegeneration in *C. elegans*. *Nature* 419: 939-944.
133. Yamashima T (1998) Inhibition of ischaemic hippocampal neuronal death in primates with cathepsin B inhibitor CA-074: A novel strategy for neuroprotection based on 'calpain-cathepsin hypothesis'. *European Journal of Neuroscience* 10: 1723-1733.
134. Syntichaki P, Samara C, Tavernarakis N (2005) The vacuolar H⁺-ATPase mediates intracellular acidification required for neurodegeneration in *C. elegans*. *Current Biology* 15: 1249-1254.
135. Goll DE, Thompson VF, Li H, Wei W, Cong J (2003) The calpain system. *Physiological Reviews* 83: 731-801.
136. Yamashima T, Tonchev AB, Tsukada T, Saido TC, Imajoh-Ohmi S, Momoi T, Kominami E (2003) Sustained calpain activation associated with lysosomal rupture executes necrosis of the postischemic CA1 neurons in primates. *Hippocampus* 13: 791-800.
137. Yamashima T (2004) Ca²⁺-dependent proteases in ischemic neuronal death. A conserved 'calpain-cathepsin cascade' from nematodes to primates. *Cell Calcium* 36: 285-293.
138. Moubarak RS, Yuste VJ, Artus C, Bouharrou A, Greer PA, Menissier-de Murcia J, Susin SA (2007) Sequential activation of poly(ADP-ribose) polymerase 1, calpains, and bax is essential in apoptosis-inducing factor-mediated programmed necrosis. *Molecular and Cellular Biology* 27: 4844-4862.
139. Slemmer JE, Zhu C, Landshamer S, Trabold R, Grohm J, Ardeshiri A, Wagner EF, Sweeney MI, Blomgren K, Culmsee C, Weber JT, Plesnila N (2008) Causal role of apoptosis-inducing factor for neuronal cell death following traumatic brain injury. *The American Journal of Pathology* 173: 1795-1805.
140. Boujrad H, Gubkina O, Robert N, Krantic S, Susin SA (2007) AIF-mediated programmed necrosis: A highly regulated way to die. *Cell Cycle* 6: 2612-2619.
141. Xu Y, Huang S, Liu ZG, Han J (2006) Poly(ADP-ribose) polymerase-1 signaling to mitochondria in necrotic cell death requires RIP1/TRAF2-mediated JNK1 activation. *Journal of Biological Chemistry* 281: 8788-8795.

142. Yoshida H, Kong YY, Yoshida R, Elia AJ, Hakem A, Hakem R, Penninger JM, Mak TW (1998) Apaf1 is required for mitochondrial pathways of apoptosis and brain development. *Cell* 94: 739-750.
143. Lindsten T, Ross AJ, King A, Zong WX, Rathmell JC, Shiels HA, Ulrich E, Waymire KG, Mahar P, Frauwirth K, Chen Y, Wei M, Eng VM, Adelman DM, Simon MC, Ma A, Golden JA, Evan G, Korsmeyer SJ, MacGregor GR, Thompson CB (2000) The combined functions of proapoptotic Bcl-2 family members Bak and Bax are essential for normal development of multiple tissues. *Molecular Cell* 6: 1389-1399.
144. Lindsten T, Thompson CB (2006) Cell death in the absence of Bax and Bak. *Cell Death and Differentiation* 13: 1272-1276.
145. Laporte C, Kosta A, Klein G, Aubry L, Lam D, Tresse E, Luciani MF, Golstein P (2007) A necrotic cell death model in a protist. *Cell Death and Differentiation* 14: 266-274.
146. Yuan J, Kroemer G (2010) Alternative cell death mechanisms in development and beyond. *Genes and Development* 24: 2592-2602.
147. Benedict CA, Norris PS, Ware CF (2002) To kill or be killed: Viral evasion of apoptosis. *Nature Immunology* 3: 1013-1018.
148. Berglund AC, Sjolund E, Ostlund G, Sonnhammer ELL (2008) InParanoid 6: Eukaryotic ortholog clusters with inparalogs. *Nucleic Acids Research* 36: D263-D266.
149. Stoll G, Jander S, Schroeter M (2002) Detrimental and beneficial effects of injury-induced inflammation and cytokine expression in the nervous system. *Advances in Experimental Medicine and Biology*. pp. 87-113.
150. Zhang M, Chen L (2008) Status of cytokines in ischemia reperfusion induced heart injury. *Cardiovascular and Hematological Disorders - Drug Targets* 8: 161-172.
151. You Z, Savitz SI, Yang J, Degterev A, Yuan J, Cuny GD, Moskowitz MA, Whalen MJ (2008) Necrostatin-1 reduces histopathology and improves functional outcome after controlled cortical impact in mice. *Journal of Cerebral Blood Flow and Metabolism* 28: 1564-1573.

152. Li Y, Yang X, Ma C, Qiao J, Zhang C (2008) Necroptosis contributes to the NMDA-induced excitotoxicity in rat's cultured cortical neurons. *Neuroscience Letters* 447: 120-123.
153. Tan S, Schubert D, Maher P (2001) Oxytosis: A novel form of programmed cell death. *Current topics in medicinal chemistry* 1: 497-506.
154. Xu X, Chua CC, Kong J, Kostrzewa RM, Kumaraguru U, Hamdy RC, Chua BHL (2007) Necrostatin-1 protects against glutamate-induced glutathione depletion and caspase-independent cell death in HT-22 cells. *Journal of Neurochemistry* 103: 2004-2014.
155. Cregan SP, Dawson VL, Slack RS (2004) Role of AIF in caspase-dependent and caspase-independent cell death. *Oncogene* 23: 2785-2796.
156. Kim S, Dayani L, Rosenberg PA, Li J (2010) RIP1 kinase mediates arachidonic acid-induced oxidative death of oligodendrocyte precursors. *International Journal of Physiology, Pathophysiology and Pharmacology* 2: 137-147.
157. Davis CW, Hawkins BJ, Ramasamy S, Irrinki KM, Cameron BA, Islam K, Daswani VP, Doonan PJ, Manevich Y, Madesh M (2010) Nitration of the mitochondrial complex I subunit NDUFB8 elicits RIP1- and RIP3-mediated necrosis. *Free Radical Biology and Medicine* 48: 306-317.
158. Smith CCT, Davidson SM, Lim SY, Simpkin JC, Hothersall JS, Yellon DM (2007) Necrostatin: A potentially novel cardioprotective agent? *Cardiovascular Drugs and Therapy* 21: 227-233.
159. Bao L, Li Y, Deng SX, Landry D, Tabas I (2006) Sitosterol-containing lipoproteins trigger free sterol-induced caspase-independent death in ACAT-competent macrophages. *Journal of Biological Chemistry* 281: 33635-33649.
160. Han W, Li L, Qiu S, Lu Q, Pan Q, Gu Y, Luo J, Hu X (2007) Shikonin circumvents cancer drug resistance by induction of a necroptotic death. *Molecular Cancer Therapeutics* 6: 1641-1649.
161. Hanahan D, Weinberg RA (2000) The hallmarks of cancer. *Cell* 100: 57-70.
162. Hu W, Kavanagh JJ (2003) Anticancer therapy targeting the apoptotic pathway. *Lancet Oncology* 4: 721-729.

163. Li QX, Yu DH, Liu G, Ke N, McKelvy J, Wong-Staal F (2008) Selective anticancer strategies via intervention of the death pathways relevant to cell transformation. *Cell Death and Differentiation* 15: 1197-1210.
164. Gescher A (2000) Staurosporine analogues - Pharmacological toys or useful antitumour agents? *Critical Reviews in Oncology/Hematology* 34: 127-135.
165. Ying S, Hacker G (2007) Apoptosis induced by direct triggering of mitochondrial apoptosis proceeds in the near-absence of some apoptotic markers. *Apoptosis* 12: 2003-2011.
166. Walczak H, Miller RE, Ariail K, Gliniak B, Griffith TS, Kubin M, Chin W, Jones J, Woodward A, Le T, Smith C, Smolak P, Goodwin RG, Rauch CT, Schuh JCL, Lynch DH (1999) Tumoricidal activity of tumor necrosis factor-related apoptosis-inducing ligand in vivo. *Nature Medicine* 5: 157-163.
167. Petak I, Vernes R, Szucs KS, Anozie M, Izeradjene K, Douglas L, Tillman DM, Phillips DC, Houghton JA (2003) A caspase-8-independent component in TRAIL/Apo-2L-induced cell death in human rhabdomyosarcoma cells. *Cell Death and Differentiation* 10: 729-739.
168. Darzynkiewicz Z, Bedner E (2000) Analysis of apoptotic cells by flow and laser scanning cytometry. *Methods in Enzymology* 322: 18-39.
169. Gong J, Traganos F, Darzynkiewicz Z (1994) A selective procedure for DNA extraction from apoptotic cells applicable for gel electrophoresis and flow cytometry. *Analytical Biochemistry* 218: 314-319.
170. Marton A, Mihalik R, Bratincsak A, Adleff V, Petak I, Vegh M, Bauer PI, Krajcsi P (1997) Apoptotic cell death induced by inhibitors of energy conservation Bcl-2 inhibits apoptosis downstream of a fall of ATP level. *European Journal of Biochemistry* 250: 467-475.
171. Daugas E, Susin SA, Zamzami N, Ferri KF, Irinopoulou T, Larochette N, Prevost MC, Leber B, Andrews D, Penninger J, Kroemer G (2000) Mitochondrio-nuclear translocation of AIF in apoptosis and necrosis. *FASEB Journal* 14: 729-739.
172. Buki KG, Bauer PI, Hakam A, Kun E (1995) Identification of domains of poly(ADP-ribose) polymerase for protein binding and self-association. *Journal of Biological Chemistry* 270: 3370-3377.

173. Wiley SR, Schooley K, Smolak PJ, Din WS, Huang CP, Nicholl JK, Sutherland GR, Smith TD, Rauch C, Smith CA, Goodwin RG (1995) Identification and characterization of a new member of the TNF family that induces apoptosis. *Immunity* 3: 673-682.
174. Gonzalvez F, Ashkenazi A (2010) New insights into apoptosis signaling by Apo2L/TRAIL. *Oncogene* 29: 4752-4765.
175. Holler N, Zaru R, Micheau O, Thome M, Attinger A, Valitutti S, Bodmer JL, Schneider P, Seed B, Tschopp J (2000) Fas triggers an alternative, caspase-8-independent cell death pathway using the kinase RIP as effector molecule. *Nature Immunology* 1: 489-495.
176. Higuchi Y (2003) Chromosomal DNA fragmentation in apoptosis and necrosis induced by oxidative stress. *Biochemical Pharmacology* 66: 1527-1535.
177. Dong Z, Saikumar P, Weinberg JM, Venkatachalam MA (1997) Internucleosomal DNA cleavage triggered by plasma membrane damage during necrotic cell death: Involvement of serine but not cysteine proteases. *American Journal of Pathology* 151: 1205-1213.
178. Whitesell L, Mimnaugh EG, De Costa B, Myers CE, Neckers LM (1994) Inhibition of heat shock protein HSP90-pp60(v-src) heteroprotein complex formation by benzoquinone ansamycins: Essential role for stress proteins in oncogenic transformation. *Proceedings of the National Academy of Sciences of the United States of America* 91: 8324-8328.
179. Lewis J, Devin A, Miller A, Lin Y, Rodriguez Y, Neckers L, Liu ZG (2000) Disruption of Hsp90 function results in degradation of the death domain kinase, receptor-interacting protein (RIP), and blockage of tumor necrosis factor-induced nuclear factor- κ B activation. *Journal of Biological Chemistry* 275: 10519-10526.
180. Ea CK, Deng L, Xia ZP, Pineda G, Chen ZJ (2006) Activation of IKK by TNF α Requires Site-Specific Ubiquitination of RIP1 and Polyubiquitin Binding by NEMO. *Molecular Cell* 22: 245-257.
181. Yang W, Guastella J, Huang JC, Wang Y, Zhang L, Xue D, Tran M, Woodward R, Kasibhatla S, Tseng B, Drewe J, Cai SX (2003) MX1013, a dipeptide caspase

- inhibitor with potent in vivo antiapoptotic activity. *British Journal of Pharmacology* 140: 402-412.
182. Bedin M, Gaben AM, Saucier C, Mester J (2004) Geldanamycin, an inhibitor of the chaperone activity of HSP90, induces MAPK-independent cell cycle arrest. *International Journal of Cancer* 109: 643-652.
183. Vande Walle L, Wirawan E, Lamkanfi M, Festjens N, Verspurten J, Saelens X, Vanden Berghe T, Vandenabeele P (2010) The mitochondrial serine protease HtrA2/Omi cleaves RIP1 during apoptosis of Ba/F3 cells induced by growth factor withdrawal. *Cell Research* 20: 421-433.
184. Lin Y, Devin A, Rodriguez Y, Liu ZG (1999) Cleavage of the death domain kinase RIP by Caspase-8 prompts TNF-induced apoptosis. *Genes and Development* 13: 2514-2526.
185. Blommaert EFC, Krause U, Schellens JPM, Vreeling-Sindelarova H, Meijer AJ (1997) The phosphatidylinositol 3-kinase inhibitors wortmannin and LY294002 inhibit in isolated rat hepatocytes. *European Journal of Biochemistry* 243: 240-246.
186. Chen WW, Yu H, Fan HB, Zhang CC, Zhang M, Zhang C, Cheng Y, Kong J, Liu CF, Geng D, Xu X (2011) RIP1 mediates the protection of geldanamycin on neuronal injury induced by oxygen-glucose deprivation combined with zVAD in primary cortical neurons. *Journal of Neurochemistry*.
187. Chan FKM, Shisler J, Bixby JG, Felices M, Zheng L, Appel M, Orenstein J, Moss B, Lenardo MJ (2003) A Role for Tumor Necrosis Factor Receptor-2 and Receptor-interacting Protein in Programmed Necrosis and Antiviral Responses. *Journal of Biological Chemistry* 278: 51613-51621.
188. Ting AT, Pimentel-Muinos FX, Seed B (1996) RIP mediates tumor necrosis factor receptor 1 activation of NFkB but not Fas/APO-1-initiated apoptosis. *EMBO Journal* 15: 6189-6196.
189. Zhang SQ, Kovalenko A, Cantarella G, Wallach D (2000) Recruitment of the IKK signalosome to the p55 TNF receptor: RIP and A20 bind to NEMO (IKKgamm) upon receptor stimulation. *Immunity* 12: 301-311.

190. He S, Wang L, Miao L, Wang T, Du F, Zhao L, Wang X (2009) Receptor Interacting Protein Kinase-3 Determines Cellular Necrotic Response to TNF- α . *Cell* 137: 1100-1111.
191. Xu C, Liu J, Hsu L, Luo Y, Xiang R, Chuang T (2011) Functional interaction of Hsp90 and Beclin 1 modulates Toll-like receptor-mediated autophagy. *FASEB Journal*.
192. Oberst A, Dillon CP, Weinlich R, McCormick LL, Fitzgerald P, Pop C, Hakem R, Salvesen GS, Green DR (2011) Catalytic activity of the caspase-8-FLIP L complex inhibits RIPK3-dependent necrosis. *Nature* 471: 363-368.
193. Simenc J, Lipnik-Stangelj M (2012) Staurosporine induces different cell death form in cultures rat astrocytes. *Radiology and Oncology* doi:10.2478/v10019-012-0036-9.
194. Kitada S, Zapata JM, Andreeff M, Reed JC (2000) Protein kinase inhibitors flavopiridol and 7-hydroxy-staurosporine down- regulate antiapoptosis proteins in B-cell chronic lymphocytic leukemia. *Blood* 96: 393-397.
195. Dohi T, Okada K, Xia F, Wilford CE, Samuel T, Welsh K, Marusawa H, Zou H, Armstrong R, Matsuzawa SI, Salvesen GS, Reed JC, Altieri DC (2004) An IAP-IAP complex inhibits apoptosis. *Journal of Biological Chemistry* 279: 34087-34090.
196. Guicciardi ME, Deussing J, Miyoshi H, Bronk SF, Svingen PA, Peters C, Kaufmann SH, Gores GJ (2000) Cathepsin B contributes to TNF α -mediated hepatocyte apoptosis by promoting mitochondrial release of cytochrome c. *Journal of Clinical Investigation* 106: 1127-1137.
197. Foghsgaard L, Wissing D, Mauch D, Lademann U, Bastholm L, Boes M, Elling F, Leist M, Jaattela M (2001) Cathepsin B acts as a dominant execution protease in tumor cell apoptosis induced by tumor necrosis factor. *Journal of Cell Biology* 153: 999-1009.
198. Hentze H, Lin XY, Choi MSK, Porter AG (2003) Critical role for cathepsin B in mediating caspase-1-dependent interleukin-18 maturation and caspase-1-independent necrosis triggered by the microbial toxin nigericin. *Cell Death and Differentiation* 10: 956-968.

199. Buttle DJ, Murata M, Knight CG, Barrett AJ (1992) CA074 methyl ester: A proinhibitor for intracellular cathepsin B. *Archives of Biochemistry and Biophysics* 299: 377-380.
200. Berghe TV, Vanlangenakker N, Parthoens E, Deckers W, Devos M, Festjens N, Guerin CJ, Brunk UT, Declercq W, Vandenabeele P (2010) Necroptosis, necrosis and secondary necrosis converge on similar cellular disintegration features. *Cell Death and Differentiation* 17: 922-930.
201. Newman ZL, Leppla SH, Moayeri M (2009) CA-074Me protection against anthrax lethal toxin. *Infection and Immunity* 77: 4327-4336.
202. Soriano FG, Virag L, Szabo C (2001) Diabetic endothelial dysfunction: role of reactive oxygen and nitrogen species production and poly(ADP-ribose) polymerase activation. *Journal of Molecular Medicine* 79: 437-448.

10. Publications

10. 1. Publications related to the thesis

1. **Dunai ZA**, Imre G, Barna G, Korcsmaros T, Petak I, Bauer PI, Mihalik R (2012) Staurosporine induces necroptotic cell death under caspase-compromised conditions in U937 cells. PLoS ONE. **IF: 4,092**

2. **Dunai ZA**, Bauer PI, Mihalik R (2011) Necroptosis: Biochemical, physiological and pathological aspects. Pathology and Oncology Research. **IF: 1,366**

3. Imre G, **Dunai ZA**, Petak I, Mihalik R (2007) Cystein cathepsin and Hsp90 activities determine the balance between apoptotic and necrotic cell death pathways in caspase-compromised U937 cells. Biochimica et Biophysica Acta - Molecular Cell Research. **IF: 4.374**

10. 2. Publications not directly related to the thesis

Stemmer U, **Dunai ZA**, Koller D, Purstinger G, Zenzmaier E, Deigner HP, Aflaki E, Kratky D, Hermetter A. (2012) Toxicity of oxidized phospholipids in cultured macrophages. Lipids in Health and Disease. **IF: 2,17**

Barna G, Sebestyen A, **Dunai ZA**, Csernus B, Mihalik R (2012) Heparin can liberate high molecular weight DNA from secondary necrotic cells. Cell Biology International. **IF: 1,482**

Fekete A, Kenesi E, Hunyadi-Gulyas E, Durgo H, Berko B, **Dunai ZA**, Bauer PI. (2012) The guanine-quadruplex structure in the human c-myc gene's promoter is converted into B-DNA form by the human poly(ADP-ribose)polymerase-1. PLoS ONE. **IF: 4,092**

Kun E, Mendeleyev J, Kirsten E, Hakam A, Kun AM, Fekete A, Bauer PI, **Dunai ZA**, Mihalik R. (2011) Regulation of malignant phenotype and bioenergetics by a π -electron donor-inducible mitochondrial MgATPase. International Journal of Molecular Medicine. **IF: 1,573**

11. Acknowledgements

I would like to dedicate the dissertation to Dr. Pal I. Bauer, and I would like to thank him both for his scientific and personal support during the intensive last years of my Ph.D. studies.

I would like to express my gratitude to my supervisor Dr. Rudolf Mihalik for his guidance throughout the whole course of my studies since 2003.

I am thankful to Prof. Laszlo Kopper and Dr. Pal I. Bauer for providing me the opportunity to work in the laboratories of the 1st Department of Pathology and Experimental Cancer Research and in the Department of Medical Biochemistry Semmelweis University, respectively.

I am grateful to Prof. Peter Sotonyi for his support as my mentor in the Kerpel-Fronius Odon talent support program.

Herein I would like to thank all the colleagues for their help and work which was indispensable for publishing the articles:

First I am beholden to Dr. Gergely Imre for giving an insight to the practical matters of the everyday research work together with my supervisor, Dr. Rudolf Mihalik. I am happy that we worked together for many years.

I am grateful to Dr. Istvan Petak for providing me with the special humanized TRAIL ligand stocks and also for his constructive suggestions and comments.

I am thankful to Dr. Gabor Barna for his help with the FACS measurements and for his helpful thoughts. I am also grateful to Prof. Andras Matolcsy and to Prof. Laszlo Budai for giving me access to the FACS instruments in their labs.

I would like to express my thanks for Dr. Tamas Korcsmaros for his invaluable ideas and suggestions, and for critically reading the manuscript.

I would like to thank Dr. Tibor Krenacs for his help in digitalization of citospin slides with Panoramic Scanner of 3DHISTECH Ltd.

I am grateful for the help of Dr. Gabor Bogel with the fluorescence microscopic studies and to Vera Pichler for her perfect assistance.

I also would like to thank Dr. Xiaodong Wang and Dr. Liming Sun for sending necrosulfonamide and for providing useful information of its use.

I would like to thank the present and past members of the laboratories I worked in:

Semmelweis University, 1st Department of Pathology and Experimental Cancer Research: Dr. Anna Sebestyén, Mrs. Marica Csorba, Dr. Lajos Berczi, Dr. Melinda Hajdu, Mrs. Györgyi Mallász.

Semmelweis University, Department of Medical Chemistry: Pal Gyulavari, Attila Varga, Anna Sipos.

Institute of Enzymology: Anna Fekete.

National Institute of Oncology, Department of Pathogenetics: Dr. Judit Olasz, Zoltan Doleschall, Andras Pazsitka, Eva Malacko, Akos Shculcz. I am grateful to Dr. Orsolya Csuka head of the Department of Pathogenetics for her tolerance and understanding which made it possible to continue the work related to my Ph.D.

I would like to thank to Cecilia Laczik for the arrangement of many administrative matters.

I am thankful for my parents for their support and for make it possible to continue my studies.

I would like to express my special thank to my friend, Dr. Zsofia Benedek for her encouragement.

Finally I would like to express my deepest thank to my fiancé Bence Somogyi for his love, encouragement and support even at the hardest times.